MASSACHUSETTS INSTITUTE OF TECHNOLOGY

TE-20

OPTIMAL MULTIPLE-IMPULSE ORBITAL RENDEZVOUS

by

John E. Prussing

August, 1967

EXPERIMENTAL ASTRONOMY LABORATORY

MASSACHUSETTS INSTITUTE OF TECHNOLOGY

CAMBRIDGE 39, MASSACHUSETTS

TE-20

OPTIMAL MULTIPLE-IMPULSE ORBITAL RENDEZVOUS

by

JOHN E. PRUSSING

S.B. (1963), S.M. (1963)
Massachusetts Institute of Technology

SUBMITTED IN PARTIAL FULFILLMENT
OF THE REQUIREMENTS FOR THE
DEGREE OF DOCTOR OF SCIENCE

at the

MASSACHUSETTS INSTITUTE OF TECHNOLOGY

Signature of Author: John E. Prussing
Department of Aeronautics and Astronautics
August 2, 1967

Certified by: Walter Wrigley
Thesis Supervisor

Thesis Supervisor

Thesis Supervisor

Accepted by: Walter Wrigley
Chairman Departmental Graduate Committee

OPTIMAL MULTIPLE-IMPULSE ORBITAL RENDEZVOUS

by

John E. Prussing

Submitted to the Department of Aeronautics and Astronautics on August 2, 1967 in partial fulfillment of the requirements for the Degree of Doctor of Science.

ABSTRACT

Minimum-fuel, multiple-impulse orbital rendezvous is investigated for the case in which the transfer time is specified (time-fixed case). A method for obtaining optimal solutions is presented which is applicable to transfers between elliptical orbits of low eccentricity. In this method optimal solutions are constructed by satisfying the necessary conditions for the primer vector. It is assumed that the terminal orbits lie close enough to each other that the linearized equations of motion can be used to describe the transfer. The boundary value problem for the rendezvous is then solved analytically.

A complete solution to a specific class of rendezvous problems is obtained for a range of transfer times. The specific case considered is multiple-impulse rendezvous between coplanar circular orbits. Two-, three-, and four-impulse transfers are minimizing solutions for this problem. Since the transfer time is fixed, a coasting period in the initial or final orbit is optimal for certain rendezvous situations.

Thesis Supervisors:

Walter Wrigley, Sc.D.
Professor of Instrumentation and Astronautics

James E. Potter, Ph.D.
Assistant Professor of Aeronautics and Astronautics

Theodore N. Edelbaum, M.S.
Analytical Mechanics Associates, Inc.

Thesis Consultant:

Walter M. Hollister, Sc.D.
Assistant Professor of Aeronautics and Astronautics

ACKNOWLEDGMENTS

The author wishes to express his appreciation to his thesis committee: to Prof. Wrigley for serving as committee chairman, to Prof. Potter for his many helpful suggestions, and to Mr. Edelbaum for assuming the major portion of the thesis supervision through many hours of invaluable discussion and criticism.

Prof. Hollister, as thesis consultant, offered helpful technical advice before his sabbatical and provided inspiration and guidance during the author's doctoral program.

The author's colleagues at the M. I. T. Experimental Astronomy Laboratory provided a stimulating research atmosphere. Special thanks in this regard are due to Dr. Robert G. Stern and the author's fellow doctoral candidates Neal Carlson and Renwick Curry.

The preparation of the final draft was ably undertaken by Jackson & Moreland. The research and publication were supported by DSR Project 76145 through NASA Contract NsG 254-62.

J. E. P.
October, 1967

TABLE OF CONTENTS

LIST OF SYMBOLS

General Notation

An underlined lower-case letter denotes a column vector. A vector symbol without the underlining denotes its scalar magnitude.

A single dot over a symbol denotes the first derivative with respect to time. Time derivatives of vectors are taken with respect to an inertial reference frame unless otherwise noted.

A prime denotes differentiation with respect to the true longitude.

Units

The system of units is described in detail in Appendix B. 5. Wherever convenient, dimensionless variables are used.

Symbols

a	radius of circular reference orbit (Appendix B. 5)
$\underline{a}$	thrust acceleration vector
A, B, C	arbitrary constants in Section 2. 4
$A^{\#}$, $B^{\#}$, $C^{\#}$, $D^{\#}$	arbitrary constants in Section 7. 4 and Section 8. 2
A_{F_J}, B_{F_J}	partitions of the state transition matrix (6 $\times$ 3) defined by Eq. (3-16)
c	effective exhaust velocity (Section 2. 1)
c	cost per radius change (Section 5. 4)
c	arbitrary constant (Section 8. 5)
e	natural logarithm base (Section 2. 1)
$\underline{f}$	a general vector-valued function

F	a general system matrix
g_p	constant defined by Eq. (6-34)
$\underline{g}$	gravitational acceleration vector
G	gravity gradient matrix (3 × 3) (Section 2.2)
h_{ij}	i^{th} component of vector $\underline{h}_j$
$\underline{h}_j$	vector defined in Eq. (5-7)
H	Hamiltonian function (Chapter 2)
H	matrix (4 × 4) defined by Eq. (5-6)
I	identity matrix
J	control cost defined by Eq. (2-2)
k	arbitrary integer (Section 8.3)
k	auxiliary variable defined by Eq. (5-16)
k_j	auxiliary variable defined by Eq. (6-36)
$\left.\begin{matrix} K \\ L \end{matrix}\right\}$	arbitrary matrices (Appendix C)
m	mass of the spacecraft
m	auxiliary variable defined by Eq. (5-16)
m_j	auxiliary variable defined by Eq. (6-35)
M	matrix (6 × 6) defined by Eq. (3-12)
n	arbitrary integer
N_{21}	partition of state transition matrix $\frac{\partial \underline{r}_2}{\partial \underline{v}_1}$
p	derivative operator $\frac{d}{dt}$ (Appendix B)
$\underline{p}$	primer vector
$\underline{q}_j$	auxiliary variable defined by Eq. (5-16)
r	radial component of position vector

$\underline{r}$	position vector of vehicle
$\underline{R}$	position vector of vehicle (Appendix B)
δR	nondimensional difference between final and initial circular orbit radii
t	time
t_p	phasing time (Eq. (2-22))
T_j	transformation matrix (6 × 6) (Appendix B)
T_{21}	partition of state transition matrix $\frac{\partial \underline{v}_2}{\partial \underline{v}_1}$
$\underline{u}$	unit vector in the direction of thrust
$\underline{v}$	velocity vector of vehicle
$\underline{\Delta V}_i$	vector velocity change due to thrust impulse at time t_i
$\underline{\Delta V}$	vector having as components the magnitudes of the velocity changes
ΔV	cost (sum of magnitudes of velocity changes)
w_{ij}	i^{th} component of vector $\underline{w}_j$
$\underline{w}_j$	vector defined by Eq. (3-19)
W	matrix having $\underline{w}_j$ as columns
$\underline{x}$	state vector (Eq. (2-5))
$\delta\tilde{\underline{x}}$	the state variation at time t minus the initial state variation propagated forward to time t (Eq. (3-15))
$\delta\underline{y}$	state variation using true longitude as independent variable
z	normal component of position
α	defined by Eq. (B-23)
α_j	dimensionless time measured from half-transfer time (Eq. 5-8))

β	initial phase angle of target body (Section B. 6)
δ	indicates first variation of variable which follows it. Unless otherwise noted, variation is assumed to be at common value of time.
Δ	denotes a change in the variable which it precedes
θ	true longitude on reference orbit
θ_1	non-dimensional transfer time for two-impulse transfer (Section 8. 3)
θ_J	nondimensional transfer time defined by Eq. (8-24)
$\delta\tilde{\theta}_F$	final value of $\delta\theta$ minus the initial value propagated forward to final time (Section 6. 6)
λ	radial component of primer vector
$\underline{\lambda}$	adjoint vector (Eq. (2-7)
μ	circumferential component of primer vector
μ	gravitational constant
$\hat{\mu}$	specific value of circumferential primer vector component (Appendix A. 3)
ν	normal component of primer vector
$\rho(\cdot)$	denotes rank of $(\cdot)$
τ	dimensionless time variable (Eq. 2-22))
τ'	arbitrary time (Appendix B. 6)
Φ_{ji}	state transition matrix associated with $\delta\underline{x}$, between times t_i and t_j
Ψ_{ji}	state transition matrix associated with $\delta\underline{y}$, between times t_i and t_j
ω	mean motion of reference orbit
$\underline{\omega}$	angular velocity of rotating frame (Appendix B)
Ω	skew-symmetric cross product matrix (3 $\times$ 3) (Appendix B)

Subscripts

0	denotes an initial value
F	denotes a final value
1, 2, 3, ...	a numerical subscript refers to the number of the thrust impulse (first, second, third, ...)
H	refers to time t_H, the half-transfer time (Section 5.2)
j	refers to time t_j
r	radial component
θ	circumferential component
I	refers to inertial reference frame
R	refers to frame rotating with respect to inertial frame

Superscripts

-1	inverse of a matrix
T	transpose of a vector or matrix
I	refers to inital coast period (Section 6.3)
F	refers to final coast period (Section 6.3)
+	denotes a transfer with a terminal coast (2^+ means two-impulse plus a terminal coast)
I	denotes variable as seen by an inertial observer (Appendix B)
R	denotes variable as seen by rotating observer
T	in Section B.6, indicates the variable is associated with target body

CHAPTER 1

INTRODUCTION

1.1 Historical Background

During the last decade the field of optimal orbital transfer has received a great amount of attention. This is due, in part, to the heightened space-age interest in orbital mechanics combined with recent theoretical and computational advances in optimization theory. However, even before it was possible to generate trajectories which would accomplish a specified objective, research began into the realization of an objective in an optimal manner.

In 1925 a book, generally agreed to be the first significant result in optimum orbital theory, was published by Hohmann,[1] concerning minimum-fuel transfer between coplanar, circular orbits. Since that time the theory of minimum-fuel orbital transfer has been developed by Lawden,[2, 3, 4] in many publications beginning about 1950, Breakwell,[5] and others.

1.2 Lawden's Problem

One aspect of the general problem of minimum fuel trajectories in an inverse square gravitational field assumes a variable thrust rocket having constant exhaust velocity and unbounded thrust magnitude. Because of the extensive work done by Lawden, this problem has been called Lawden's Problem. This thesis investigation of minimum-fuel, multiple-impulse rendezvous is a specific case of Lawden's Problem.

In a paper by Edelbaum,[6] the known (1966) solutions to Lawden's Problem are cited and discussed. Many important results have been obtained for optimal multiple-impulse transfer. Examples include the results of Lawden,[3] the extensions of the Hohmann transfer made by Shternfeld,[7] Edelbaum,[8] and Hoelker and Silber,[9] optimal transfer between coaxial ellipses by Marchal,[10] optimal transfer in the vicinity of a circular orbit by Edelbaum,[11] and optimal transfer between hyperbolas by Gobetz[12] and Marchal.[13]

These and other solutions have been obtained for the optimal time-open transfer, in which the transfer time is unspecified. Not many results, in comparison, have been obtained for the time-fixed case. The publications in this area are quite recent and include theoretical studies by Lawden,[4] and Lion and Handelsman,[14] solutions for long transfer times by Marec,[15] and applications to interplanetary mission planning by Doll and Gobetz.[16]

1.3 Thesis Objective

The objective of this investigation is to describe a method for obtaining fixed-time, minimum-fuel, multiple-impulse transfers between close orbits, to apply the method to the specific case of coplanar, circle-to-circle rendezvous, and to describe those rendezvous for which transfers using more than two impulses are superior to two-impulse transfers. The circle-to-circle coplanar rendezvous is of interest since it is the simplest case which demonstrates the optimality of time-fixed transfers requiring more than two impulses.

1.4 Synopsis

In Chapter 2 the necessary conditions for minimum-fuel impulsive orbital transfers are obtained from Pontryagin's Maximum Principle. Lawden's primer vector is defined and its use in constructing optimal multiple-impulse transfers is discussed. Appendix A contains the details of the construction of optimal solutions.

In Chapter 3 the linearized boundary value problem for a rendezvous between close orbits is formulated. Appendix B describes in detail the linearized equations of motion and the boundary conditions for a circle-to-circle rendezvous.

The fact that only two-, three-, and four-impulse transfers need be considered for optimal solutions to a linearized coplanar rendezvous is discussed in Chapter 4. The necessity of considering initial or final coasting periods in time-fixed optimal solutions is demonstrated.

Chapters 5, 6, and 7 present analytical solutions to the linearized four-, three-, and two-impulse circle-to-circle coplanar rendezvous.

The reachable final states for minimum-fuel rendezvous using different numbers of impulses are displayed for a range of transfer times.

In Chapter 8 a set of non-unique optimal solutions is presented. This set includes the linearized Hohmann transfer and multiple-impulse solutions which use the same amount of fuel as the Hohmann transfer.

The optimal solutions to the circle-to-circle coplanar rendezvous problem are summarized in Chapter 9 and several example transfers are shown. Recommendations for further study are included.

CHAPTER 2

NECESSARY CONDITIONS FOR AN OPTIMAL TRANSFER

2.1 Introduction

The necessary conditions for a solution to Lawden's Problem can be deduced through Pontryagin's Maximum Principle.[17] For a variable thrust rocket having constant exhaust velocity and unbounded thrust magnitude, the mass of fuel expended during a transfer is given by,

$$\Delta m = m_o(1 - e^{-J/c}) \tag{2-1}$$

where m_o is the initial mass of the vehicle, c is the constant exhaust velocity, and

$$J = \int_0^{t_F} |\underline{a}| \, dt \tag{2-2}$$

where $\underline{a}$ is the thrust acceleration due to the propulsion system. Due to the monotonic behavior of Δm with J, minimization of J will minimize Δm. Since the control variable, $\underline{a}$, appears explicitly in the equation of motion, the control cost J is a convenient criterion for the minimization of fuel.

2.2 Necessary Conditions for an Optimal Impulsive Transfer

The equations of motion of a thrusting vehicle in a gravitational field in terms of the position, $\underline{r}$, and the velocity, $\underline{v}$, are:

$$\dot{\underline{r}} = \underline{v} \tag{2-3}$$

$$\dot{\underline{v}} = \underline{g}(\underline{r}) + \underline{a} \tag{2-4}$$

where $\underline{g}$ is the gravitational acceleration and $\underline{a}$ is the acceleration due to the propulsion. In terms of the state vector,

$$\underline{x} \triangleq \begin{bmatrix} \underline{r} \\ \underline{v} \end{bmatrix} \tag{2-5}$$

Equations (2-3) and (2-4) are of the form:

$$\dot{\underline{x}} = \underline{f}(\underline{x}, \underline{a}) \tag{2-6}$$

The differential equation for a first order change in the state, $\delta\underline{x}$, is

$$\delta\dot{\underline{x}} = \left(\frac{\partial \underline{f}}{\partial \underline{x}}\right)\delta\underline{x} = \begin{bmatrix} 0 & I \\ G(\underline{r}) & 0 \end{bmatrix}\delta\underline{x} \tag{2-7}$$

where $G(\underline{r})$ is the (symmetric) gravity gradient matrix, $(\partial\underline{g}/\partial\underline{r})$, evaluated along a reference solution to the state equation (2-6).

The adjoint (costate) vector, $\underline{\lambda}$, satisfies a related differential equation:

$$\dot{\underline{\lambda}} = -\left(\frac{\partial \underline{f}}{\partial \underline{x}}\right)^T \underline{\lambda} \tag{2-8}$$

The adjoint vector is important in optimization problems since it is a measure of the sensitivity of the cost to a small change in the state.

To obtain the necessary conditions to minimize J (maximize -J) of Eq. (2-2), the Maximum Principle is applied by defining a Hamiltonian function,

$$H = -a + \underline{\lambda}^T \underline{f} \tag{2-9}$$

By partitioning the adjoint vector into components,

$$\underline{\lambda} = \begin{bmatrix} \underline{\lambda}_r \\ \underline{\lambda}_v \end{bmatrix} \tag{2-10}$$

and defining the thrust unit vector,

$$\underline{u} = \frac{\underline{a}}{a} \quad (u=1,\ a>0) \tag{2-11}$$

the terms in the Hamiltonian which depend on the thrust control, $\underline{a}$, can be collected to yield:

$$H = \underbrace{(\underline{\lambda}_v^T \underline{u} - 1)\, a}_{H_o} + \underline{\lambda}_r^T \underline{v} + \underline{\lambda}_v^T \underline{g} \tag{2-12}$$

H_o is a function of the thrust control, $\underline{a}$, and the $\underline{\lambda}_v$-component of the adjoint vector, which Lawden[4] refers to as the primer vector, $\underline{p}$. Adopting this notation,

$$H_o = (\underline{p}^T \underline{u} - 1)\, a \tag{2-13}$$

H_o (and hence H) is maximized over the choice of $\underline{u}$ by taking

$$\underline{u} = \frac{\underline{p}}{p} \tag{2-14}$$

which aligns the thrust vector with the primer vector. Then

$$H_o = (p - 1)\, a \tag{2-15}$$

If $p < 1$, H_o is maximized by taking $a = 0$ (no thrust). If $p > 1$, H_o is maximized by making a infinite. This is not physically realizable since it corresponds to an infinite thrust over a finite time interval. Therefore the thrusts occur when,

$$p = 1$$

and the direction of the impulse is

$$\underline{u} = \underline{p}$$

In addition, the primer vector and its first derivative must be continuous.

To summarize, the necessary conditions, first obtained by Lawden,[4] for an optimal impulsive transfer are:

1. The primer vector and its first derivative must be continuous everywhere.
2. The thrust impulses are applied in the direction of the primer vector at the times for which $p = 1$.
3. $p \leq 1$ during the transfer

4. As a consequence of these conditions, for impulses which are not at the initial or final times, $\dot{p} = 0$.

A typical time history of a primer vector magnitude for an optimal three-impulse transfer is shown in Fig. 2-1.

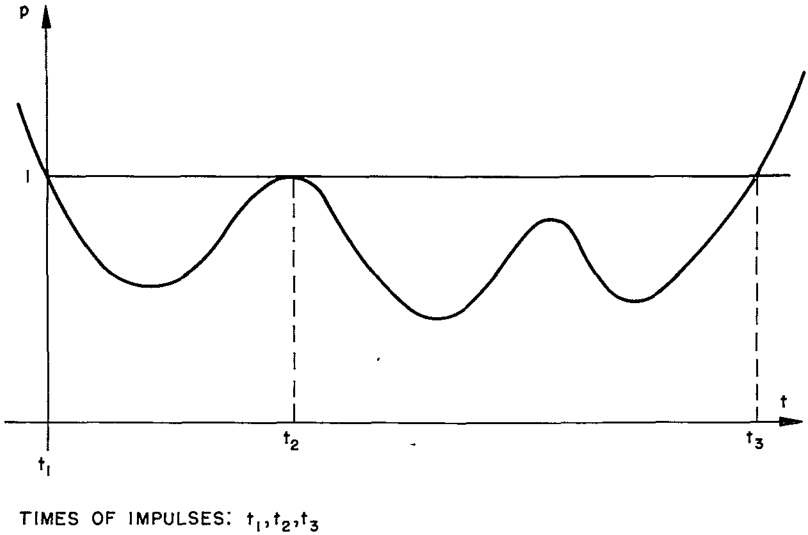

Fig. 2-1. Optimal three-impulse primer magnitude time history.

2.3 The Primer Vector and the Linearized Equations of Motion

The differential equation for the adjoint vector (Eq. (2-8)), written in second order form in terms of the primer vector is

$$\ddot{\underline{p}} = G(\underline{r})\,\underline{p} \tag{2-15a}$$

By comparison with Eq. (3-3), the primer vector satisfies the same differential equation as the first order variation in position, $\delta\underline{r}$.

If one considers rendezvous between orbits which lie close together, the equations of motion can be linearized about an intermediate reference orbit (Section 3.2). In this case the primer vector is evaluated along the reference trajectory and, to first order, is independent of the perturbed trajectory described by the linearized equations of motion. Thus the linearized equations of motion and the adjoint equations can be solved separately. This is in contrast to a problem with a nonlinear state equation, in which the adjoint vector is a function of the state.

Because of this separability a solution to the primer vector equation which satisfies the necessary conditions for an optimum is independent of the boundary conditions for a specific rendezvous. Once the times of application and the directions of the thrust impulses are determined from the primer solution, a linear boundary value problem is solved to determine the magnitudes of the impulses to satisfy the boundary conditions for a specified rendezvous (Chapter 3).

2.4 The Primer Vector along a Circular Orbit

For rendezvous between elliptical orbits of low eccentricity a convenient reference trajectory is a circular orbit lying between the terminal orbits. For linear theory to be valid, both the inclination between the terminal orbits and the radial separation of the orbits relative to the semi-major axis of either orbit must be small. A circular reference orbit is convenient because the linearized equations of motion and the primer vector equations are analytically simple. However, closed-form analytical solutions to the linearized motion equations for elliptical reference orbits are also available[18] and could be useful in other applications.

Since the primer vector satisfies the same differential equation as the first order variation in position (Section 2.3), the solution to the primer vector equation has the same form as the solution to the motion equations given in Appendix B.4. Coordinatizing the primer vector in a frame rotating with a body in the reference orbit,

$$\underline{p} = \begin{bmatrix} \lambda \\ \mu \\ \nu \end{bmatrix} \tag{2-16}$$

where λ, μ, ν are the radial, circumferential, and out-of-plane components, respectively. The component equations are then analogous to Eq. (B-22). In terms of ω, the mean motion of the circular reference orbit:

$$\ddot{\lambda} = 3\omega^2\lambda + 2\omega\dot{\mu} \tag{2-17}$$

$$\ddot{\mu} = -2\omega\dot{\lambda} \tag{2-18}$$

$$\ddot{\nu} = -\omega^2\nu \tag{2-19}$$

The out-of-plane component, ν, is uncoupled from the other components and satisfies a linear oscillator equation. The solution for the in-plane components can be written in the form:

$$\lambda = A(\cos\tau + 2B) \tag{2-20}$$

$$\mu = A(-2\sin\tau - 3B\tau + C) \tag{2-21}$$

where $\tau \triangleq \omega(t - t_p)$ and A, B, C, t_p are arbitrary constants.

2.5 Geometrical Construction of Primer Vector Solutions Satisfying the Necessary Conditions

Equations (2-20) and (2-21) are a parametric description of a locus in the λ-μ plane. With B=0 the locus is a 1 $\times$ 2 ellipse shown in Fig. 2-2. For B $\neq$ 0 the locus is the cycloid-like curve shown in Figs. 2-3 and 2-4. In Eqs. (2-20) and (2-21) the constant A normalizes length in the λ-μ plane, B determines the shape of the locus, and C positions the locus along the μ-axis. Since the transfer begins at t=0, t_p corresponds to the initial value of $\tau(\tau_o = -\omega t_p)$.

For a two-dimensional problem, solutions to the primer vector equation which satisfy the necessary conditions for an optimal transfer can be constructed geometrically using the primer vector locus diagram. For the fixed transfer time $\tau_F - \tau_o$, the necessary conditions (Section 2.2) require that the locus be smooth, that the locus lie on or inside a unit circle in the λ-μ plane ($p \leq 1$) for all $\tau\epsilon[\tau_o, \tau_F]$, and that the locus be tangent to the unit circle for impulses not at the terminal times ($\dot{p} = 0$). The optimum times to apply the impulses are then those times

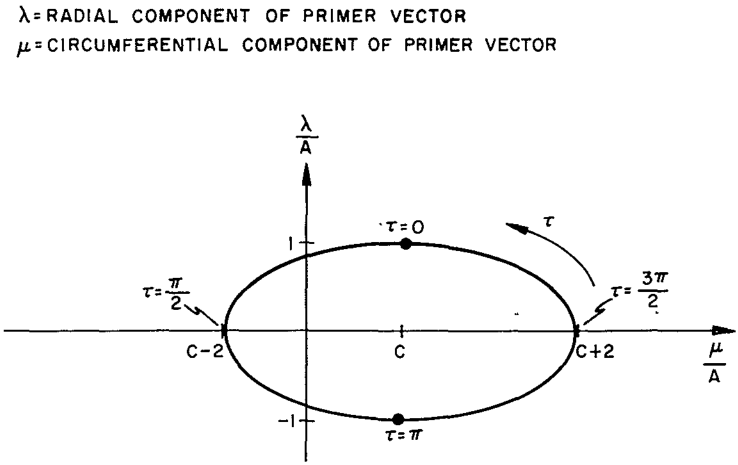

Fig. 2-2. Primer locus diagram for B = 0.

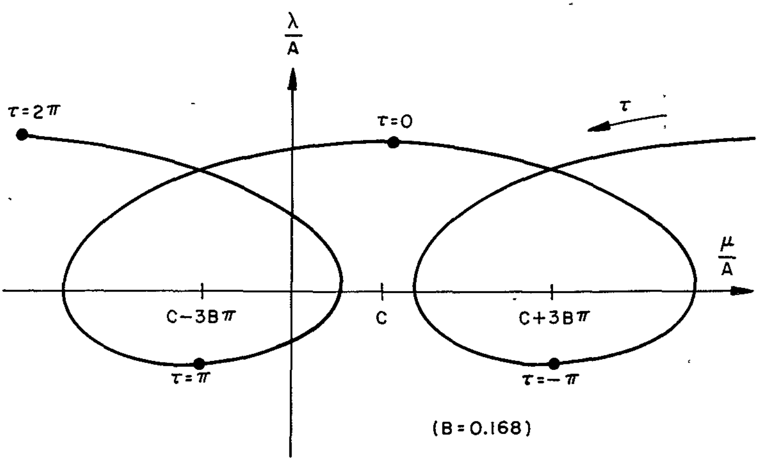

Fig. 2-3. Primer locus diagram for B > 0.

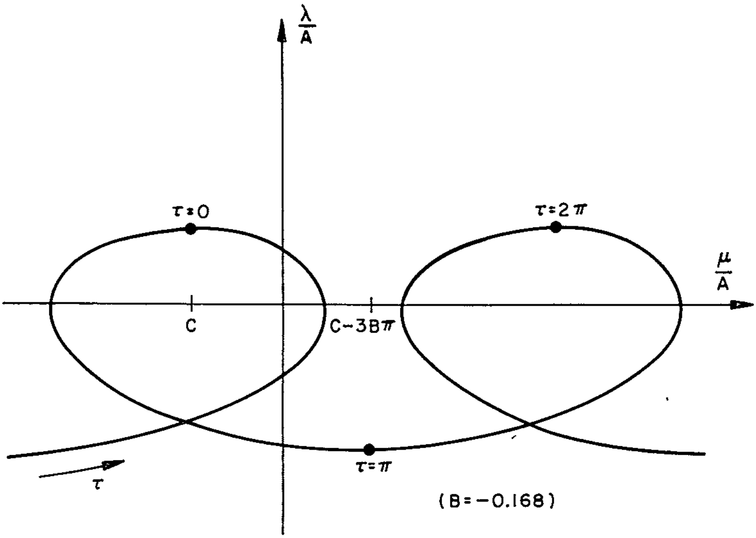

Fig. 2-4. Primer locus diagram for B < 0.

for which the locus touches the unit circle ($p = 1$); the thrust directions are given by the components of the primer vector at these times. Figures 2-5 through 2-7 show examples of constructions of optimal multiple-impulse primer vector solutions. The $\underline{u}_1$ vectors are the unit vectors in the directions of thrust.

A more detailed description of the technique used to construct optimal solutions is discussed in Appendix A.

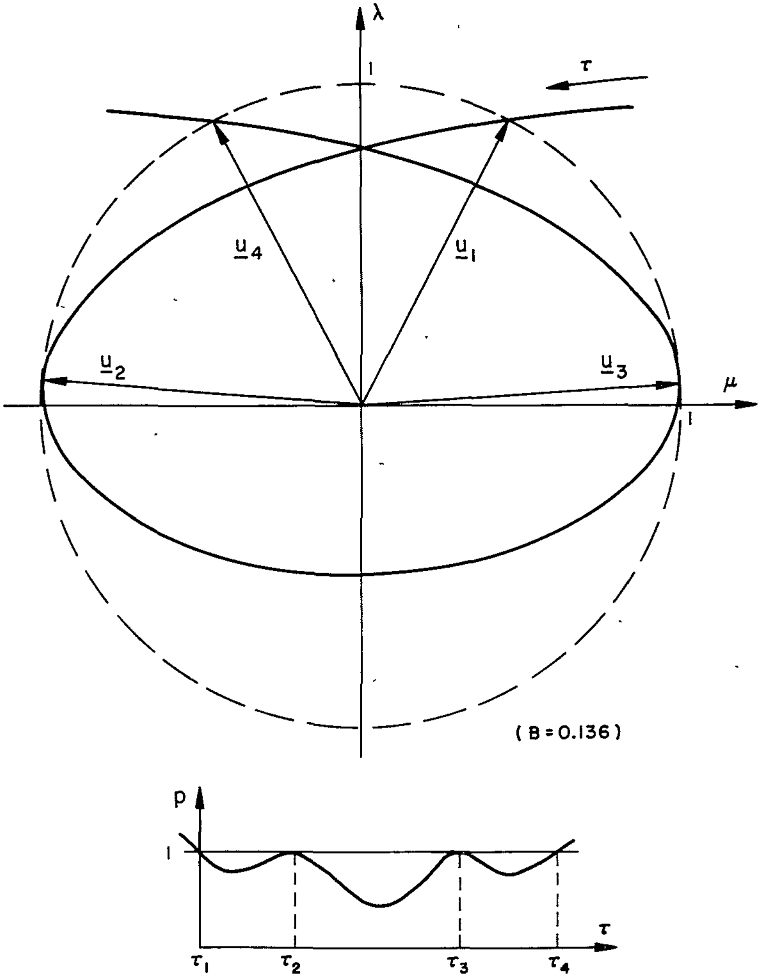

Fig. 2-5. Primer locus construction for four-impulse optimal.

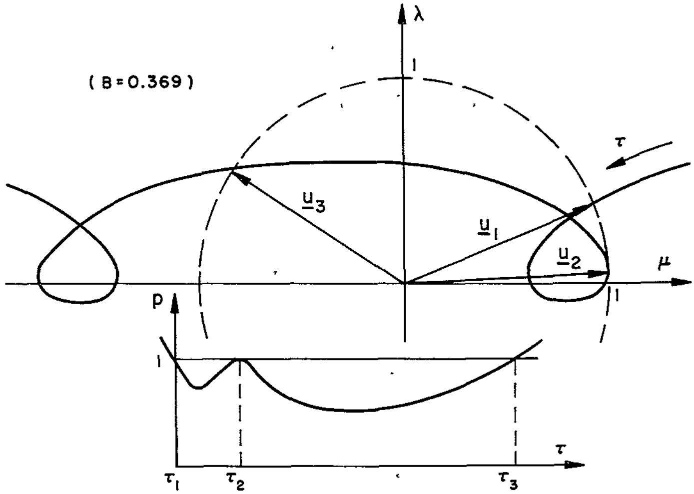

Fig. 2-6. Primer locus construction for three-impulse optimal.

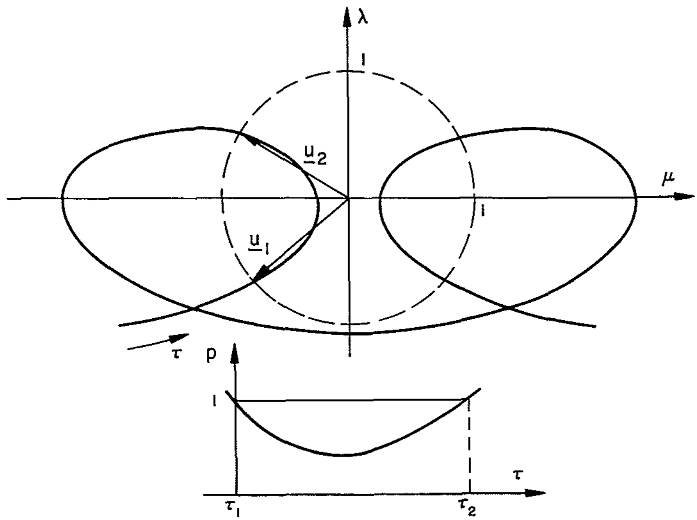

Fig. 2-7. Primer locus construction for two-impulse optimal.

CHAPTER 3

THE RENDEZVOUS BOUNDARY VALUE PROBLEM

3.1 Introduction.

For a circular orbit, primer vector solutions which satisfy the necessary conditions for an optimal fixed-time impulsive transfer can be obtained by the method of Chapter 2. These solutions are valid for trajectories which lie close enough to the circular orbit to be described by first order variations of the circular orbit motion. Using these linearized equations of motion, optimal solutions to the orbital rendezvous problem can be determined for the case in which both of the terminal orbits lie within the linear range of the reference orbit.

Once primer vector solutions have been obtained which satisfy the necessary conditions for an optimal transfer, the times of application and the directions of the thrust impulses are determined. The only additional information necessary to completely describe the transfer is the magnitude of the instantaneous velocity change caused by each thrust impulse. These magnitudes depend on the specified transfer time, the given initial conditions and the desired final boundary conditions for the rendezvous and must therefore be determined by solving a linear boundary value problem.

For an orbital rendezvous the desired final boundary conditions require that the position and velocity of the vehicle at the final time be the position and velocity of the target body. Optimal solutions to other types of transfers require less restrictive final boundary conditions. For example, an "orbital interception" requires matching only the positions of the vehicle and the target at the final time. In an "orbital transfer" the location in the desired final orbit at the final time is not prescribed.

This investigation is concerned with optimal solutions to the time-fixed orbital rendezvous problem.

3.2 Linearization of the Equations of Motion

The differential equations of motion of a vehicle moving under the influence of gravitational forces are:

$$\dot{\underline{r}} = \underline{v} \qquad\qquad (3\text{-}1)$$
$$\dot{\underline{v}} = \underline{g}(\underline{r})$$

where, for two-body motion,

$$\underline{g}(\underline{r}) = -\frac{\mu}{r^3}\underline{r} \qquad\qquad (3\text{-}2)$$

Equation (3-1) can be linearized by assuming small variations about a known reference solution:

$$\begin{aligned} \delta\dot{\underline{r}} &= \delta\underline{v} \\ \delta\dot{\underline{v}} &= G(\underline{r})\ \delta\underline{r} \end{aligned} \qquad\qquad (3\text{-}3)$$

where $G(\underline{r}) = \partial\underline{g}(\underline{r})/\partial\underline{r}$ is the gravity gradient matrix evaluated along the reference trajectory. For two-body motion,

$$G(\underline{r}) = \frac{\mu}{r^5}[3\,\underline{r}\,\underline{r}^T - r^2 I] \qquad\qquad (3\text{-}4)$$

Defining a six-component state vector

$$\underline{x} \triangleq \begin{bmatrix} \underline{r} \\ \underline{v} \end{bmatrix} \qquad\qquad (3\text{-}5)$$

Equation (3-3) can be written as

$$\delta\dot{\underline{x}} = \begin{bmatrix} 0 & I \\ G & 0 \end{bmatrix} \delta\underline{x} \qquad\qquad (3\text{-}6)$$

If the state variation, $\delta\underline{x}$, is defined to be the difference between the actual state and the reference state at some time t, then the operations of differentiation and variation can be interchanged to yield:

$$\frac{d}{dt}\,\delta\underline{x} = \begin{bmatrix} 0 & I \\ G & 0 \end{bmatrix} \delta\underline{x} \qquad\qquad (3\text{-}7)$$

For the state variation defined in this way, time is said to be the independent variable for the linearization, since $\delta t \equiv 0$.

The solution of Eq. (3-7) is then

$$\delta \underline{x}(t_j) = \Phi(t_j, t_i)\, \delta \underline{x}(t_i) \tag{3-8}$$

where $\Phi(t_j, t_i)$ is the state transition matrix (fundamental matrix) of the system (3-7).

Appendix B discusses the linearized equations of motion in more detail.

3.3 An Alternative Independent Variable for the Linearization

The two-body nonlinear equations of motion expressed in polar coordinates are:

$$\ddot{r} - r\dot{\theta}^2 = -\frac{\mu r}{(r^2 + z^2)^{3/2}} \tag{3-9}$$

$$r\ddot{\theta} + 2\dot{r}\dot{\theta} = 0 \tag{3-10}$$

$$\ddot{z} = -\frac{\mu z}{(r^2 + z^2)^{3/2}} \tag{3-11}$$

Linearization of these equations about the reference circular orbit $r = a$, $z = 0$ results in Eq. (B-23). In order for these linearized equations to be valid, the velocity variations must be small, but the only position components which need be small are $\delta r/a$ and δz.[19] $\delta\theta$ is unrestricted since the gravitational attraction is independent of θ. Thus, for the linear theory to be valid, the motion is confined to a torus about the reference orbit.

For moderately long transfer times (less than two reference orbit periods), the value of $\delta\theta$ can become appreciable due to the secular term in transition matrix (Eq. (B-24)). While not violating linearity, this results in a significant circumferential displacement between the actual position of the vehicle and the point on the reference orbit at which the primer vector is evaluated for that same time. Because the primer vector is evaluated as a function of position in the reference orbit and because of the inherent geometrical characteristics of the orbits and the somewhat artificial introduction of time as a parameter, it seems reasonable to associate the primer vector with a point on the actual trajectory which is geometrically close to the point at which the primer vector is evaluated. This can be accomplished by comparing the reference state and the actual state at a common value of the longitude angle, θ, rather than at the same time.

In the linear theory this implies taking θ (in the three-dimensional case the true longitude) as the independent variable for the linearization ($\delta\theta \equiv 0$) and treating δt as a state variable. This has been applied to elliptical orbits by Stern and Potter.[20]

The state variations for the two different independent variables are related by a linear transformation. Let $\delta \underline{y}$ denote the state variation with θ as the independent variable. Then

$$\delta \underline{y} = M \, \delta \underline{x} \tag{3-12}$$

The state transition matrix, $\Psi(\theta_j, \theta_i)$ for $\delta \underline{y}$ is related to the original transition matrix, $\Phi(t_j, t_i)$ by

$$\Psi_{ji} = M_j \Phi_{ji} M_i^{-1} \tag{3-13}$$

Appendix B.7 presents the matrix M for a circular orbit and demonstrates how the solutions to the rendezvous problem using time as the independent variable are related to solutions with θ as the independent variable.

In the remainder of this investigation, time is considered to be the independent variable since a position-velocity state is conceptually simpler and easier to display geometrically. However, the transformed solutions to the rendezvous problem probably yield a better approximation to the nonlinear solution.

3.4 Formulation of the Boundary Value Problem

In terms of the linearized equations of motion, the effect of several velocity changes during a transfer is obtained by superposition. Let $\delta \underline{x}_0$ be the state variation at the initial time, $t = 0$, and let $\delta \underline{x}_F$ be the final state variation. In terms of velocity changes $\underline{\Delta V}_j$ made at times t_j ($j = 1, 2, 3, \ldots, n$):

$$\delta \underline{x}_F = \Phi_{Fo} \, \delta \underline{x}_o + \sum_{j=1}^{n} \Phi_{Fj} \begin{bmatrix} \underline{0} \\ \underline{\Delta V}_j \end{bmatrix} \tag{3-14}$$

For convenience, define

$$\delta \tilde{\underline{x}}_F = \delta \underline{x}_F - \Phi_{Fo} \, \delta \underline{x}_o \tag{3-15}$$

and partition the transition matrix such that

$$\Phi_{Fj} = [A_{Fj} \;\; \vdots \;\; B_{Fj}] \tag{3-16}$$

Then Eq. (3-14) becomes:

$$\delta \tilde{\underline{x}}_F = \sum_{j=1}^{n} B_{Fj} \, \underline{\Delta V}_j \tag{3-17}$$

In terms of the unit vector in the direction of thrust

$$\underline{u}_j = \frac{\underline{\Delta V}_j}{\Delta V_j} \tag{3-18}$$

and the definition

$$\underline{w}_j \triangleq B_{Fj} \underline{u}_j \tag{3-19}$$

Equation (3-17) becomes

$$\delta \tilde{\underline{x}}_F = W(t_j, u_j) \, \underline{\Delta V} \tag{3-20}$$

where

$$W = [\underline{w}_1, \, \underline{w}_2, \, \ldots, \, \underline{w}_n] \tag{3-21}$$

$$\underline{\Delta V} = \begin{bmatrix} \Delta V_1 \\ \Delta V_2 \\ \vdots \\ \Delta V_n \end{bmatrix} \tag{3-22}$$

The matrix W is a function of the times of the impulses and their directions. These t_j and $\underline{u}_j$ for an optimal transfer are obtained directly from the primer vector locus of Chapter 2 and contain the information which is necessary for an optimum transfer.

The vector $\underline{w}_j$ has the physical interpretation of being the change in the final state variation due to a unit magnitude velocity change at time t_j in the optimal direction $\underline{u}_j$ (the direction of the primer vector).

The boundary value problem is now formulated for the fixed transfer time t_F. The desired final state variation, $\delta\underline{x}_F$, is the state variation of the target at t_F, a known quantity. The initial state variation is known and the W matrix is constructed from the optimization. The solution to the boundary value problem is then the $\underline{\Delta V}$ which will accomplish the optimal rendezvous.

In terms of the n components of $\underline{\Delta V}$ and a q-component state variation vector, Eq. (3-20) represents q equations in the n unknowns.

However, not all solutions for $\underline{\Delta V}$ are admissible, since some components may turn out to be negative. Since the line in space along which the thrust is directed is determined by the primer vector, a negative component of $\underline{\Delta V}$ requires that the thrust be directed in a sense opposite to the primer vector. The solution will satisfy the boundary conditions, but violate a necessary condition for the optimum and is therefore inadmissible. The condition for an admissible solution is then

$$\Delta V_i \geq 0 \qquad i = 1, 2, \ldots, n \tag{3-23}$$

CHAPTER 4

TYPES OF TIME-FIXED OPTIMAL SOLUTIONS

4.1 Introduction

The purpose of this investigation is to obtain a complete optimal multiple-impulse solution to a specific class of rendezvous problem for a wide range of transfer times. The complete optimal solution to the problem is complicated by two factors: (1) For an initial location of the target, the number of impulses to realize the optimal rendezvous depends on the transfer time, and (2) for a fixed transfer time and initial conditions, either an initial or final coast period in one of the terminal orbits may be optimal.

In order to obtain a complete optimal solution for a class of rendezvous problems and be able to reasonably display and interpret the results, a very simple class of problems is considered, namely, rendezvous between coplanar, circular orbits.

The reference orbit for the linearization is taken to be a circular orbit lying half-way between the initial and final circular orbits. The linearized analysis is valid if the difference in radii of the terminal orbits is small compared to the reference orbit radius.

4.2 The Number of Impulses and Uniqueness of the Solutions

For impulsive solutions to problems described by linear differential equations, several results are known which are useful in obtaining solutions. The first, obtained by Neustadt[21] and by Potter[22] is the following:

> For a linear system the <u>maximum</u> number of impulses necessary to realize the optimum transfer is equal to the number of constraints on the state variables at the specified final time.

Thus a fixed-time, coplanar rendezvous may require as many as four impulses. An optimal three-dimensional rendezvous may require as many as six.

For the coplanar case the state variation has four components and the boundary value equation (3-20) represents four equations in the n unknown velocity change magnitudes ($n \leq 4$). If the terminal orbits do not intersect, at least two impulses are required to perform a rendezvous (optimal or non-optimal). Therefore the types of thrust programs which must be investigated for the optimal, coplanar, circle-to-circle rendezvous are two-, three-, and four-impulse transfers.

Another result due to Potter[23] is the condition for uniqueness of the optimal solutions and the demonstration that the Maximum Principle is a sufficient as well as necessary condition for the optimum in this problem. The optimal thrust program is unique if and only if the columns $\underline{w}_1$, $\underline{w}_2$, . . . , $\underline{w}_n$ of the matrix W of Eq. (3-20) are linearly independent. The special cases of non-unique solutions are discussed in Chapter 8.

4.3 Solutions with Initial or Final Coasting Periods

For a specified transfer time and specified initial states of the target and rendezvous vehicles, a coasting period in either the initial or final orbit may be optimal. An initial coast implies waiting in the initial orbit before applying the first thrust impulse. A final coast implies that the rendezvous takes place earlier than the specified final time.

Since the fuel expended depends greatly on the position of the target relative to the rendezvous vehicle at launch, a certain amount of the specified transfer time in some cases is best invested in a coast period, allowing a geometrically more favorable rendezvous.

Rendezvous requiring coasting periods to realize minimum fuel can be illustrated by considering a two-impulse rendezvous between coplanar, circular orbits. In Fig. 4-1 contours of total velocity requirement per difference in terminal orbit radii for the linearized rendezvous are plotted on a time-of-launch, time-of-arrival plane. (Velocity is measured in units of orbital velocity, radius difference is in fractions of reference orbit radius.) Any point in this plane represents a possible rendezvous since the launch time and transfer time are specified. Note that points

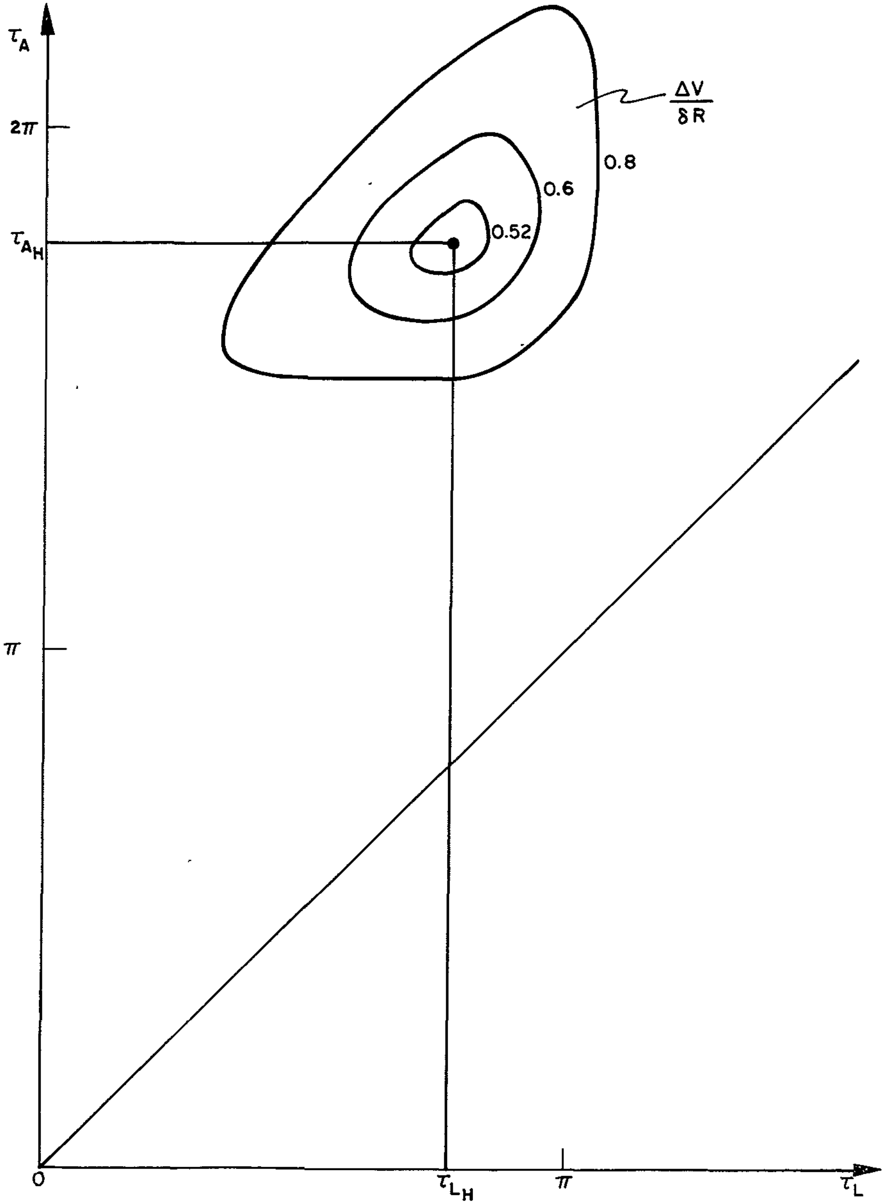

Fig. 4-1. Contours of velocity requirements for linearized two-impulse rendezvous.

representing positive transfer times lie above the line for which launch and arrival times are equal. Time is nondimensionalized such that in one reference orbit period τ changes by 2π (Section B. 5).

Specifying the launch time fixes the initial geometry in terms of the phase angle between the launch point and the target (Section B. 6). For example, the launch time for the Hohmann transfer, τ_{LH}, corresponds to an initial phase angle, β, of

$$\beta_H = \frac{3}{4}\pi \ \delta R \tag{4-1}$$

where δR is the difference between the final and initial circular orbit radii (non-dimensionalized by being measured in fractions of reference orbit radius).

A situation for which an initial coast is optimal is shown in Fig. 4-2. The specified initial and final times are τ_1 and τ_2, respectively. The transfer represented by point P requires launching at time τ_1 and arriving at time τ_2. Any point on the line PQ, e. g. point M, represents a transfer which also arrives at τ_2 but launches at a later time, τ_M. This transfer occurs in the fixed transfer time $\tau_2 - \tau_1$, but requires an initial coast of duration $\tau_M - \tau_1$ and a correspondingly shorter time-in-flight of $\tau_2 - \tau_M$. Point Q is the limiting case where the total fixed transfer time is used for the initial coast and the time-in-flight is zero.

Analogously, for any transfer represented by a point on the line PR, the launch occurs at τ_1, but the rendezvous takes place earlier than τ_2 and requires a coasting period in the final orbit.

Any transfer inside the shaded triangle of Fig. 4-2 can be achieved in the fixed time $\tau_2 - \tau_1$ by using both an initial and final coast. Of these trips, point M evidently requires the smallest two-impulse velocity requirement. For this rendezvous situation an initial coast of duration $\tau_M - \tau_1$ results in the minimum two-impulse transfer. If this transfer is optimal (no multiple-impulse transfer has a smaller velocity requirement), the primer vector magnitude has the form shown in Fig. 4-3.

Figure 4-4 shows that for the same initial time, τ_1, and a longer fixed transfer time, $\tau_2' - \tau_1$, the absolute minimum (Hohmann transfer at

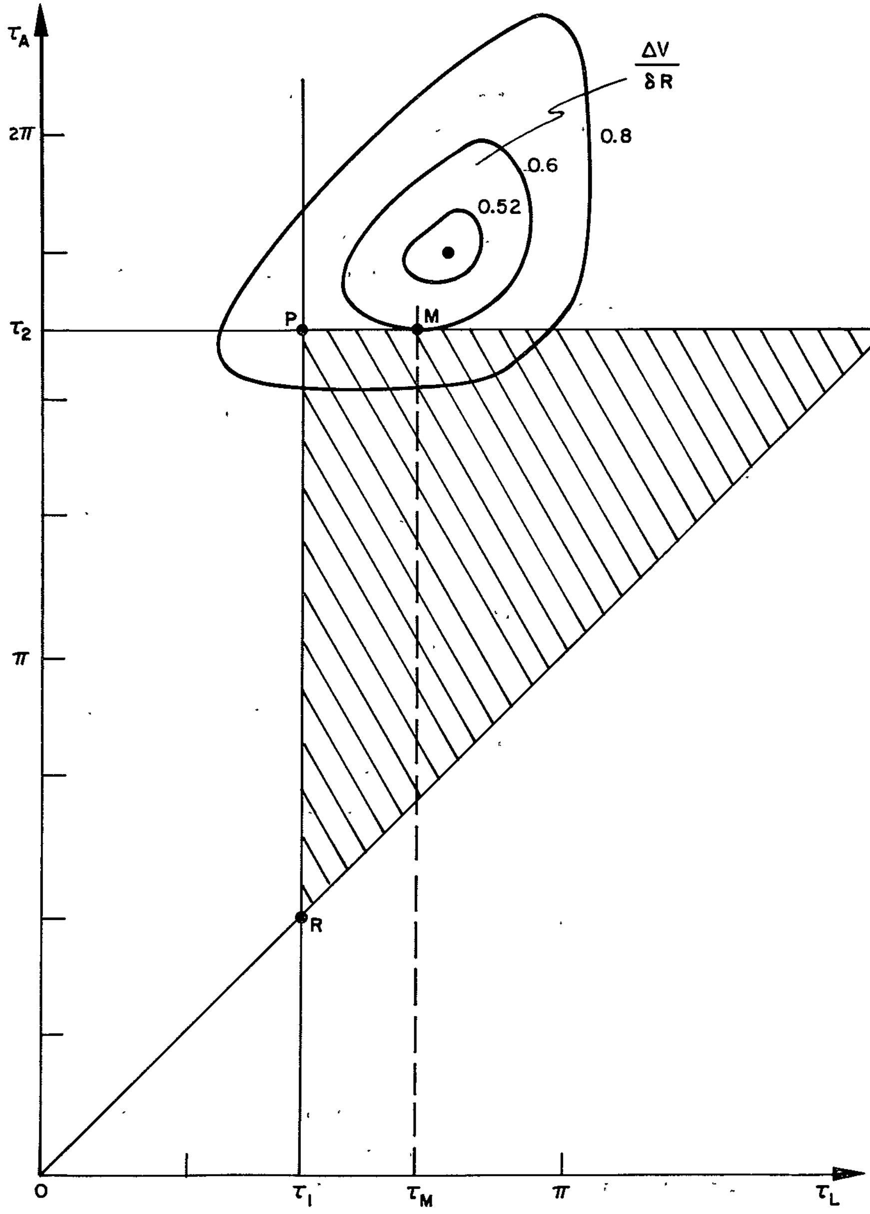

Fig. 4-2. Optimal two-impulse rendezvous requiring initial coast.

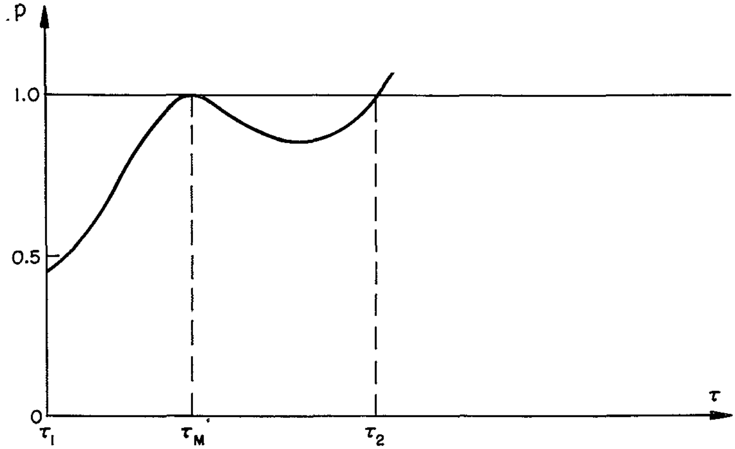

Fig. 4-3. Primer vector magnitude for optimal two-impulse transfer with initial coast.

point M) can be employed. This requires an initial coast of duration $\tau_{LH} - \tau_1$ and a final coast of duration $\tau_2' - \tau_{AH}$.

In Fig. 4-5 the initial time τ_1', is later than the launch time for the Hohmann transfer. The minimum two-impulse rendezvous for the final time τ_2 occurs at the point M and requires no coasting periods.

For this same initial time and a later final time, τ_2', the minimum two-impulse rendezvous occurs at time τ_M, and requires a coast in the final orbit until τ_2' (Fig. 4-6).

The velocity requirement contours of the type shown in Fig. 4-6 repeat every synodic period of the terminal orbits. Thus for any initial time, e.g. τ_1', and a sufficiently long transfer time, the absolute minimum of the Hohmann transfer can always be realized. However, the synodic period varies inversely with δR, which, strictly speaking, is an infinitesimal, although reasonaly good approximations are obtained

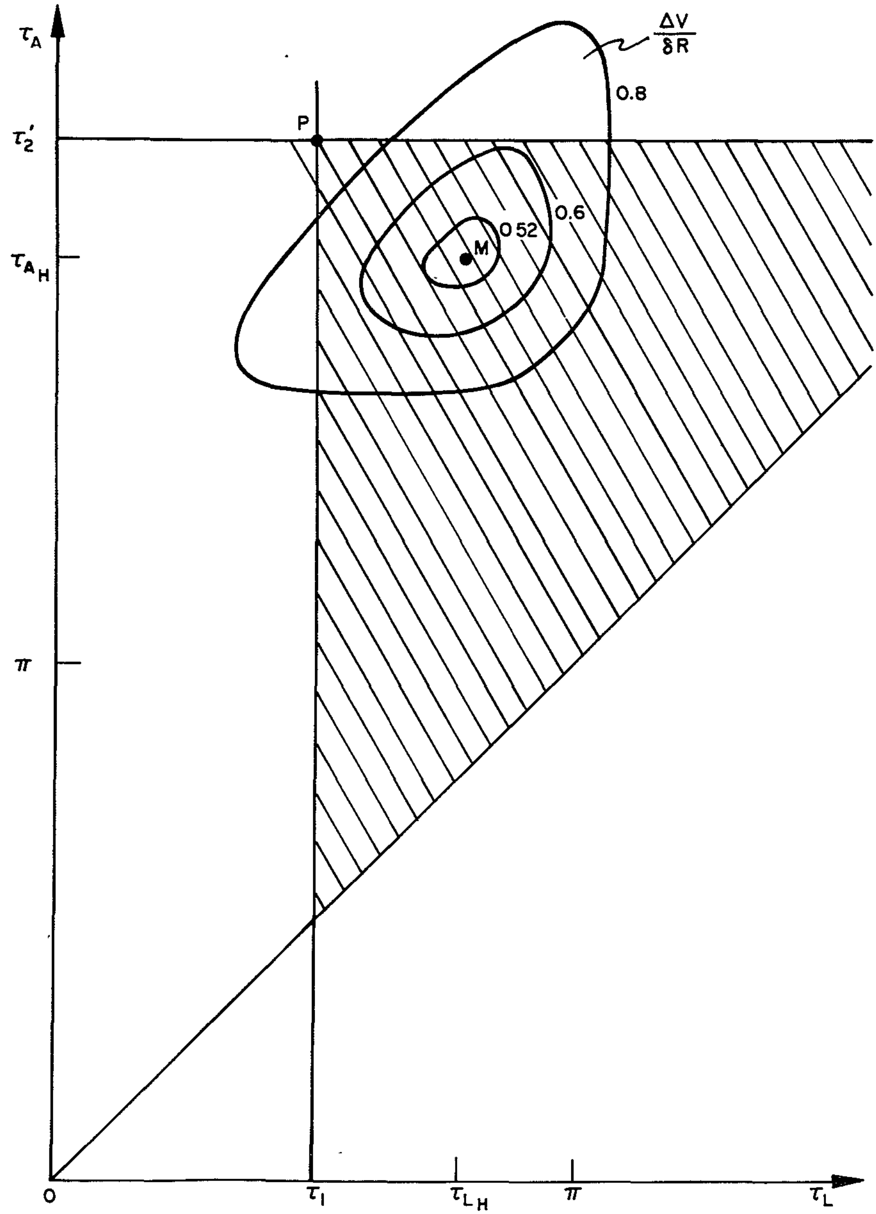

Fig. 4-4. Optimal rendezvous requiring initial and final coast.

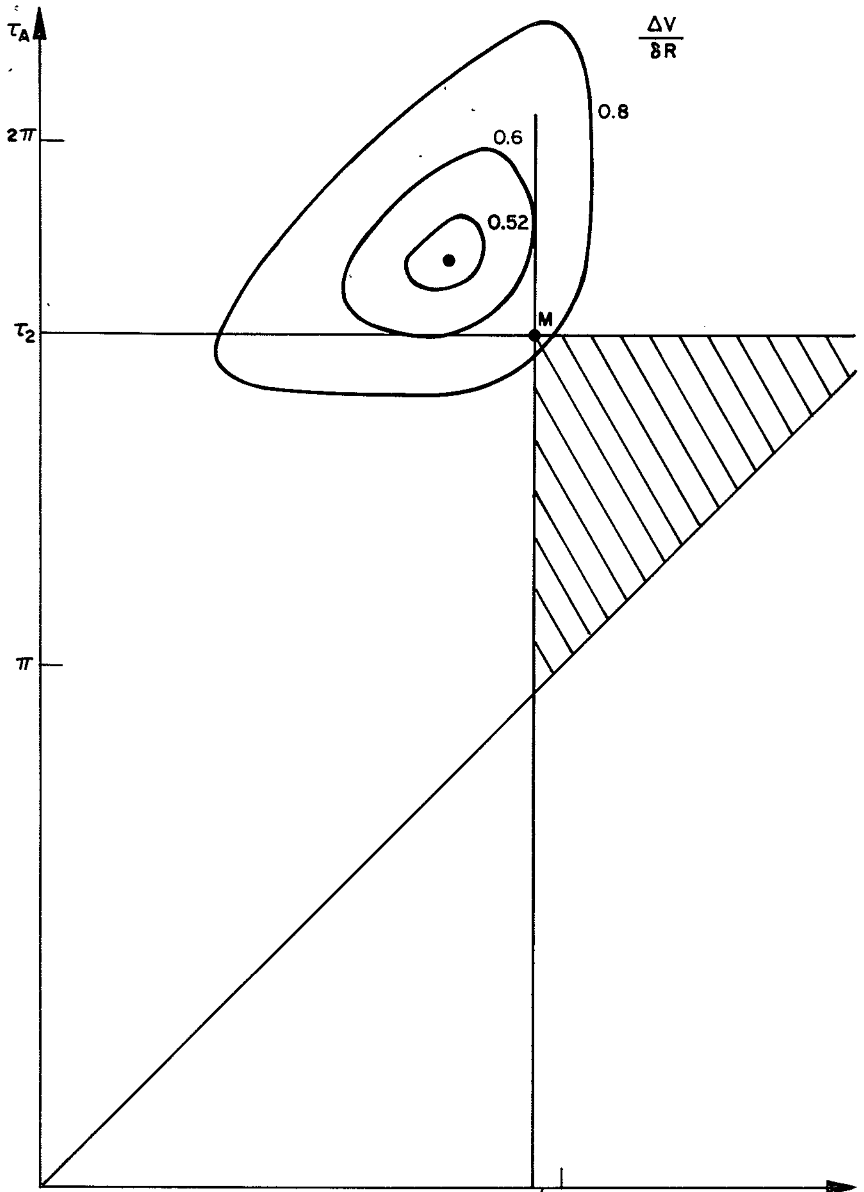

Fig. 4-5. Optimal rendezvous requiring no coasting periods.

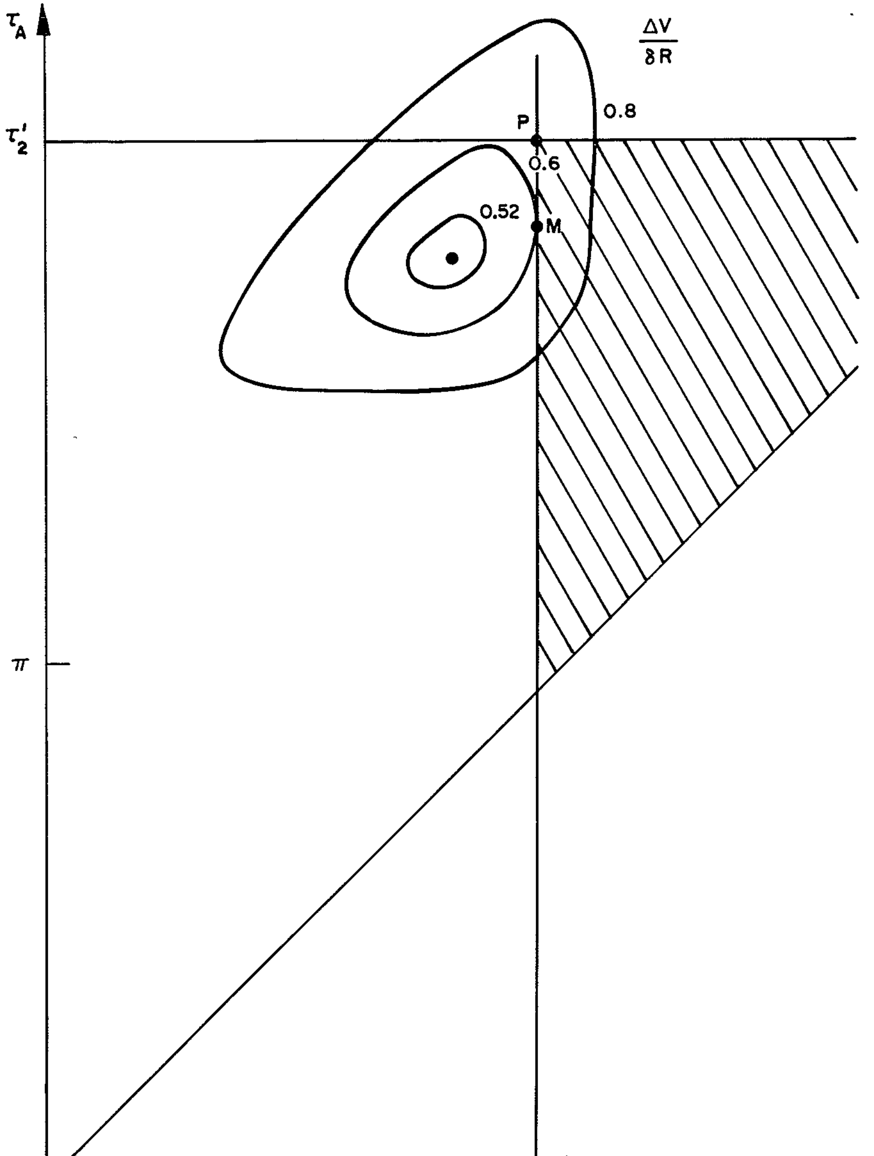

Fig. 4-6. Optimal rendezvous requiring final coast.

for δR of the order of 0.1. For infinitesimally close orbits, however, the synodic period is arbitrarily large and a Hohmann transfer for the initial time τ_1' is attainable only asymptotically. In this investigation of moderate transfer times (less than two reference orbit periods) a single synodic cycle of the terminal orbits is considered.

The example of a two-impulse rendezvous has been used to demonstrate initial and final coast solutions. Analogously, three-impulse minimizing transfers may require terminal coasts (Chapter 6). In Chapter 5 it is shown that no four-impulse solutions with terminal coasts exist other than the non-unique case discussed in Chapter 8.

4.4 Reciprocal and Dual Primer Vector Solutions

For each solution to the primer vector equation which satisfies the necessary conditions, there are other solutions for the same transfer time which result in related boundary value solutions. The simplest of these is the reciprocal solution, in which the thrust unit vectors are the negatives of those in the original solution. This is shown in Fig. 4-7 for a three-impulse optimum.

The dotted primer locus of Fig. 4-7 is obtained from the original locus (described by Eq. (2-20)) by replacing the constant B by its negative. Since B is the coefficient of the secular term in the μ-component, the time parameter travels along the locus in the opposite direction. Since the primer vector differential equation (Eq. (2-15)) is homogeneous, the reciprocal solution is merely the statement that, given a solution, $\underline{p}$, $-\underline{p}$ is also a solution.

Physically the reciprocal solution using the same $\underline{\Delta V}$ as the original solution represents a rendezvous from an initial state variation, $-\delta\underline{x}_O$, to a final variation, $-\delta\underline{x}_F$. Thus if the original optimal solution transfers the vehicle from the inner orbit to the outer orbit with a rendezvous behind the reference point, the reciprocal solution represents an optimal transfer from the outer to the inner orbit with rendezvous ahead of the reference point as shown in Fig. 4-8. In this figure the transfer is plotted in a frame rotating with a point in the reference orbit. The transfer time and the cost of these two rendezvous is the same. The

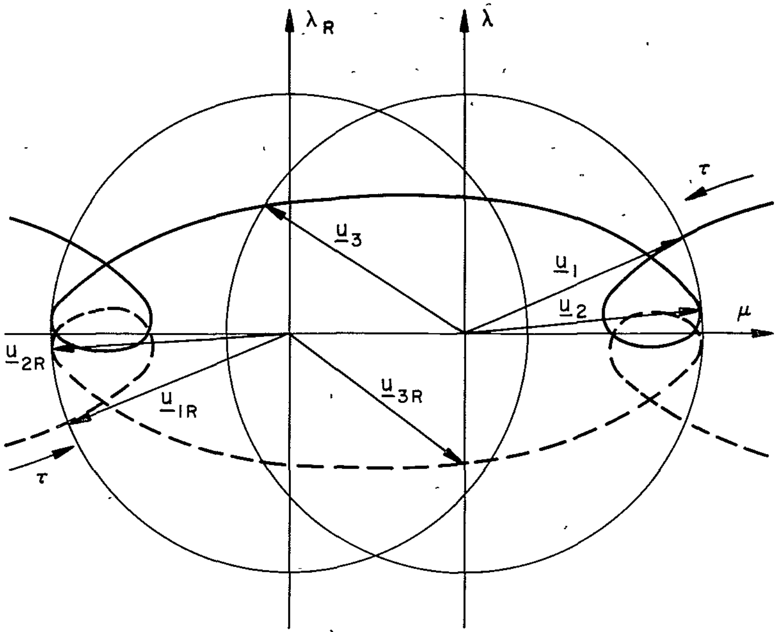

Fig. 4-7. Construction of reciprocal solution.

initial phase angle, β (Section B. 6), for the reciprocal solution is the negative of the original phase angle. The other type of solution is the dual solution shown in Fig. 4-9. The dual primer solution for a given number of impulses is the original solution run backwards in time. Since the primer vector satisfies a second order differential equation involving no first derivative terms (Eq. (2-15a)), a solution run backwards in time is also a solution.

This dual solution represents the rendezvous shown in Fig. 4-10, in which the sign of δR is reversed (since the final orbit of the original solution becomes the initial orbit of the dual solution). The value of $\delta\theta_F$ remains unchanged, due to the fact that the reference orbit is

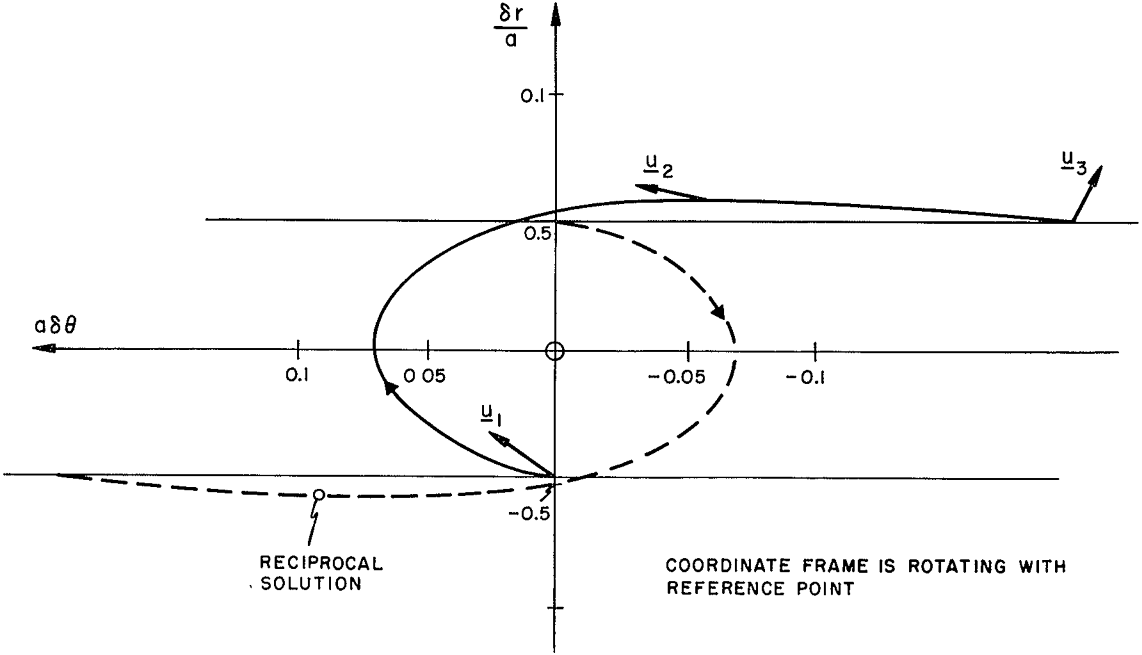

Fig. 4-8. Original solution and reciprocal solution (three-impulse).

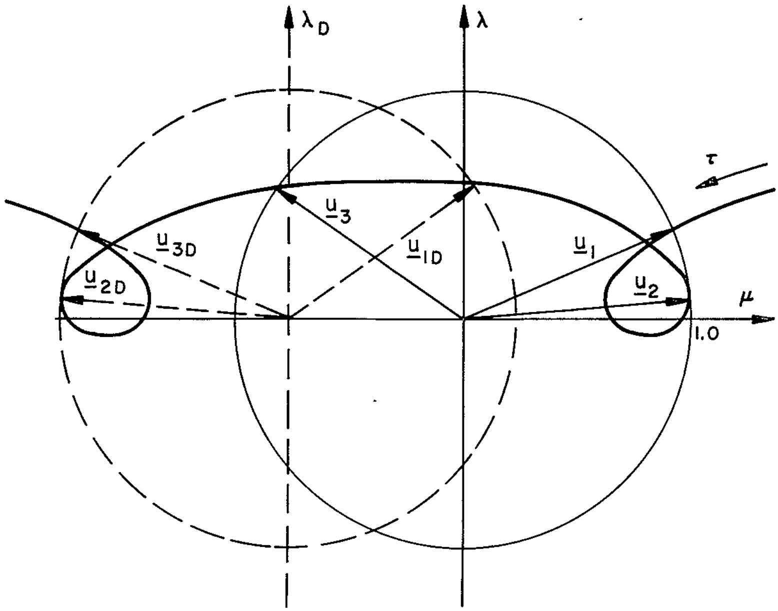

Fig. 4-9. Construction of dual primer solution (dotted solution is dual solution).

half-way between the terminals. The relationship of the impulse directions is shown in Fig. 4-9. The relationship between the velocity change magnitudes is treated in the sections discussing the solution to the boundary value problem.

The transfer time, t_F, and the cost of the two solutions is the same. The initial phase angle for the dual solution is related to the phase angle of the original solution by

$$\beta^D = \beta - \frac{3}{2}(\tau_F - \tau_0)\,\delta R$$

The dual solution also has a reciprocal solution, obtained by reversing the thrust directions. This results in a boundary value solution for which δR is unchanged, while $\delta\theta_F$ changes sign.

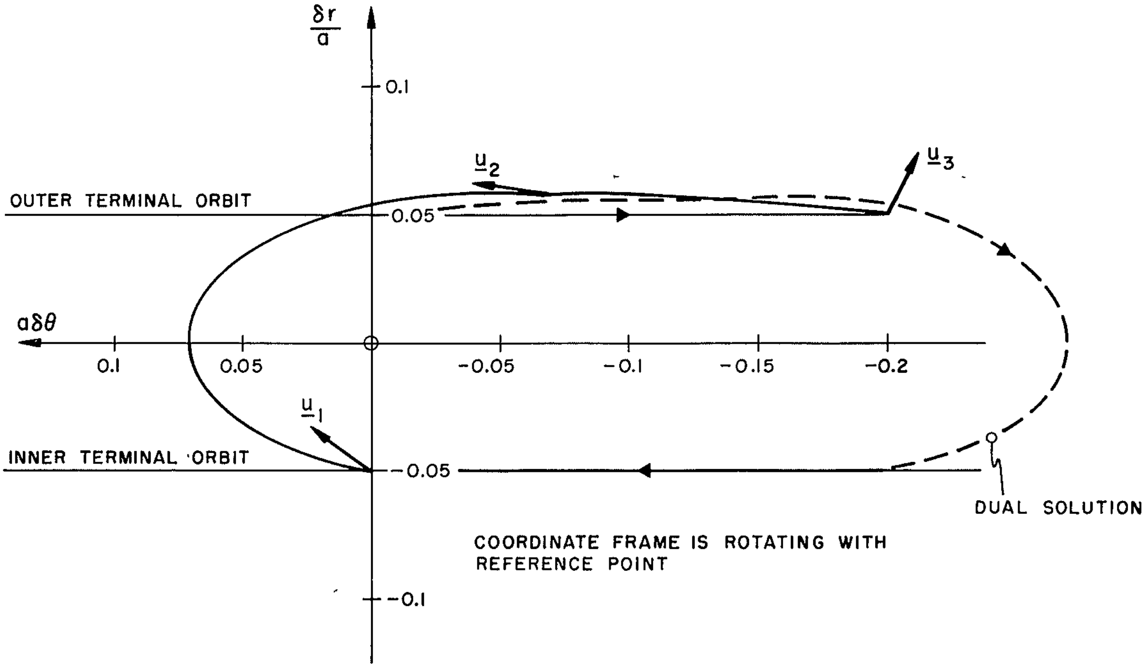

Fig. 4-10. Original solution and dual solution (three-impulse).

Thus a given primer vector solution satisfying the necessary conditions gives rise to four related but distinct boundary value problems, each of which requires the same number of impulses and the same cost.

CHAPTER 5

OPTIMAL FOUR-IMPULSE SOLUTIONS

5.1 Introduction

Optimal four-impulse transfers are of interest because they employ the maximum number of impulses necessary to realize minimum fuel solutions to the linearized, coplanar, time-fixed rendezvous problem. In this chapter primer vector solutions satisfying the necessary conditions for a four-impulse optimal transfer are described and the circle-to-circle, coplanar rendezvous trajectories which correspond to these solutions are obtained.

The four-impulse primer solutions obtained exist in families, characterized by the number of loops of the primer locus for which the magnitude of the primer vector is less than unity. One of these families for a circular orbit, as well as solutions for elliptical orbits, has been obtained previously by Winston.[24] Of the two families of solutions for a circular orbit obtained in this investigation, only one family provides optimal solutions to the circle-to-circle rendezvous problem. The specific types of optimal four-impulse transfers resulting from the other, shorter-transfer-time family remain an open area of investigation.

5.2 Four-Impulse Primer Vector Solutions

Figures 5-1 and 5-2 show primer vector solutions which satisfy the necessary conditions for a four-impulse optimal transfer. To obtain these minimizing solutions the center of the unit circle must lie at a point on the horizontal axis which is either in the center of a loop of the locus (Fig. 5-1) or midway between two loops (Fig. 5-2). This geometrical consideration results in the following symmetry properties of four-impulse optimal solutions:

1. The impulse times are symmetric about the time halfway through the transfer.

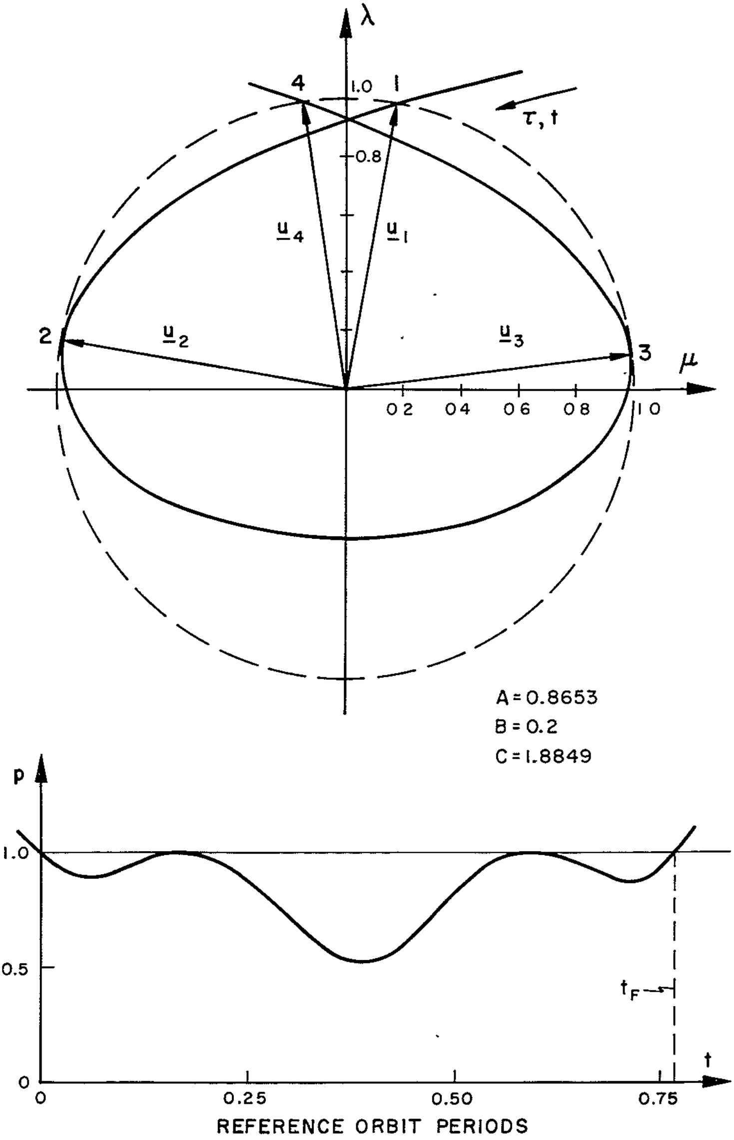

Fig. 5-1. "One-loop" four-impulse primer solution.

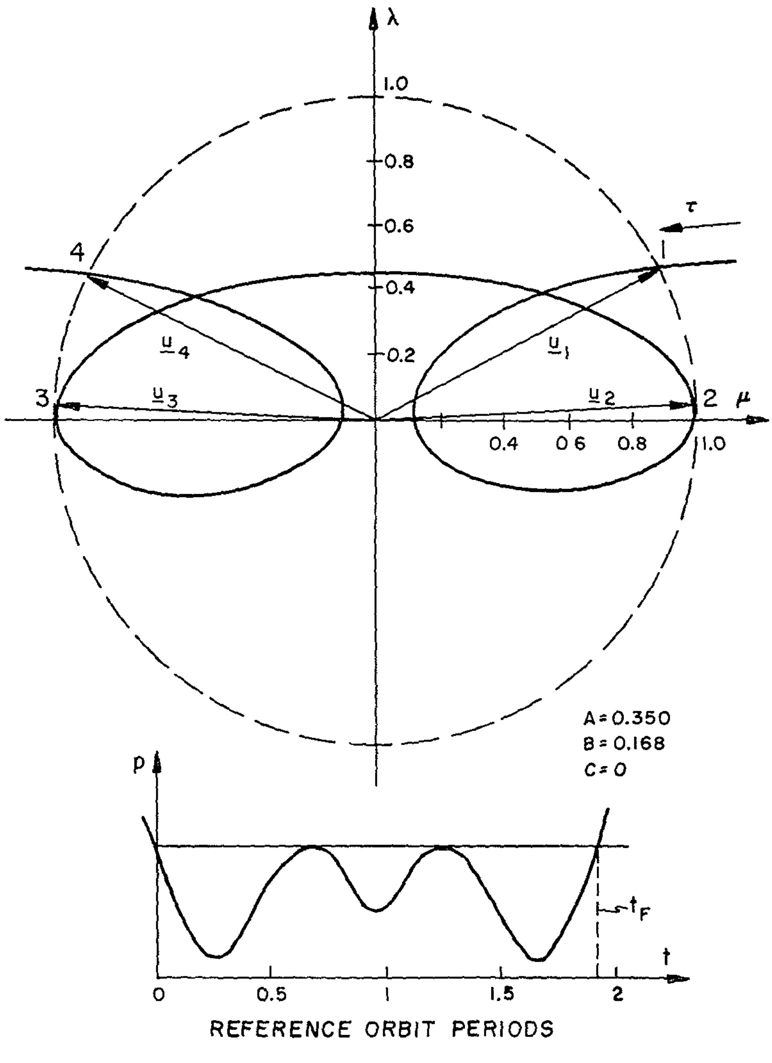

Fig. 5-2. "Two-loop" four-impulse primer solution.

2. The first and fourth impulse directions have equal radial components and tangential components which are the negative of each other.

3. The second and third impulse directions also satisfy the property (2).

Figure 5-3 shows the reciprocal solution (Section 4.5) to the solution of Fig. 5-2. From Fig. 5-2 it is evident that the dual primer solution (Section 4.5) is identical with the original solution.

Each family of primer solutions exists for a range of transfer times, t_F. (The final time, t_F, is the transfer time since the initial time is chosen to be $t = 0$). One-loop solutions exist for $0.46 \leq t_F \leq 1.5$ reference orbit periods. Two-loop solutions exist for $1 < t_F \leq 2.5$ reference periods.

For these solutions Fig. 5-4 displays the times of the second and third impulses for an optimal transfer. Figures 5-5 and 5-6 show the elevation angles for the impulse directions. The elevation angle is measured with respect to the positive μ-axis (local horizontal).

5.3 Coplanar Four-Impulse Boundary Value Solutions

The coplanar four-impulse boundary value problem for a rendezvous is represented by four equations in the four unknown velocity changes. From Section 3.4:

$$\delta \underline{\tilde{x}}_F = W \underline{\Delta V} \tag{5-1}$$

In order to use these symmetry properties of four-impulse solutions in solving Eq. (5-1), it is convenient to measure time from the half-transfer time, t_H:

$$t_H \triangleq \frac{t_F}{2} \tag{5-2}$$

Since

$$\delta \underline{x}_H = \Phi_{HF}\, \delta \underline{x}_F \tag{5-3}$$

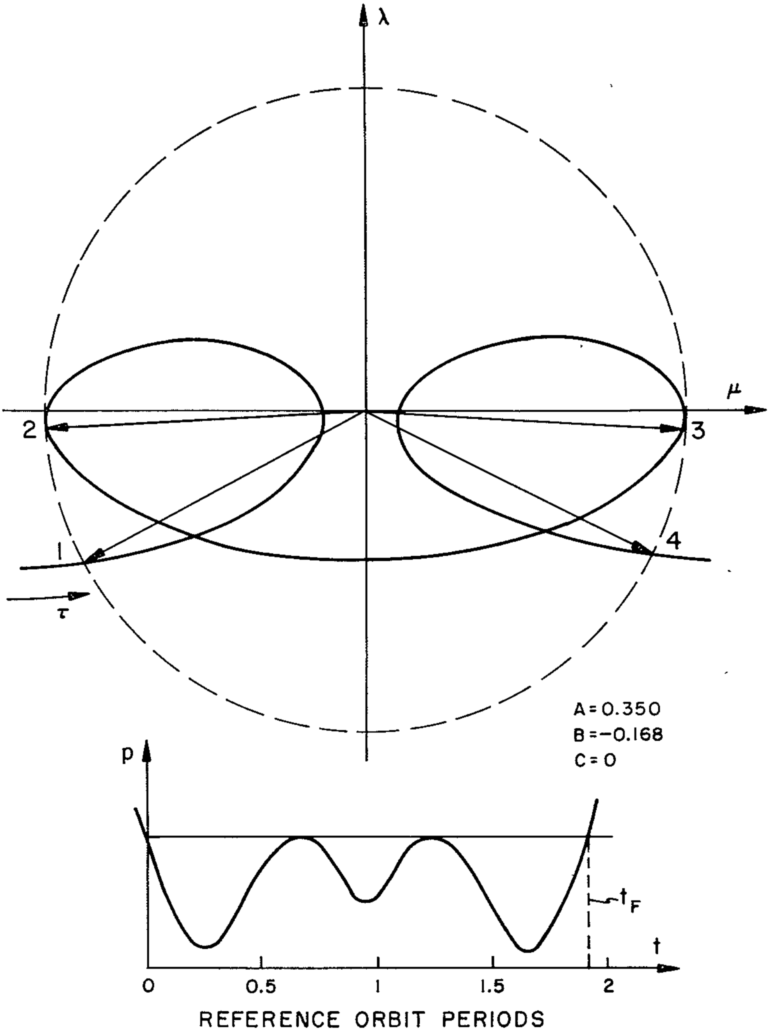

Fig. 5-3. Reciprocal primer vector solution to Fig. 5-2.

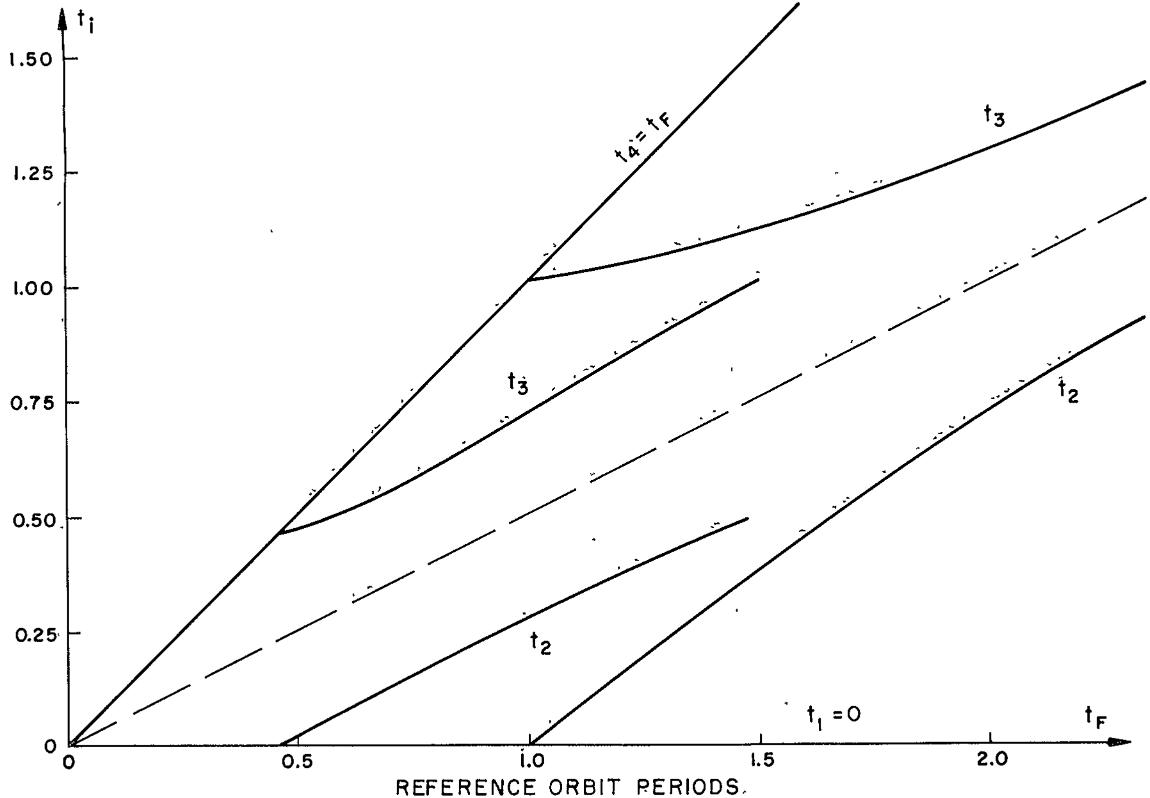

Fig. 5-4. Impulse times for two families of four-impulse solutions.

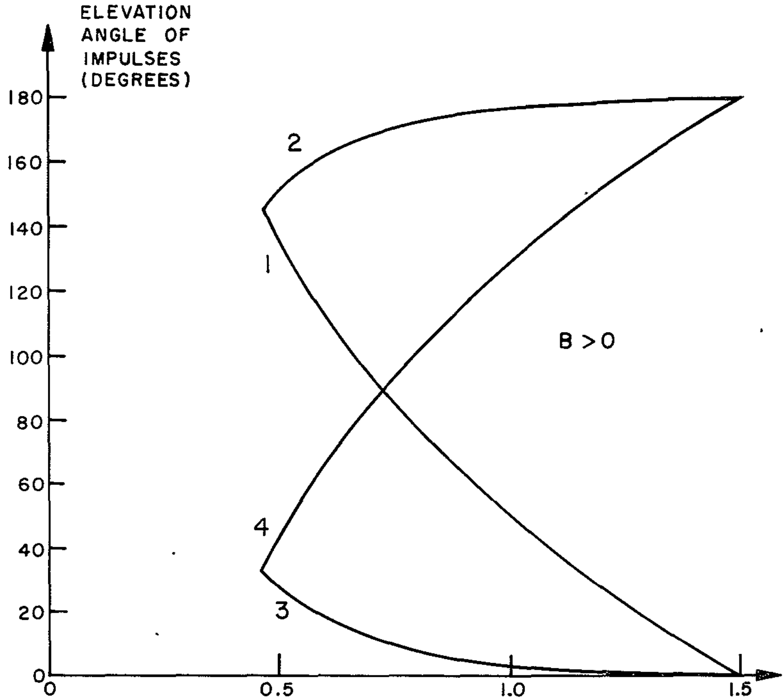

Fig. 5-5. Impulse elevation angle for one-loop solutions.

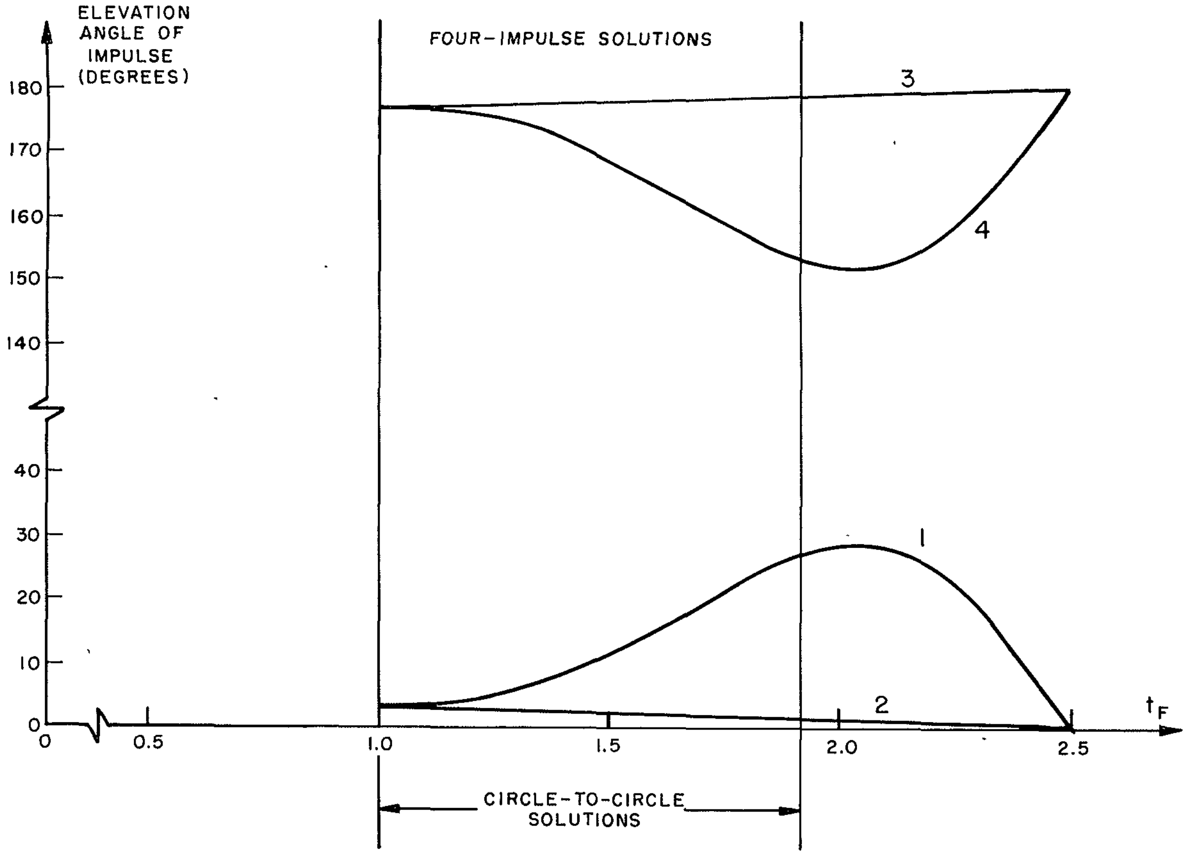

Fig. 5-6. Impulse elevation angle for two-loop solutions (B > 0).

Equation (5-1) can be rewritten as

$$\delta\underline{\tilde{x}}_H = H\,\underline{\Delta V} \tag{5-4}$$

where

$$\delta\underline{\tilde{x}}_H = \Phi_{HF}\,\delta\underline{\tilde{x}}_F = \delta\underline{x}_H - \Phi_{Ho}\,\delta\underline{x}_o \tag{5-5}$$

and

$$H = \Phi_{HF}\,W = [\underline{h}_1\;\underline{h}_2\;\underline{h}_3\;\underline{h}_4] \tag{5-6}$$

where

$$\underline{h}_j = B_{Hj}\,\underline{u}_j \qquad (j = 1,\ 2,\ 3,\ 4) \tag{5-7}$$

Note that $\delta\underline{x}_H$ is not the state variation of the vehicle at time t_H during the transfer. It is the final state variation, $\delta\underline{x}_F$ (which includes the effect of <u>all</u> the velocity changes made during the transfer), transformed back to the time t_H. Since, for a rendezvous, $\delta\underline{x}_F$ is also the state variation of the target at t_F, and since it is assumed that no velocity changes are made on the target, $\delta\underline{x}_H$ can be interpreted as the state variation of the target at time t_H.

Using the circular orbit state transition matrix of Appendix B, Eq. (5-7) can be written in component form:

$$\underline{h}_j = \begin{bmatrix} h_{1j} \\ h_{2j} \\ h_{3j} \\ h_{4j} \end{bmatrix} = \begin{bmatrix} \sin\alpha_j & 2(1 - \cos\alpha_j) \\ 2(\cos\alpha_j - 1) & 4\sin\alpha_j - 3\alpha_j \\ \cos\alpha_j & 2\sin\alpha_j \\ -2\sin\alpha_j & 4\cos\alpha_j - 3 \end{bmatrix} \begin{bmatrix} u_{jr} \\ u_{j\theta} \end{bmatrix} \tag{5-8}$$

where

$$\alpha_j \triangleq \tau_H - \tau_j = \omega(t_H - t_j) \tag{5-9}$$

The symmetry properties of the primer solution can be used to simplify H, since

$$\alpha_4 = -\alpha_1 \;;\; \alpha_3 = -\alpha_2 \tag{5-10}$$

$$\underline{u}_4 = \begin{bmatrix} u_{4r} \\ u_{4\theta} \end{bmatrix} = \begin{bmatrix} u_{1r} \\ -u_{1\theta} \end{bmatrix} \tag{5-11}$$

$$\underline{u}_3 \doteq \begin{bmatrix} u_{3r} \\ u_{3\theta} \end{bmatrix} = \begin{bmatrix} u_{2r} \\ -u_{2\theta} \end{bmatrix} \tag{5-12}$$

Since an element of B_{Hj} is either an even or odd function of α_j, these symmetry properties result in the following form for H:

$$H = \begin{bmatrix} h_{11} & h_{12} & -h_{12} & -h_{11} \\ h_{21} & h_{22} & h_{22} & h_{21} \\ h_{31} & h_{32} & h_{32} & h_{31} \\ h_{41} & h_{42} & -h_{42} & -h_{41} \end{bmatrix} \tag{5-13}$$

5.4 Circle-to-Circle Coplanar Solutions

As shown in Appendix B.6, for a circular reference trajectory lying half-way between the terminal orbits, the final state variation is

$$\delta \underline{x}_F = \begin{bmatrix} \delta R/2 \\ \delta\theta_F \\ 0 \\ -\frac{3}{4}\,\delta R \end{bmatrix} \tag{5-14}$$

where δR is the difference between the non-dimensional final and initial orbit radii.

Since $\tau_F - \tau_H = \tau_H - \tau_o$,

$$\delta \underline{\tilde{x}}_H = \begin{bmatrix} \delta R \\ \delta\theta_F \\ 0 \\ -\frac{3}{2}\,\delta R \end{bmatrix} = H\,\underline{\Delta V} \tag{5-15}$$

Using the form of H in Eq. (5-13), the solution for the magnitudes of the velocity changes is expedited by defining the following variables:

$$
\begin{aligned}
m &= h_{11}h_{42} - h_{12}h_{41} \\
k &= h_{22}h_{31} - h_{12}h_{32} \qquad (5\text{-}16) \\
q_j &= 2h_{4j} + 3h_{1j} \qquad (j = 1, 2)
\end{aligned}
$$

In terms of these variables

$$|H| = 4mk \qquad (5\text{-}17)$$

If H is non-singular, a unique solution for the velocity changes for an optimal rendezvous exists.[25] For circular terminal orbits, the solution is a function of two variables:

$$\underline{\Delta V} = \begin{bmatrix} \Delta V_1 \\ \Delta V_2 \\ \Delta V_3 \\ \Delta V_4 \end{bmatrix} = \frac{1}{4}\begin{bmatrix} q_2/m & -2\frac{h_{32}}{k} \\ -q_1/m & 2\frac{h_{31}}{k} \\ q_1/m & 2\frac{h_{31}}{k} \\ -q_2/m & -2\frac{h_{32}}{k} \end{bmatrix} \begin{bmatrix} \delta R \\ \delta\theta_F \end{bmatrix} \qquad (5\text{-}18)$$

In Figs. 5-7 and 5-8 it is shown that H is singular only at the maximum and minimum transfer times for a given family of primer vector solutions.

Note that in Eq. (5-18) for the special case $\delta R = 0$ (rendezvous with a target in the initial (reference) orbit):

$$
\begin{aligned}
\Delta V_1 &= \Delta V_4 \\
\Delta V_2 &= \Delta V_3
\end{aligned}
\qquad (5\text{-}19)
$$

The solution to the boundary value problem given by Eq. (5-18) results in admissible solutions only if

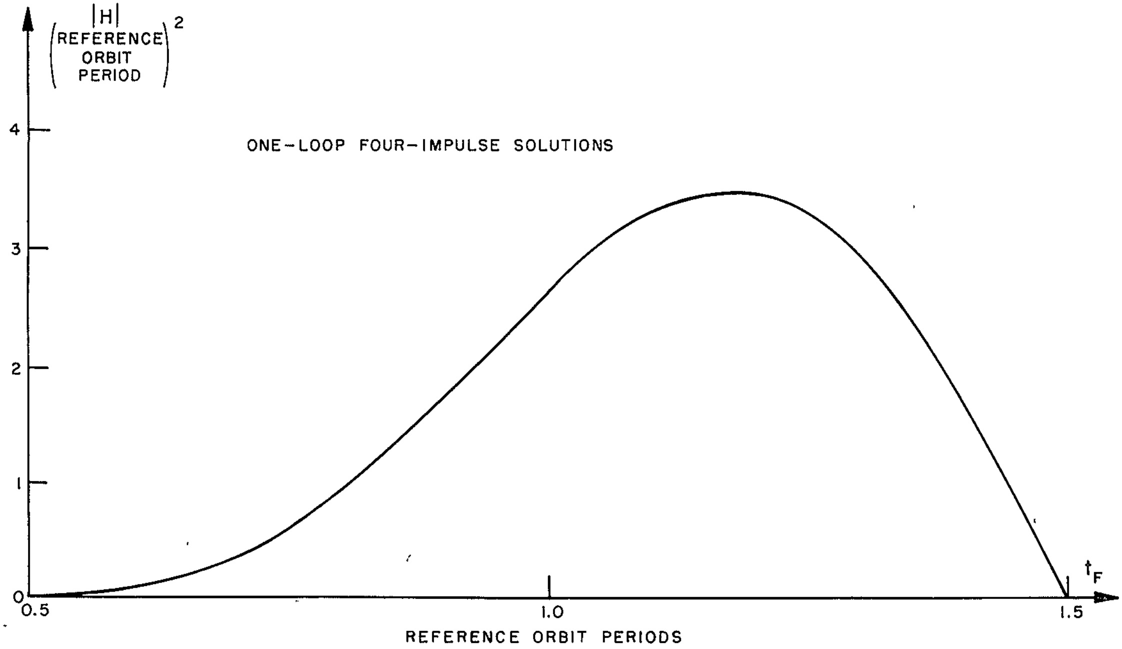

Fig. 5-7. Determinant of H matrix.

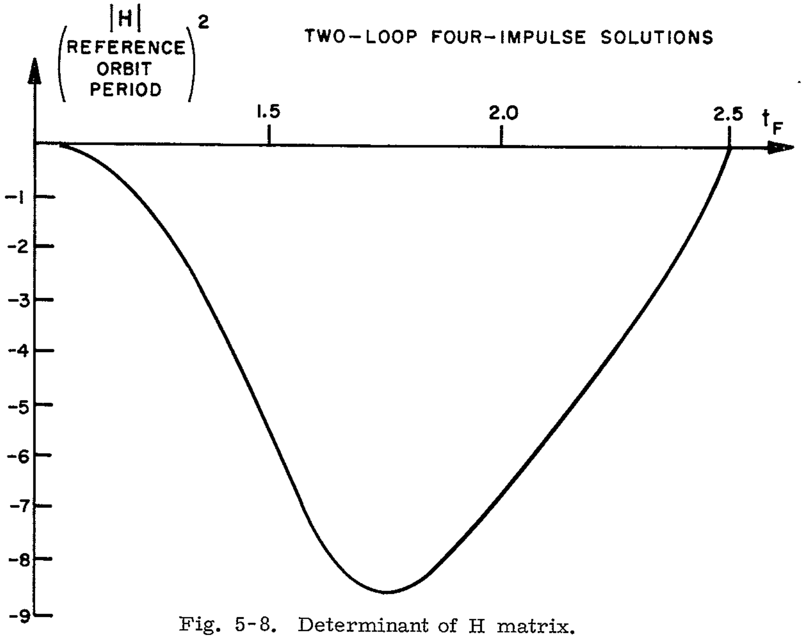

Fig. 5-8. Determinant of H matrix.

$$\Delta V_i \geq 0 \qquad i = 1, 2, 3, 4 \tag{5-20}$$

This constraint can be included without first solving the boundary value problem by considering the third row of the matrix Eq. (5-15):

$$0 = h_{31}\Delta V_1 + h_{32}\Delta V_2 + h_{32}\Delta V_3 + h_{31}\Delta V_4$$

For an admissible four-impulse solution in which the velocity changes are uniquely determined, it is necessary that

$$\frac{h_{31}}{h_{32}} < 0 \tag{5-21}$$

The specific primer vector solutions which result in admissible four-impulse solutions are the two-loop solutions as shown in Fig. 5-9.

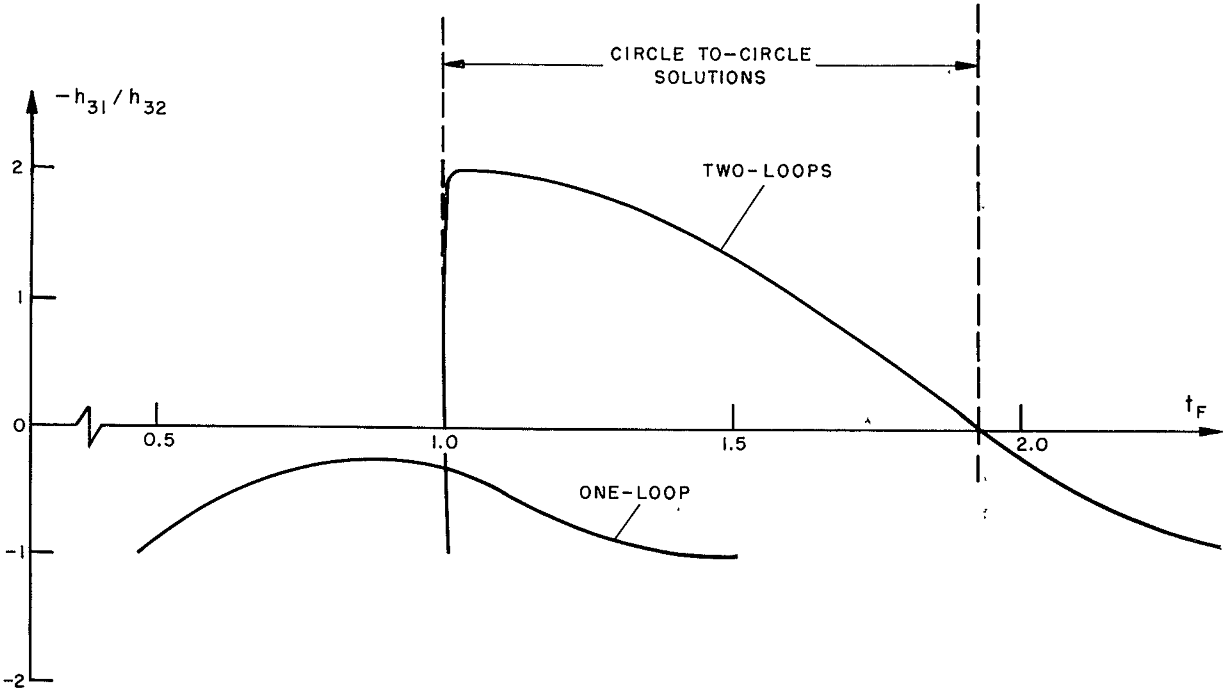

Fig. 5-9. Transfer times allowing circle-to-circle solutions (four-impulses).

The condition for admissible solutions restricts the set of reachable states, as shown by the example in Fig. 5-10. In this example $k/2m(q_1/h_{31})$ is the limiting value of $\delta\theta_F/\delta R$, but in other situations $k/2m(q_2/h_{32})$ may be the limiting value. In Fig. 5-10 the reachable final states are those for which

$$\delta\theta_F \geq \frac{k}{2m}\left(\frac{q_1}{h_{31}}\right)\delta R \qquad (\delta R > 0)$$

$$\delta\theta_F \geq -\frac{k}{2m}\left(\frac{q_1}{h_{31}}\right)\delta R \qquad (\delta R < 0) \tag{5-22}$$

The cost for these admissible solutions is given by

$$J = \sum_{i=1}^{4} \Delta V_i \tag{5-23}$$

Substituting ΔV_i from Eq. (5-18)

$$J = \left(\frac{h_{31} - h_{32}}{k}\right)\delta\theta_F \tag{5-24}$$

or, explicitly in terms of the initial phase angle of the target, β (Appendix B.6):

$$J = \left(\frac{h_{31} - h_{32}}{k}\right)\left(\beta - \frac{3}{4}(\tau_F - \tau_o)\,\delta R\right) \tag{5-25}$$

The set of reachable states using the reciprocal solution of the primer vector equation is obtained by noting that since the thrust direction unit vectors change sign, the H matrix changes sign. Figure 5-11 shows the restricted final state variations for the same example as Fig. 5-10. For the same $\underline{\Delta V}$, the initial and final state variations using the reciprocal primer solution are the negatives of those using the original primer solution.

Figure 5-12 displays the reachable states as a function of transfer time. Due to symmetry $|\delta\theta_F/\delta R|$ is plotted in the upper-half plane. The dotted lines represent boundaries for the four-impulse solutions

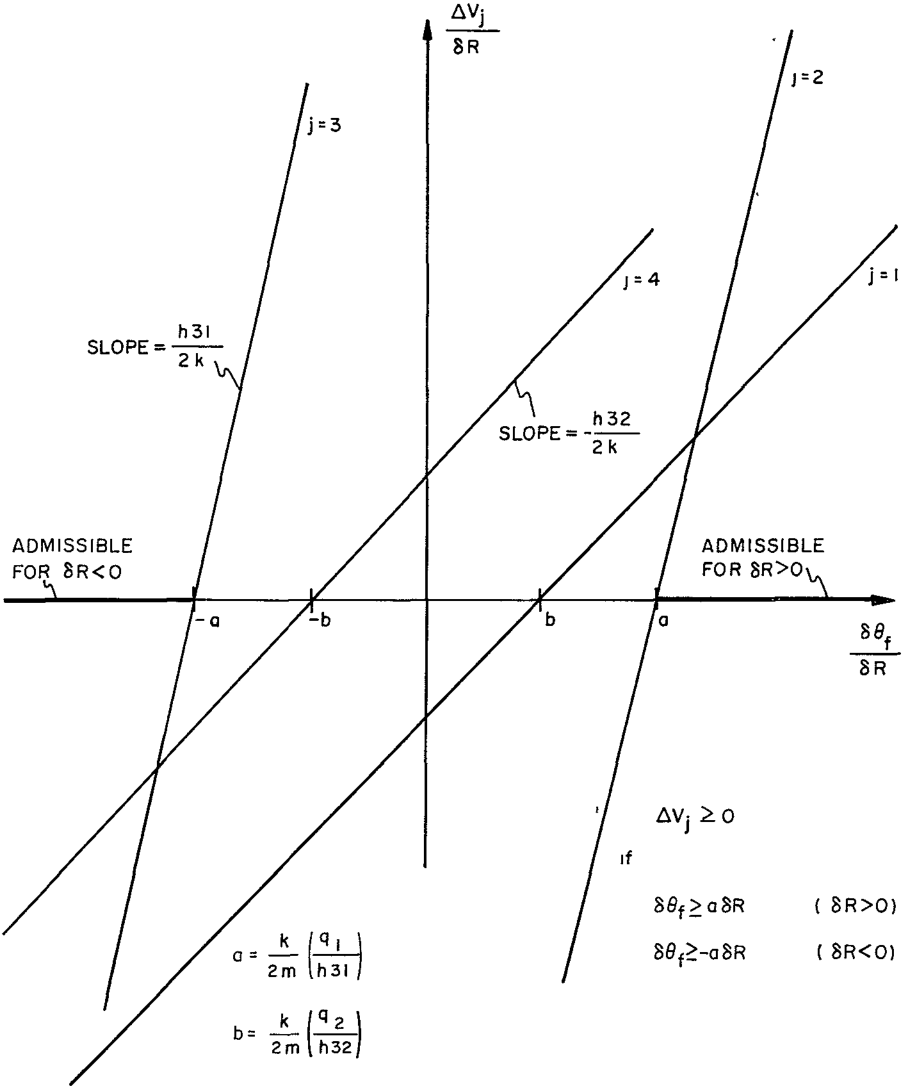

Fig. 5-10. Admissible solutions.

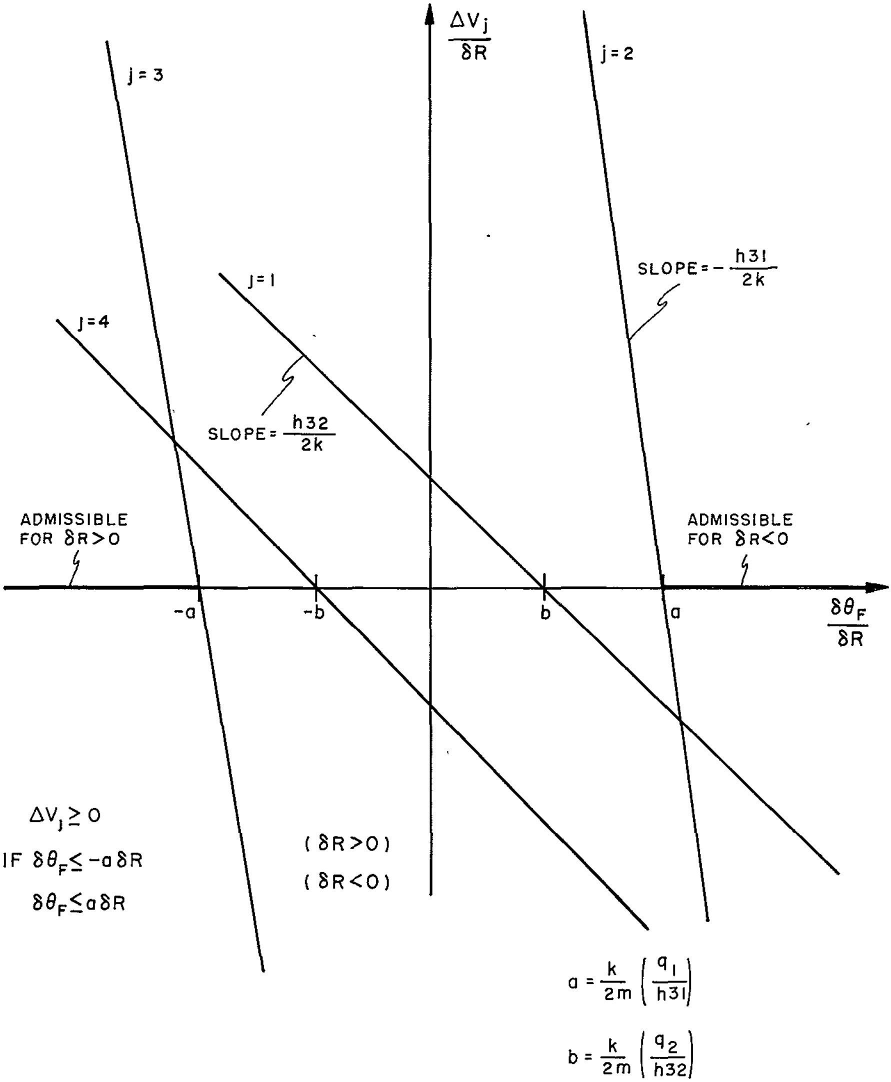

Fig. 5-11. Admissible reciprocal solutions.

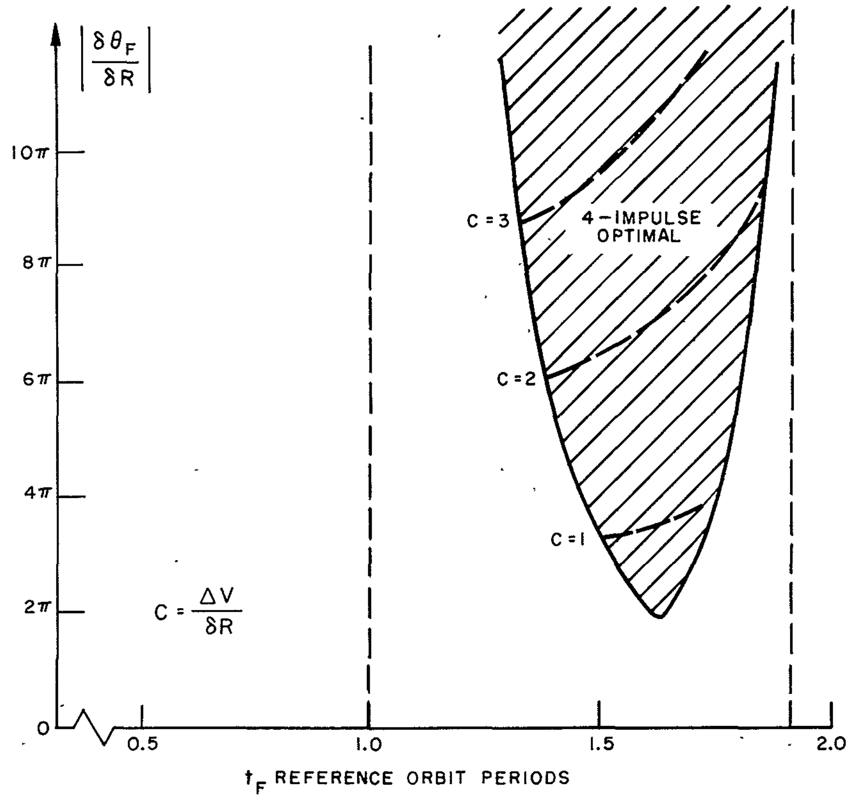

Fig. 5-12. Reachable final state variations for optimal four-impulse rendezvous.

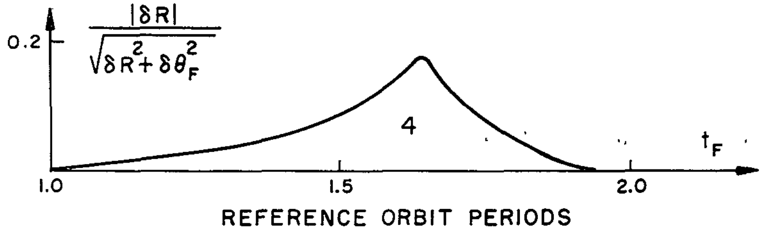

Fig. 5-13. Alternative display of Fig. 5-12.

(attainable when $\delta R = 0$). An alternative display is given by Fig. 5-13, in which, through a change of variable, the same information is plotted in a finite portion of a plane.

5.5 Solutions with Terminal Coasts

Aside from the non-unique solutions discussed in Chapter 8, the primer locus shape which allows initial or final coasting periods for four-impulses is the locus for which $B = 0$ (see Fig. 2-1). In this case the primer vector magnitude is periodic, as shown in Fig. 5-14. However, the admissibility condition (Eq. (5-21)) is violated for this case and no circle-to-circle solutions exist. As discussed in Chapters 6 and 7, optimal coast solutions for three- and two-impulse transfers do exist for the circle-to-circle case.

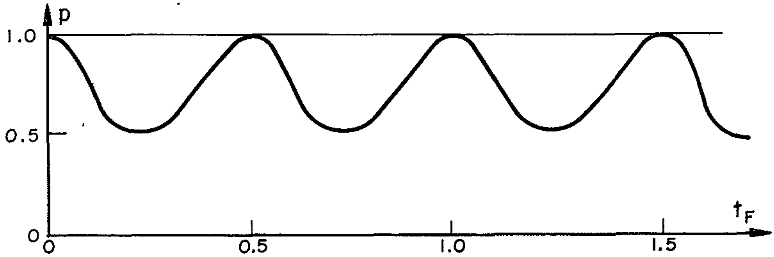

Fig. 5-14. Primer magnitude for $B = 0$ ($A = 0.5$, $C = 0$).

CHAPTER 6

OPTIMAL THREE-IMPULSE SOLUTIONS

6.1 Three-Impulse Primer Vector Solutions

As shown by previous examples of three-impulse primer vector solutions which satisfy the necessary conditions, e.g. Fig. 4-9, the symmetry of impulse times and directions which exists in the four-impulse case is lacking in the three-impulse case. For this reason the method of constructing three-impulse primer solutions is slightly different and is discussed in Appendix A.4.

6.2 Coplanar Three-Impulse Boundary Value Solutions

For the coplanar three-impulse problem the boundary value problem is represented by four equations in three unkonwn velocity changes:

$$\delta \underline{\tilde{x}}_F = W \, \underline{\Delta V} \tag{6-1}$$

where

$$W = [\underline{w}_1 \ \ \underline{w}_2 \ \ \underline{w}_3] \ (4 \times 3) \tag{6-2}$$

and

$$\underline{\Delta V} = \begin{bmatrix} \Delta V_1 \\ \Delta V_2 \\ \Delta V_3 \end{bmatrix} \tag{6-3}$$

A unique solution to Eq. (6-1) exists only if the columns of W are linearly independent. The boundary conditions for which a unique solution exists are those for which the augmented matrix, formed by adjoining the column $\delta \underline{\tilde{x}}_F$ to the columns of W, has rank three. For the three-impulse case this requires that the augmented matrix (4 X 4) be singular:

$$\left| \delta \underline{\tilde{x}}_F \ \ \underline{w}_1 \ \ \underline{w}_2 \ \ \underline{w}_3 \right| = 0 \tag{6-4}$$

6.3 Solutions with Terminal Coasts

In Section 4.4 the situation in which an optimal fixed-time rendezvous requires an initial or final coasting period is discussed. In order to satisfy the necessary conditions for an optimal transfer, the primer vector magnitude must not exceed unity during the coasting period. As an example, Fig. 6-1 shows a primer magnitude time history for an optimal three-impulse rendezvous with a final coast. The fixed transfer time is $\tau_F - \tau_o$. ($\tau_o = \tau_1$ since the initial time and the time of the first impulse are the same.) The duration of the final coast is $\tau_F - \tau_3$.

The dotted continuation of the primer magnitude for $\tau > \tau_F$ demonstrates that this three-impulse solution with a final coast is actually a portion of an optimal four-impulse primer vector solution. Since the rendezvous occurs using three impulses, this consideration of a four-impulse solution is tantamount to interpreting the optimal three-impulse solution with a final coast as an optimal four-impulse solution for which the fourth impulse has zero magnitude. An initial coast can be treated in an analogous manner, as shown by Fig. 6-2.

Based on these considerations, the primer vector solutions for optimal three-impulse rendezvous with terminal coast can be generated

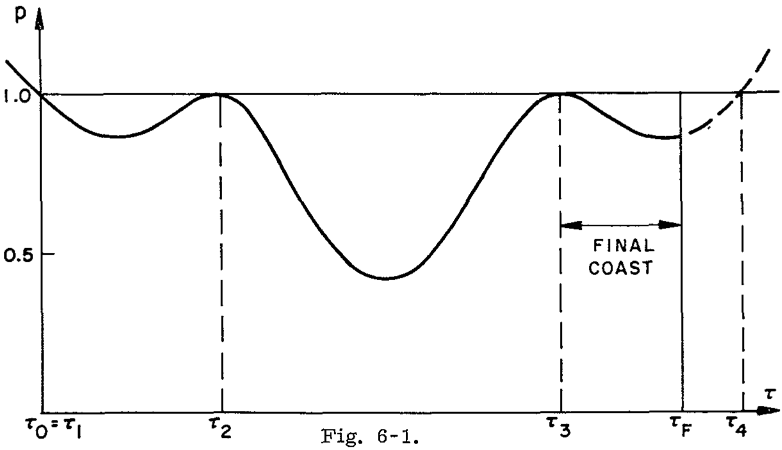

Fig. 6-1.

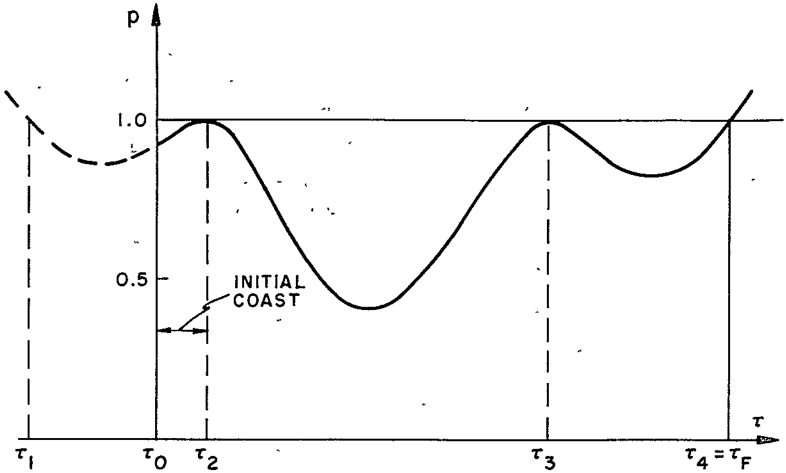

Fig. 6-2.

directly from the four-impulse solutions of Chapter 5. The final coast system of Fig. 6-1 is valid for all fixed transfer times $\tau_F - \tau_o$ for which $\tau_3 \leq \tau_F \leq \tau_4$. The initial coast solution of Fig. 6-2 is valid for all $\tau_F - \tau_o$ for which $\tau_1 \leq \tau_o \leq \tau_2$.

The boundary conditions satisfied by the three-impulse with terminal coast solutions differ from those satisfied by the corresponding four-impulse solution. The boundary conditions for three-impulses are determined by Eq. (6-4).

6.4 Circle-to-Circle, Coplanar Solutions with Terminal Coasts

To make use of the four-impulse primer vector solutions of Section 5.5, it is convenient to define

$$H = \Phi_{HF} W \tag{6-5}$$

where H is (4 X 3) and τ_H is the half-transfer time of the four-impulse solution. Then, by analogy with Eq. (5-15), the boundary value equation for three impulses is.

$$\delta \underline{\tilde{x}}_H = H \, \underline{\Delta \dot{V}} \tag{6-6}$$

where

$$\delta \underline{x}_H = \begin{bmatrix} \delta R \\ \delta\theta_F \\ 0 \\ -\frac{3}{2}\,\delta R \end{bmatrix} \tag{6-7}$$

To distinguish between initial and final coasts, define:

$$H^I \triangleq \Phi_{HF}\, W^I \tag{6-8}$$

and

$$H^F \triangleq \Phi_{HF}\, W^F \tag{6-9}$$

where

$$W^I = [\underline{w}_2 \;\; \underline{w}_3 \;\; \underline{w}_4] \tag{6-10}$$

and

$$W^F = [\underline{w}_1 \;\; \underline{w}_2 \;\; \underline{w}_3] \tag{6-11}$$

The $\underline{w}_i$ are those determined by the four-impulse primer solution.

Since Φ_{HF} is nonsingular, it can be shown by Sylvester's Law (Appendix C) that the rank of H is equal to the rank of W, which is three if the $\underline{w}_i$ are linearly independent. Therefore the condition for the existence of a unique three-impulse solution, $\underline{\Delta V}$, is:

For initial coast:

$$\left| \delta\tilde{\underline{x}}_H \;\; \underline{h}_2 \;\; \underline{h}_3 \;\; \underline{h}_4 \right| = 0 \tag{6-12}$$

For final coast:

$$\left| \delta\tilde{\underline{x}}_H \;\; \underline{h}_1 \;\; \underline{h}_2 \;\; \underline{h}_3 \right| = 0 \tag{6-13}$$

Substituting Eq. (6-7) for $\delta\tilde{\underline{x}}_H$ and the appropriate columns from Eq. (5-8), one obtains (since $\tau_F = \tau_4$ for four-impulse case)

For initial coast:

$$\delta\theta_4 = \frac{q_2 k}{2 h_{32} m}\, \delta R \tag{6-14}$$

For final coast:

$$\delta\theta_4 = -\frac{q_2 k}{2h_{32} m}\,\delta R \tag{6-15}$$

As one would expect, by comparison with the boundary value solution, Eq. (5-18), Eq. (6-14) is the condition $\Delta V_1 = 0$ and Eq. (6-15) is the condition $\Delta V_4 = 0$.

Unlike the four-impulse solution, Eqs. (6-14) and (6-15) show that $\delta\theta_F$ and δR for a unique three-impulse solution must be linearly related.

The velocity changes necessary to perform the rendezvous are (using notation of Eq. (5-16)):

For initial coast:

$$\Delta V_2^I = \frac{\delta R}{4m}\left(q_2 \frac{h_{31}}{h_{32}} - q_1\right) \tag{6-16}$$

$$\Delta V_3^I = \frac{\delta R}{4m}\left(q_2 \frac{h_{31}}{h_{32}} + q_1\right) \tag{6-17}$$

$$\Delta V_4^I = -\frac{q_2}{2m}\,\delta R \tag{6-18}$$

The cost,

$$J^I = \frac{q_2}{2m}\left(\frac{h_{31}}{h_{32}} - 1\right)\delta R \tag{6-19}$$

For final coast:

$$\Delta V_1^F = \frac{q_2}{2m}\,\delta R \tag{6-20}$$

$$\Delta V_2^F = \frac{\delta R}{4m}\left(-q_2 \frac{h_{31}}{h_{32}} - q_1\right) \tag{6-21}$$

$$\Delta V_3^F = \frac{\delta R}{4m}\left(-q_2 \frac{h_{31}}{h_{32}} + q_1\right) \tag{6-22}$$

$$J^F = \frac{q_2}{2m}\left(1 - \frac{h_{31}}{h_{32}}\right)\delta R$$

If the solution obtained is an initial coast, the dual solution (Section 4.4) represents a final coast, since the dual solution is the original solution run backwards in time. This is shown by the relationship of the velocity change magnitudes:

For the same value of δR:

$$\Delta V_1^F = -\Delta V_4^I \tag{6-23}$$

$$\Delta V_2^F = -\Delta V_3^I \tag{6-24}$$

$$\Delta V_3^F = -\Delta V_2^I \tag{6-25}$$

$$J^F = -J^I$$

for both the final coast and initial coast solutions.

To satisfy the admissibility condition, $\Delta V_i \geq 0$, an admissible solution and the reciprocal of the dual solution must be used. Use of the reciprocal solution is equivalent to reversing the sign of δR by reversing the sign of the ΔV_i.

The conditions that a coasting three-impulse solution is admissible differ slightly from the four-impulse conditions. For an admissible three-impulse solution:

1. $$\frac{h_{31}}{h_{32}} < 0 \tag{6-27}$$

and

2. $$\left|\frac{q_2}{h_{32}}\right| > \left|\frac{q_1}{h_{31}}\right| \tag{6-28}$$

Condition (1) is the same as the four-impulse solution and will be satisfied if only admissible four-impulse solutions are used to generate three-impulse solutions. Condition (2) is evident from Fig. 5-10. The critical value of $\delta\theta_F / \delta R$ for the four-impulse solution must be the value for which ΔV_1 (ΔV_4 for the dual solution) vanishes to allow an initial (or final) coast.

For the coplanar circle-to-circle case, conditions (1) and (2) are satisfied along the lower-transfer-time boundary of the four-impulse region (Fig. 6-3). This indicates that three-impulse coasting solutions lie to the left of this boundary. These are shown in Fig. 6-3; the 3^+ notation indicates three impulses plus a coast period. Along the higher-transfer-time boundary of the four-impulse region of Fig. 6-3 condition (2) is violated. This means that ΔV_2 (or ΔV_3) vanishes along this

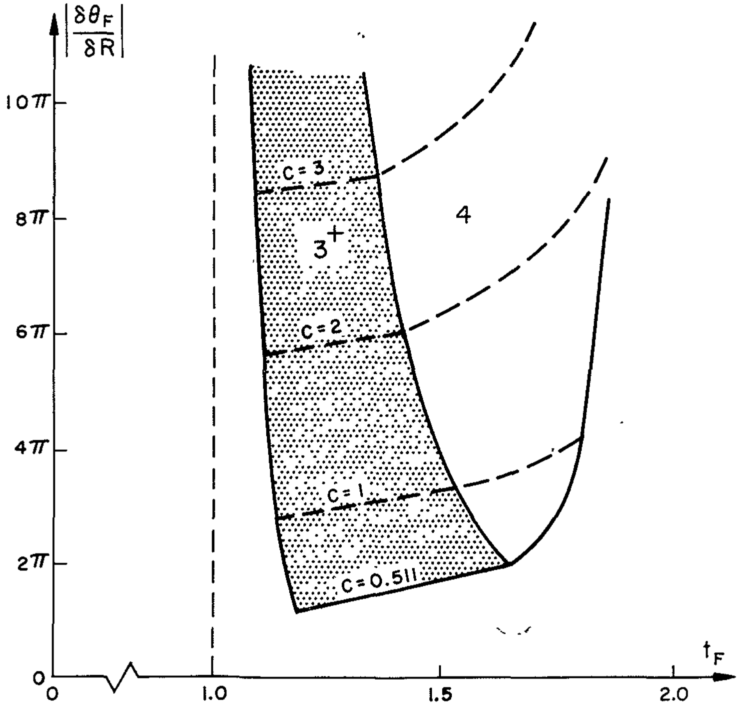

Fig. 6-3. Final state variations reached optimally by four and three-plus-coast solutions $C = \frac{\Delta V}{\delta R}$.

boundary and three-impulse transfers with no terminal coasts lie to the right of the boundary.

At the point on the four-impulse boundary for which $\delta\theta_F / \delta R$ is a minimum in Fig. 6-3:

$$\frac{q_2}{h_{32}} = \frac{q_1}{h_{31}} \qquad (6\text{-}29)$$

so that $\Delta V_1 = \Delta V_2 = 0$ ($\Delta V_3 = \Delta V_4 = 0$ for the dual solution). This indicates that this point borders on a region of two-impulse with terminal coast.

In Fig. 6-3 the reachable final state variations using three-impulses plus a terminal coast (3^+) are shown. The lower-transfer-time boundary of the 3^+ region is the same as the boundary for the four-impulse region because both sets of solutions are obtained from the same primer vector solutions.

The lines of constant cost per radius change are straight in the 3^+ region. Their slope reflects the rate at which the value of $\delta\theta_F$ changes due to a terminal coast. For a final coast $\tau_3 \leq \tau_F \leq \tau_4$ (see Fig. 6-1):

$$\frac{\delta\theta_F}{\delta R} = \frac{\delta\theta_3}{\delta R} - \frac{3}{4}(\tau_F - \tau_3)$$

since the final coast is of duration $\tau_F - \tau_3$ and

$$\delta\dot{\theta} = -\frac{3}{4}\,\delta R$$

for the final circular orbit (Appendix B).

Likewise, for an initial coast $\tau_1 \leq \tau_o \leq \tau_2$ (Fig. 6-2);

$$\frac{\delta\theta_F}{\delta R} = \frac{\delta\theta_3}{\delta R} + \frac{3}{4}(\tau_2 - \tau_o)$$

since

$$\delta\dot{\theta} = \frac{3}{4}\,\delta R$$

for a coast in the initial orbit and $\tau_4 - \tau_3 = \tau_2 - \tau_1$ by symmetry.

In Fig. 6-3 the cost per radius change is constant along these coasting lines since the cost of the three-impulse transfer is not changed due to the terminal coast. As before, only the magnitude of $\delta\theta_F / \delta R$ is plotted due to the symmetry of the plot. The important point is that during a final coast $\delta\theta_F / \delta R$ decreases; during an initial coast it increases. The magnitudes of the rates of change are the same because the reference orbit lies half-way in between the terminal orbits.

6.5 Circle-to-Circle Coplanar Solutions with No Terminal Coasts

The three-impulse boundary value problem is represented by Eq. (6-1):

$$\delta\underline{\tilde{x}}_F = W\,\underline{\Delta V} \tag{6-1}$$

since

$$\delta\underline{x}_F = \begin{bmatrix} \delta R/2 \\ \delta\theta_F \\ 0 \\ -\frac{3}{4}\,\delta R \end{bmatrix} \tag{6-30}$$

$$\delta\underline{\tilde{x}}_F = \delta\underline{x}_F - \Phi_{Fo}\,\delta\underline{x}_o = \begin{bmatrix} \delta R \\ \delta\tilde{\theta}_F \\ 0 \\ -\frac{3}{2}\,\delta R \end{bmatrix} \tag{6-31}$$

where

$$\delta\tilde{\theta}_F = \delta\theta_F - \frac{3}{4}(\tau_F - \tau_o)\,\delta R \tag{6-32}$$

Since there are no terminal coasts $\tau_F = \tau_3$, and $\tau_o = \tau_1$. In this case the vector $\underline{w}_3$ is given by

$$\underline{w}_3 = \begin{bmatrix} \underline{0} \\ \underline{u}_3 \end{bmatrix} = \begin{bmatrix} 0 \\ 0 \\ u_{3r} \\ u_{3\theta} \end{bmatrix} \tag{6-33}$$

The boundary conditions for which a unique solution for $\underline{\Delta V}$ exists are given by Eq. (6-4). Evaluating the determinant for $\delta\underline{\tilde{x}}_F$ and $\underline{w}_3$ given above:

$$\frac{\delta \tilde{\theta}_F}{\delta R} = \frac{u_{3r}(2k_4 + 3m_2) - 2k_3 u_{3\theta}}{2(m_3 u_{3\theta} - m_4 u_{3r})} \triangleq g_p \tag{6-34}$$

where, by analogy with the definition of k and m for the four-impulse solution (Eq. (5-16)):

$$m_j = w_{11} w_{j2} - w_{12} w_{j1} \tag{6-35}$$

$$k_j = w_{22} w_{j1} - w_{21} w_{j2} \tag{6-36}$$

To obtain a unique solution the columns of W (4×3) must be linearly independent. If this is true at least one (3×3) submatrix of W must be nonsingular. Assuming it is the submatrix formed by the first three rows;

$$u_{3r} m_2 \neq 0 \tag{6-37}$$

Eq. (6-37) was found to be satisfied for all the three-impulse transfers examined. If Eq. (6-37) is satisfied, the solution to Eq. (6-1) can be written as:

$$\Delta V_1 = \left(\frac{w_{22} - g_p w_{12}}{m_2} \right) \delta R \tag{6-38}$$

$$\Delta V_2 = \left(\frac{w_{11} g_p - w_{21}}{m_2} \right) \delta R \tag{6-39}$$

$$\Delta V_3 = - \frac{\delta R}{u_{3r} m_2} \left(m_3 g_p + k_3 \right) \tag{6-40}$$

Since $\delta\theta_F$ and δR are proportional to one another, the solution for the velocity changes is written in terms of the one independent state variable, δR.

As before, the admissibility condition is $\Delta V_i \geq 0$. This condition is quite restrictive in comparison with the four-impulse case. In the four-impulse solution (Eq. (5-18)) $\delta\theta_F$ and δR could be specified independently for a given transfer time. Thus solutions existed along vertical lines in the plane of reachable states (Fig. 6-3). The admissibility condition restricted the solutions to lie along certain segments of the lines.

However, in the three-impulse case $\delta\theta_F$ is proportional to δR for a given transfer time. This corresponds to a point in the plan of reachable states rather than a line. The admissibility conditions determine whether or not this point is admissible; no range of values is allowed. This restriction, however, tends to be outweighed by the fact that there are many more three-impulse primer solutions which satisfy the necessary conditions than there are four-impulse solutions for a given range of transfer times. This results in the large part of the plane of reachable states occupied by admissible three-impulse solutions (Fig. 6-4). Figure 6-5 shows the regions of three-impulse transfers in a finite-plane representation.

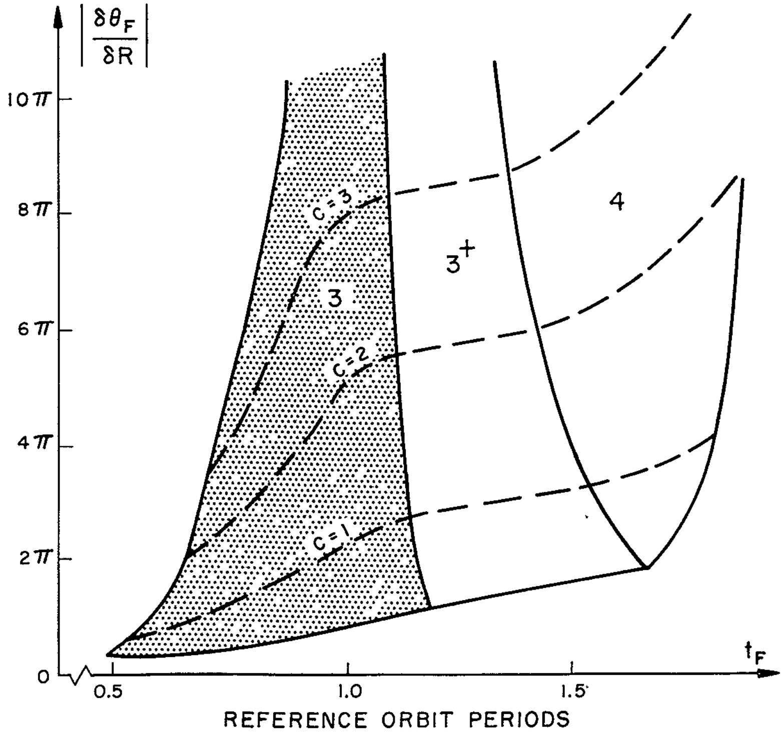

Fig. 6-4. Final state variations reached optimally by three- and four-impulse solutions.

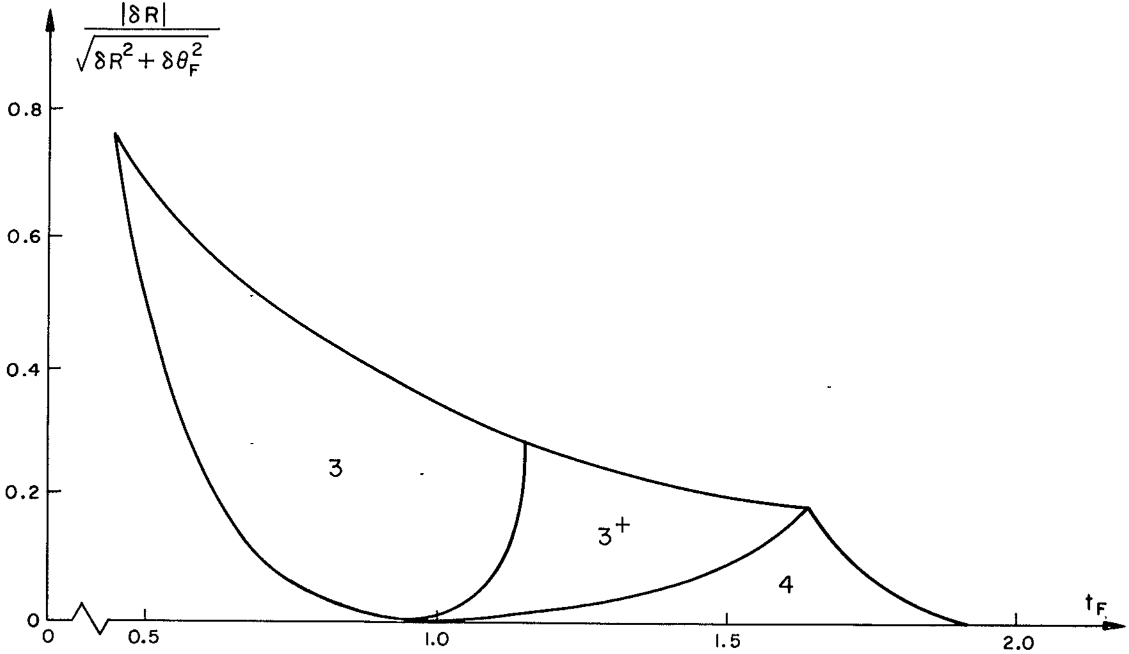

Fig. 6-5. Alternative display of three-impulse solutions.

6.6 Characteristics of an Example Set of Three-Impulse Optimal Solutions

Because of the great number of three-impulse solutions, only the characteristics of an example set of solutions are given in this section. These examples are three-impulse optimal solutions constructed from the primer vector locus having a value B = 0.35. Appendix A.4 discusses the method of obtaining solutions from the locus diagram.

The transfer times which yield circle-to-circle solutions for this locus are $0.645 \leq t_F \leq 0.911$ reference orbit periods. Figure 6-6 shows the time of the midcourse impulse for these solutions. The fact that the time of the second impulse is essentially constant is not in itself significant, but due primarily to the fact that the same locus shape is being used.

The sizes of the velocity changes and the ratio $\delta\theta_F / \delta R$ are shown in Fig. 6-7. As seen in this figure, the lower boundary of this set of solutions is determined by the admissibility condition, since C_2 is negative for $t < 0.645$. The upper boundary, $t_F = 0.911$, is due to the fact that the magnitude of $\delta\theta_F / \delta R$ becomes infinite. This requires that δR be zero. As seen in Fig. 6-5, no three-impulse solutions are optimal for $\delta R = 0$ for the transfer times considered.

Figure 6-8 shows the elevation angles of the impulses (measured with respect to the local horizontal, as in Chapter 5). The impulse directions become quite highly inclined to the local horizontal near the lower boundary of the transfer times. At the lower boundary the third impulse is directed along the local vertical.

In Chapter 9 an example three-impulse transfer is shown and the percentage saving of optimal three-impulse transfers over two-impulse transfers is discussed.

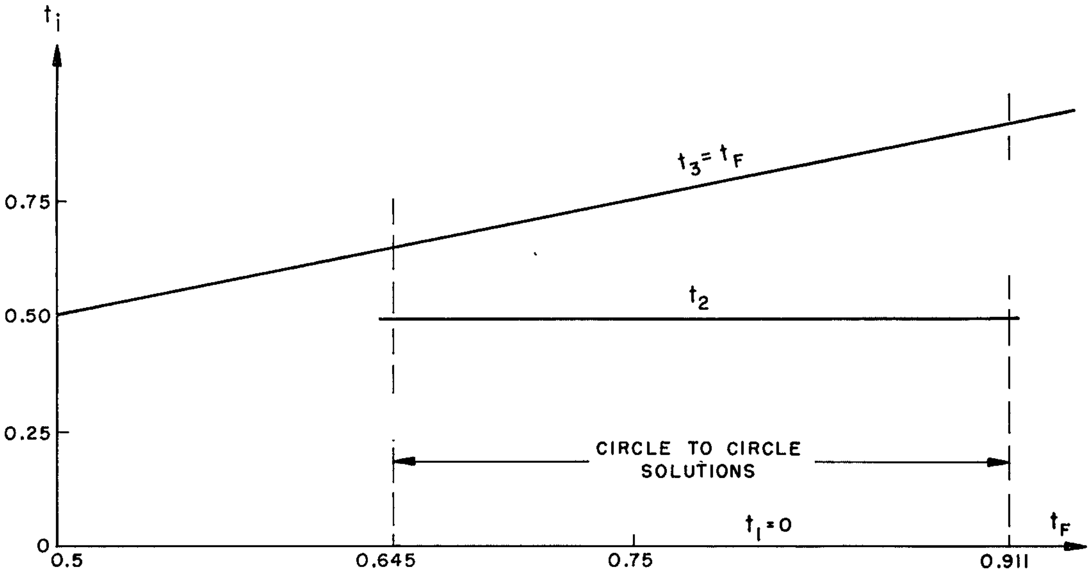

Fig. 6-6. Impulse times for example three-impulse transfers (B = 0.35).

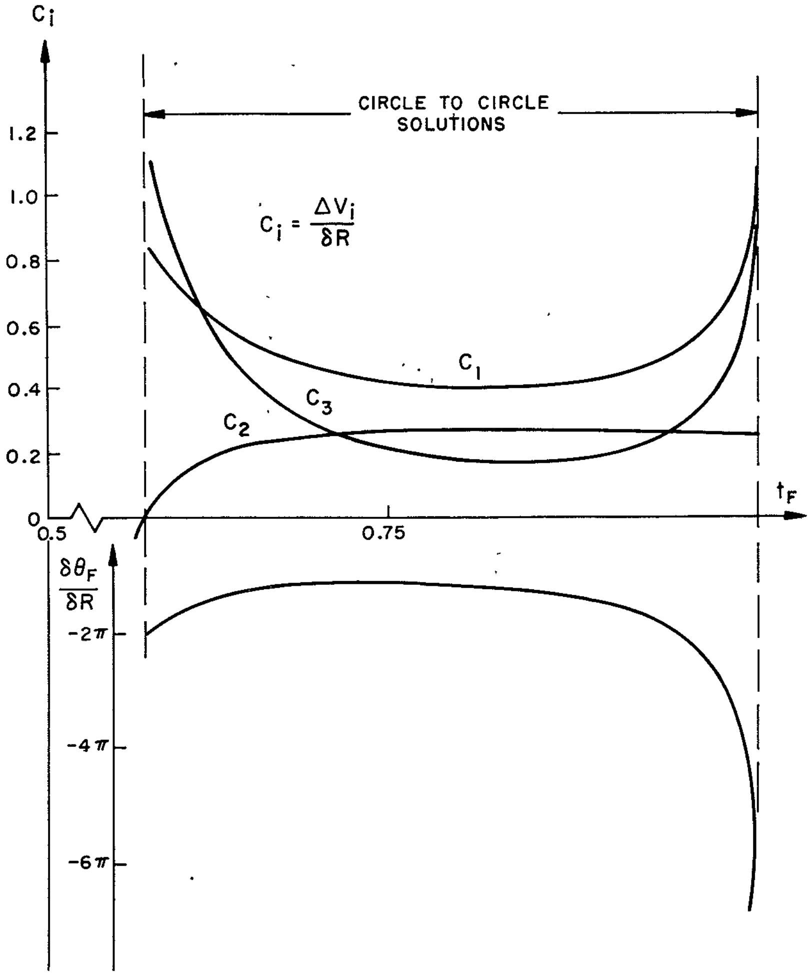

Fig. 6-7. Velocity change magnitudes and final state variations for example three-impulse solutions.

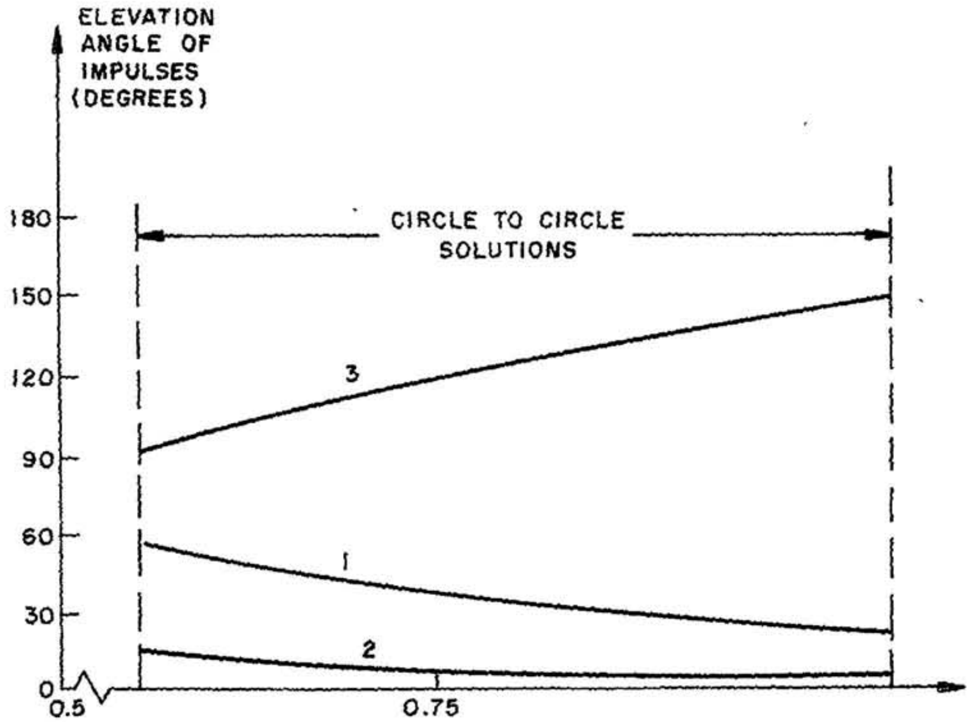

Fig. 6-8. Elevation angles of impulses for example three-impulse solutions.

CHAPTER 7

OPTIMAL TWO-IMPULSE SOLUTIONS

7.1 Introduction

For non-intersecting terminal orbits two-impulses is the minimum number necessary to perform a rendezvous. In the coplanar case the four velocity change components (two for each impulse) are determined to satisfy the four desired final values of the state (two coordinates of position, two of velocity).

For the linearized two-impulse case this offers a simplification, since, for a given transfer time and boundary conditions the two-impulse solution is unique. Whether or not this solution is optimal can be determined by evaluating the primer vector corresponding to this solution and seeing if it satisfies the necessary conditions. This is more convenient than constructing two-impulse primer vector solutions from the primer locus.

7.2 The Two-Impulse Boundary Value Problem

The two-impulse boundary value problem can be written in the form of Eq. (3-17):

$$\delta\underline{\tilde{x}}_F = [B_{F1} \ \vdots \ B_{F2}] \begin{bmatrix} \underline{\Delta V}_1 \\ \hline \underline{\Delta V}_2 \end{bmatrix} \tag{7-1}$$

or

$$\delta\underline{\tilde{x}}_2 = [B_{21} \ \vdots \ B_{22}] \begin{bmatrix} \underline{\Delta V}_1 \\ \hline \underline{\Delta V}_2 \end{bmatrix} \tag{7-2}$$

where

$$\delta\underline{\tilde{x}}_2 = \Phi_{2F}\,\delta\underline{\tilde{x}}_F \tag{7-3}$$

In Eq. (7-2)

$$B_{22} = \begin{bmatrix} 0 \\ I \end{bmatrix} \tag{7-4}$$

and let

$$B_{21} = \begin{bmatrix} N_{21} \\ T_{21} \end{bmatrix} \tag{7-5}$$

The boundary value problem is then

$$\delta \underline{\tilde{x}}_2 = \begin{bmatrix} N_{21} & 0 \\ T_{21} & I \end{bmatrix} \begin{bmatrix} \underline{\Delta V}_1 \\ \underline{\Delta V}_2 \end{bmatrix} \tag{7-6}$$

The condition for a solution is that N_{21} be invertible. Then:

$$\begin{bmatrix} \underline{\Delta V}_1 \\ \cdot \\ \underline{\Delta V}_2 \end{bmatrix} = \begin{bmatrix} N_{21}^{-1} & 0 \\ -T_{21}N_{21}^{-1} & I \end{bmatrix} \delta \underline{\tilde{x}}_2 \tag{7-7}$$

7.3 Circle-to-Circle, Coplanar Solutions

For circular terminal orbits

$$\delta \underline{\tilde{x}}_2 = \begin{bmatrix} \delta R \\ \delta\theta_2 - \frac{3}{4}(\tau_2 - \tau_1)\, \delta R \\ 0 \\ -\frac{3}{2}\, \delta R \end{bmatrix} \tag{7-8}$$

For a circular reference orbit, the partitions of the state transition matrix are given in Appendix B. In units for which $a = \omega = 1$

$$\left| N_{21} \right| = 8(1 - \cos\theta) - 3\theta \sin\theta \tag{7-9}$$

where $\theta = \tau_2 - \tau_1$, the non-dimensional time between the impulses.

The solution to the boundary value problem (Eq. (7-7)) can be written as:

$$\begin{bmatrix} \Delta \underline{V}_1 \\ \\ \Delta \underline{V}_2 \end{bmatrix} = \frac{1}{|N_{21}|} \begin{bmatrix} 4 \sin\theta - 3\theta & -2(1-\cos\theta) & 0 & 0 \\ 2(1-\cos\theta) & \sin\theta & 0 & 0 \\ 3\theta\cos\theta - 4\sin\theta & -2(1-\cos\theta) & 8(1-\cos\theta) - 3\theta\sin\theta & 0 \\ 14(1-\cos\theta) - 6\theta\sin\theta & -\sin\theta & 0 & 8(1-\cos\theta) - 3\theta\sin\theta \end{bmatrix} \delta\underline{\tilde{x}}_2 \tag{7-10}$$

$|N_{21}|$ is zero for θ which are multiples of 2π and also for other isolated values such as 2.82π, as shown by Fig. 7-1.

7.4 The Primer Vectors Corresponding to the Two-Impulse Solutions

From the velocity changes determined by Eq. (7-10), the corresponding primer vector components are determined by:

$$\lambda_i = \frac{\Delta V_{ir}}{\Delta V_i} \tag{7-11}$$

$$\mu_i = \frac{\Delta V_{i\theta}}{\Delta V_i} \tag{7-12}$$

$$i = 1, 2$$

To determine the arbitrary constants in the primer vector solution which satisfy Eq. (7-11) and (7-12) for the given transfer time, it is convenient to write the primer solution in an alternative form (discussed in Section 8.2):

$$\lambda = A^{\#}\cos\omega t + B^{\#}\sin\omega t + 2C^{\#} \tag{7-13}$$

$$\mu = 2B^{\#}\cos\omega t - 2A^{\#}\sin\omega t - 3C^{\#}\omega t + D^{\#} \tag{7-14}$$

Considering the first impulse to occur at $t = 0$ and the second at $t = t_2$, Eqs. (7-13) and (7-14) can be written as:

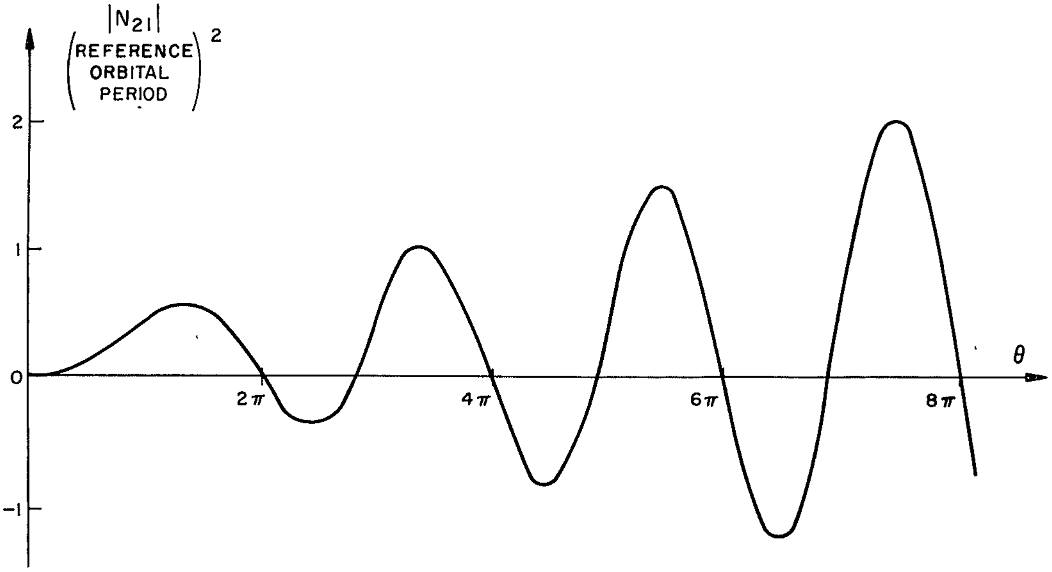

Fig. 7-1. Determinant of N_{21} matrix.

$$
\begin{bmatrix} \lambda_1 \\ \mu_1 \\ \lambda_2 \\ \mu_2 \end{bmatrix} = \begin{bmatrix} 1 & 0 & 2 & 0 \\ 0 & 2 & 0 & 1 \\ \cos\theta & \sin\theta & 2 & 0 \\ -2\sin\theta & 2\cos\theta & -3\theta & 1 \end{bmatrix} \begin{bmatrix} A^{\#} \\ B^{\#} \\ C^{\#} \\ D^{\#} \end{bmatrix} \tag{7-15}
$$

where $\theta = \tau_2 - \tau_1 = \omega t_2$.

Inversion of this matrix yields the values of the constants in terms of the known primer vector components. The determinant of this matrix is the same as $|N_{21}|$ and is given by Eq. (7-9).

$$
\begin{bmatrix} A^{\#} \\ B^{\#} \\ C^{\#} \\ D^{\#} \end{bmatrix} = \frac{1}{|N_{21}|} \begin{bmatrix} 4(1-\cos\theta) - 3\theta\sin\theta & 2\sin\theta & -4(1-\cos\theta) & -2\sin\theta \\ 3\theta\cos\theta - 4\sin\theta & 2(1-\cos\theta) & 4\sin\theta - 3\theta & -2(1-\cos\theta) \\ 2(1-\cos\theta) & -\sin\theta & 2(1-\cos\theta) & \sin\theta \\ 8\sin\theta - 6\theta\cos\theta & 4(1-\cos\theta) - 3\theta\sin\theta & 6\theta - 8\sin\theta & 4(1-\cos\theta) \end{bmatrix} \begin{bmatrix} \lambda_1 \\ \mu_1 \\ \lambda_2 \\ \mu_2 \end{bmatrix}
$$

Determination of the constants and substitution into Eqs. (7-13) and (7-14) determines whether the primer vector satisfies the necessary conditions for an optimal.

7.5 Rendezvous Accomplished by Optimal Two-Impulse Solutions

Figure 7-2 shows a typical primer magnitude history for an optimal two-impulse transfer. Figure 7-3 displays the final state variations reachable by two-impulse solutions of this type. As one might expect, the two-impulse transfers are optimal for shorter transfer times than other multiple-impulse solutions.

7.6 Rendezvous Accomplished by Optimal Two-Impulse with Coast Solutions

Figure 7-4 shows a primer magnitude history which allows a two-impulse solution with a final coast. The impulses are applied at times t_1 and t_2. The dual to this solution then allows an initial coast. In the

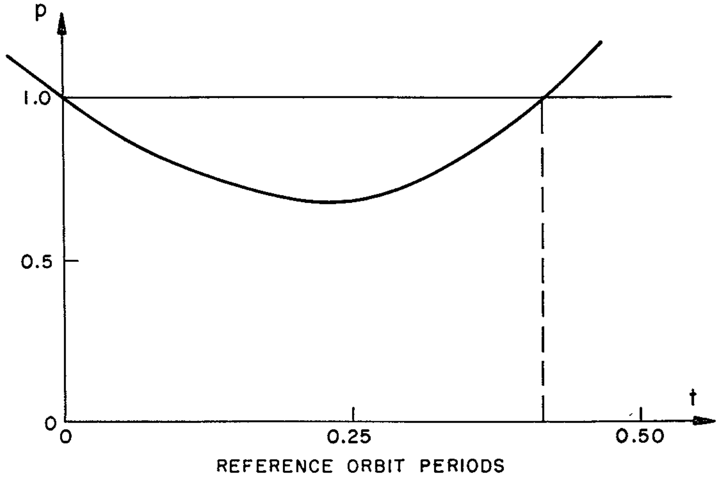

Fig. 7-2. Primer magnitude for optimal two-impulse rendezvous.

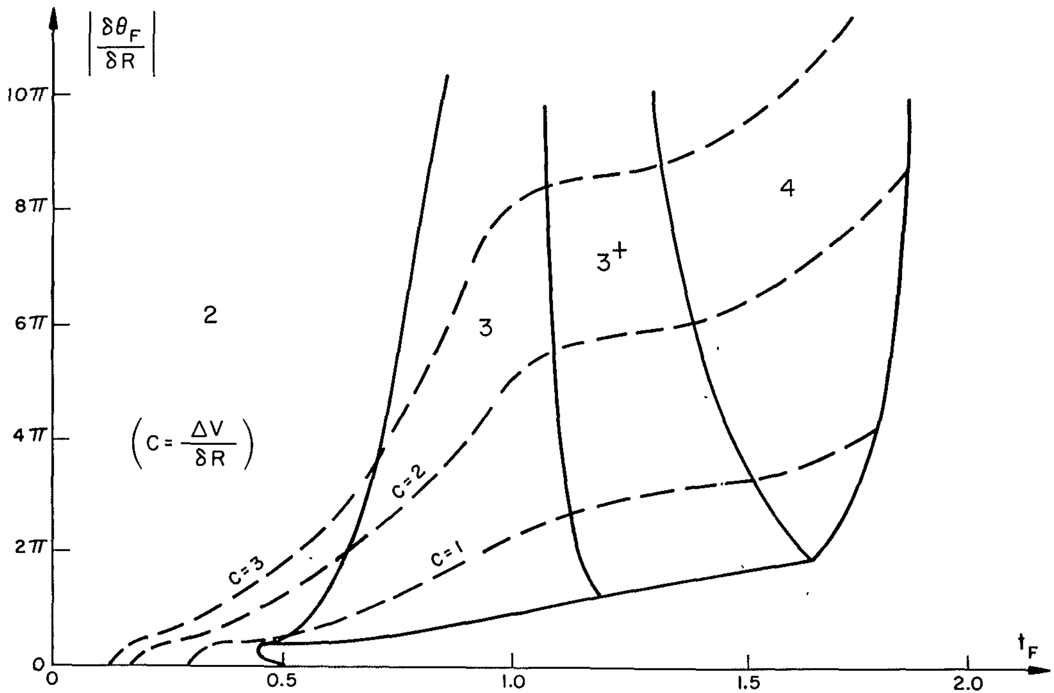

Fig. 7-3. Reachable final state variations for optimal two-, three-, and four-impulse rendezvous.

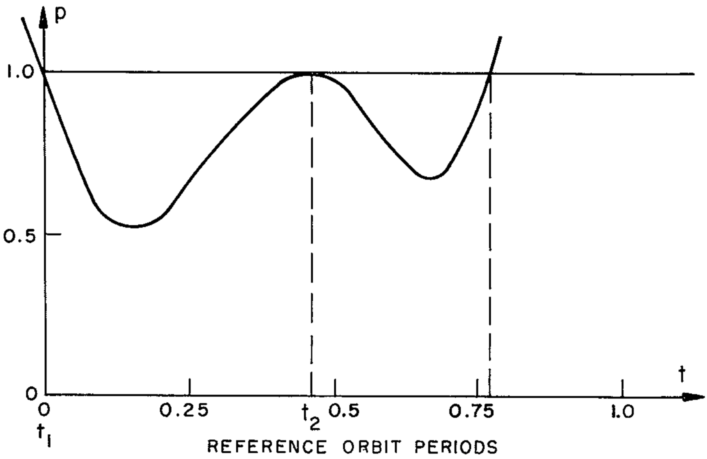

Fig. 7-4. Primer magnitude for optimal two-impulse with final coast.

specific example shown in Fig. 7-4 the two-impulse solution meets the boundary of the three-impulse region for time slightly larger than 0. 75 reference orbit period, as shown.

The reachable final state variations for optimal two-impulse with coast solutions are shown in Fig. 7-5. The region occupied by these solutions (denoted by 2^+) is quite small. This is due to the fact that three-impulse solutions for transfer times slightly longer than those required for optimal two-impulse solutions require less fuel than the two-impulse with coast solutions for the same transfer times.

Figure 7-6 is an alternative representation of the regions of optimal two-impulse solutions.

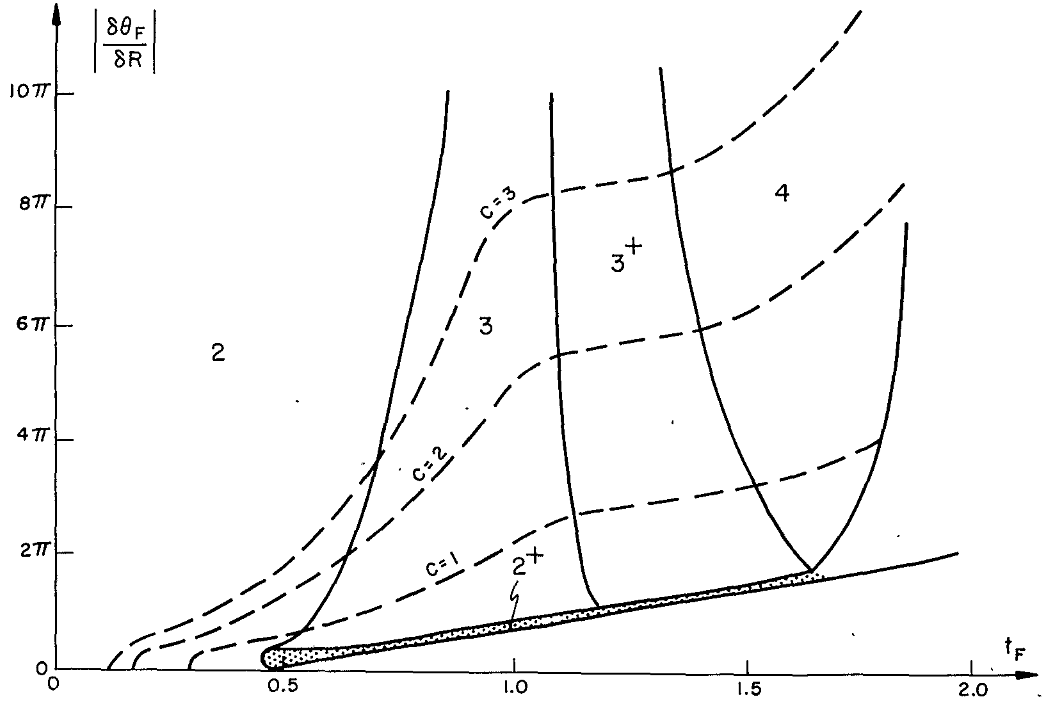

Fig. 7-5. Reachable final state variations showing optimal two-impulse with coast solutions.

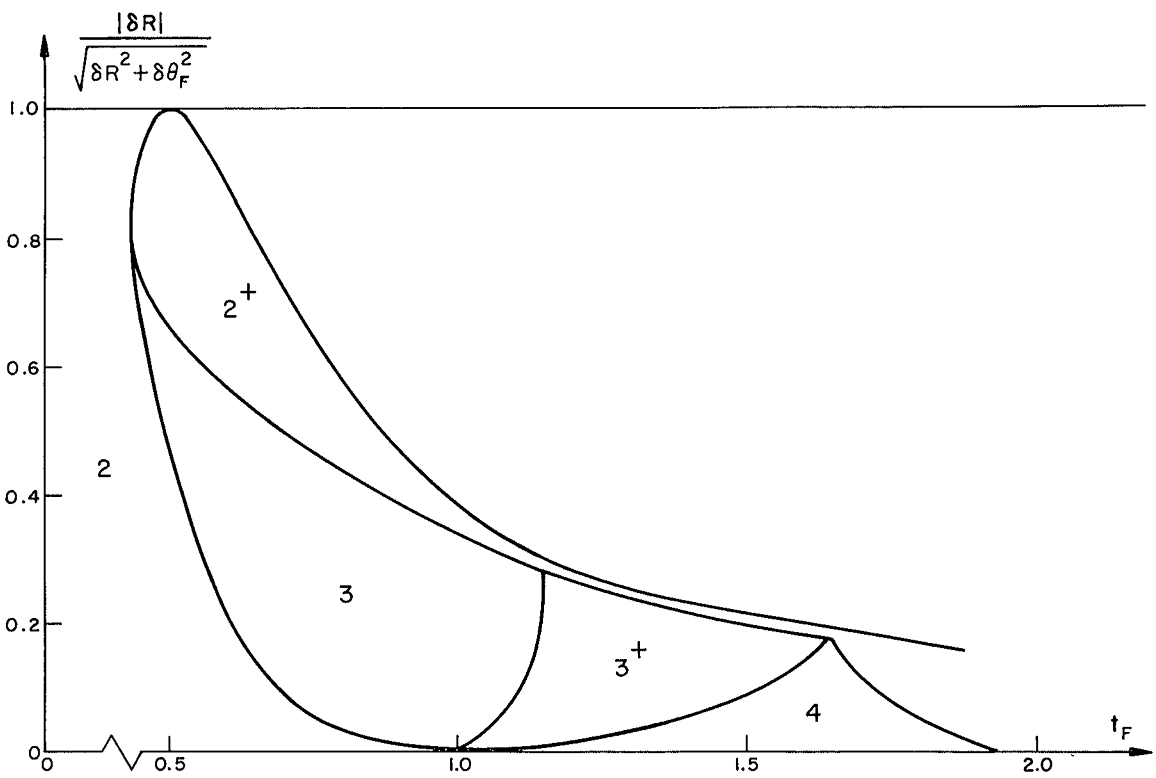

Fig. 7-6. Alternative display of regions of two-impulse optimal solutions.

CHAPTER 8

NON-UNIQUE MULTIPLE-IMPULSE SOLUTIONS

8.1 Introduction

This chapter investigates a set of multiple-impulse solutions to the circle-to-circle rendezvous problem for which the Maximum Principle is degenerate. The case occurs when the magnitude of the primer vector is unity during the entire transfer. Although this solution satisfies the necessary conditions for an optimal transfer, the impulse times are not determined by the Maximum Principle.

This behavior is analogous to the singular arc[4, 26] which arises in nonlinear problems when the switch function[4, 26] is zero over a finite time interval. However, in the nonlinear case the primer vector is a function of the state and is influenced by the control, whereas in the linear case the primer vector is a function only of the reference state and is not influenced to first order by variations in the control.

For linear problems this type of degeneracy results in non-unique solutions. A discussion of this is found in a paper by McIntyre and Crocco.[27] In this chapter the rendezvous trajectories which correspond to this type of primer vector solution are examined for the case of two, three, and four impulses. These solutions are more than theoretically interesting since the two-impulse solution is the linearized form of the Hohmann transfer, known to be the absolute minimum-fuel transfer solution to the circle-to-circle problem being investigated.[28]

8.2 Primer Vector Solution for Degenerate Case

Considering the two-dimensional problem, the primer vector solution for which the vector has unit magnitude during the entire transfer is evident by writing the solution of Chapter 2 (Eq. (2-20)) in the alternative form:

$$\lambda = A^{\#}\cos\omega t + B^{\#}\sin\omega t + 2C^{\#} \tag{8-1}$$

$$\mu = 2B^{\#}\cos\omega t - 2A^{\#}\sin\omega t - 3C^{\#}\omega t + D^{\#} \tag{8-2}$$

where the arbitrary constants of Eq. (2-20) are related to the above constants by:

$$A^2 = A^{\#2} + B^{\#2} \tag{8-3}$$

$$B = \frac{C^{\#}}{A} \tag{8-4}$$

$$t_p = \frac{1}{\omega} \tan^{-1}\left(\frac{B^{\#}}{A^{\#}}\right) \tag{8-5}$$

$$C = \frac{D^{\#} - 3C^{\#}\omega t_p}{A} \tag{8-6}$$

The solution for which the primer vector has unit magnitude for all time is obtained from Eqs. (8-1) and (8-2) by choosing

$$A^{\#} = B^{\#} = C^{\#} = 0 \tag{8-7}$$

$$D^{\#} = 1 \tag{8-8}$$

This corresponds to a primer locus which is a point in the λ-μ plane located at (0, 1).

This primer solution satisfies the necessary conditions for an optimal impulsive transfer, but the impulse times are not uniquely determined. The optimal thrust direction, however, is always circumferential. Since the primer magnitude never exceeds unity, any solution to the boundary value problem is also valid with unlimited initial or final coasting periods. The reciprocal solution is obtained by choosing $D^{\#} = -1$.

8.3 Two-Impulse Non-Unique Solutions

For the two-impulse non-unique solution the unit vectors in the direction of thrust are:

$$\underline{u}_1 = \underline{u}_2 = \begin{bmatrix} 0 \\ 1 \end{bmatrix} \tag{8-9}$$

and the sensitivity vectors, $\underline{w}_j$ (Eq. (3-19)) are

$$\underline{w}_1 = \begin{bmatrix} 2(1 - \cos\theta_1) \\ 4\sin\theta_1 - 3\theta_1 \\ 2\sin\theta_1 \\ 4\cos\theta_1 - 3 \end{bmatrix} ; \quad \underline{w}_2 = \begin{bmatrix} 0 \\ 0 \\ 0 \\ 1 \end{bmatrix} \qquad (8\text{-}10)$$

where $\theta_1 = \tau_2 - \tau_1$.

The two-impulse boundary value equation (3-20) becomes:

$$\begin{bmatrix} \delta R \\ \delta\tilde{\theta}_F \\ 0 \\ -\frac{3}{2}\,\delta R \end{bmatrix} = \begin{bmatrix} 2(1 - \cos\theta_1) & 0 \\ 4\sin\theta_1 - 3\theta_1 & 0 \\ 2\sin\theta_1 & 0 \\ 4\cos\theta_1 - 3 & 1 \end{bmatrix} \begin{bmatrix} \Delta V_1 \\ \Delta V_2 \end{bmatrix} \qquad (8\text{-}11)$$

where, as before,

$$\delta\tilde{\theta}_F = \delta\theta_F - \frac{3}{4}\,\delta R\,(\tau_F - \tau_o)$$

Satisfaction of the third-row equation of matrix equation (8-11) for $\Delta V_1 \neq 0$ requires

$$\sin\theta_1 = 0 \qquad (8\text{-}12)$$

or

$$\theta_1 = n\pi \qquad n = 1, 2, \ldots \qquad (8\text{-}13)$$

Allowing $\Delta V_1 = 0$ results in the uninteresting solution $\Delta V_1 = \Delta V_2 = 0$.

For n an even integer

$$\begin{bmatrix} \delta R \\ \delta\tilde{\theta}_F \\ 0 \\ -\frac{3}{2}\,\delta R \end{bmatrix} = \begin{bmatrix} 0 & 0 \\ -3n\pi & 0 \\ 0 & 0 \\ 1 & 1 \end{bmatrix} \begin{bmatrix} \Delta V_1 \\ \Delta V_2 \end{bmatrix} \qquad (8\text{-}14)$$

which requires

$$\delta R = 0 \tag{8-15}$$

$$\Delta V_2 = -\Delta V_1 \tag{8-16}$$

Equation (8-16) violates the admissibility condition, $\Delta V_i \geq 0$ $(i = 1, 2)$.

For n an odd integer

$$\begin{bmatrix} \delta R \\ \delta\tilde{\theta}_F \\ 0 \\ -\frac{3}{2}\delta R \end{bmatrix} = \begin{bmatrix} 4 & 0 \\ -3n\pi & 0 \\ 0 & 0 \\ -7 & 1 \end{bmatrix} \begin{bmatrix} \Delta V_1 \\ \Delta V_2 \end{bmatrix} \tag{8-17}$$

which has the admissible solution

$$\Delta V_1 = \Delta V_2 = \frac{\delta R}{4} \tag{8-18}$$

$$\delta\theta_F = 0 \tag{8-19}$$

For n = 1 this is the linearized version of the Hohmann transfer. Equation (8-19) results from the fact that the period of the Hohmann transfer ellipse and the reference orbit period are equal if the reference orbit lie half-way between the terminal orbits. The initial target phase angle (Eq. (B-34)) for the Hohmann transfer is then

$$\beta_H = \frac{3}{4}\pi\ \delta R \tag{8-20}$$

For n = 3, 5, 7, ... the transfers correspond to applying the second impulse 1, 2, 3, ... full reference orbit periods after the time of the second impulse for a normal Hohmann transfer. The cost of all these thrust programs is the same; each corresponds to a different inital target phase angle:

$$\beta = \frac{3}{4}(n\pi)\ \delta R \tag{8-21}$$

Since the primer magnitude never exceeds unity, unlimited initial and final coasting periods are allowed by the necessary conditions for an optimal. For the Hohmann transfer without final coast, $\tau_F = \tau_2$, the time of the second impulse. In this case $\delta\theta_F = 0$ (Eq. (8-19)). However, if a coast in the final orbit is included ($\tau_F > \tau_2$),

$$\delta\theta_F = -\frac{3}{4}\delta R(\tau_F - \tau_2) \tag{8-22}$$

since $\delta\dot{\theta} = \frac{-3}{4}\delta R$ for the final circular orbit (Appendix B. 6).

In like manner, for an initial coast ($\delta\dot{\theta} = \frac{3}{4}\delta R$):

$$\delta\theta_F = \frac{3}{4}\delta R(\tau_1 - \tau_o) \tag{8-23}$$

where $\tau_1 - \tau_o$ is the duration of the initial coast, and, as before, $\delta\theta_o = 0$.

These two coasting solutions for the Hohmann transfer appear as straight lines in Fig. 8-1. Any point inside the wedge formed by the coasting lines can be reached by a unique combination of an initial coast and final coast plus a Hohmann transfer. The cost of any transfer inside this wedge is then the cost of a Hohmann transfer, the absolute minimum cost.

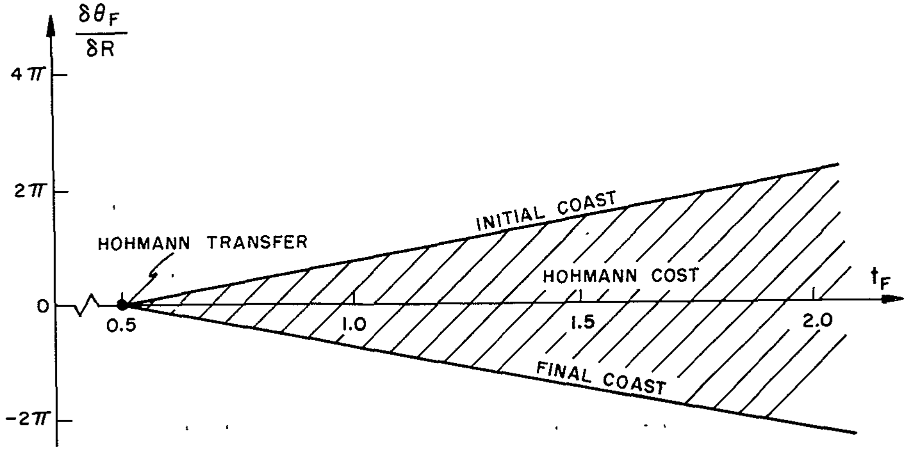

Fig. 8-1. Reachable final states of non-unique transfers.

8.4 Three-Impulse Non-Unique Solutions

For the three-impulse non-unique solution the boundary value Eq. (8-11) becomes:

$$\begin{bmatrix} \delta R \\ \delta\tilde{\theta}_F \\ 0 \\ -\frac{3}{2}\delta R \end{bmatrix} = \begin{bmatrix} 2(1 - \cos\theta_1) & 2(1 - \cos\theta_2) & 0 \\ 4\sin\theta_1 - 3\theta_1 & 4\sin\theta_2 - 3\theta_2 & 0 \\ 2\sin\theta_1 & 2\sin\theta_2 & 0 \\ 4\cos\theta_1 - 3 & 4\cos\theta_2 - 3 & 1 \end{bmatrix} \begin{bmatrix} \Delta V_1 \\ \Delta V_2 \\ \Delta V_3 \end{bmatrix} \tag{8-24}$$

where

$$\theta_j = \tau_3 - \tau_j \qquad j = 1, 2$$

By analogy with the two-impulse case we investigate the cases for which

$$\begin{aligned} \theta_1 &= n\pi \\ \theta_2 &= k\pi \qquad k, n = 1, 2, 3 \ldots \end{aligned} \tag{8-25}$$

Case I:

For both n and k even integers, Eq. (8-24) becomes

$$\begin{bmatrix} \delta R \\ \delta\theta_F \\ 0 \\ -\frac{3}{2}\delta R \end{bmatrix} = \begin{bmatrix} 0 & 0 & 0 \\ -3n\pi & -3k\pi & 0 \\ 0 & 0 & 0 \\ 1 & 1 & 1 \end{bmatrix} \begin{bmatrix} \Delta V_1 \\ \Delta V_2 \\ \Delta V_3 \end{bmatrix} \tag{8-26}$$

This solution requires $\delta R = 0$ (equation of the first row) and then

$$\Delta V_1 + \Delta V_2 + \Delta V_3 = 0 \tag{8-27}$$

by the equation of the fourth row. Equation (8-27) cannot be satisfied by an admissible solution unless all the velocity changes are zero.

Case II:

For the case in which both n and k are odd, the boundary value problem is:

$$\begin{bmatrix} \delta R \\ \delta\tilde{\theta}_F \\ 0 \\ -\frac{3}{2}\delta R \end{bmatrix} = \begin{bmatrix} 4 & 4 & 0 \\ -3n\pi & -3k\pi & 0 \\ 0 & 0 & 0 \\ -7 & -7 & 1 \end{bmatrix} \begin{bmatrix} \Delta V_1 \\ \Delta V_2 \\ \Delta V_3 \end{bmatrix} \tag{8-28}$$

which has solution

$$\Delta V_1 = \frac{\delta R}{4} - \frac{\delta\theta_F}{3\pi(n-k)} \tag{8-29}$$

$$\Delta V_2 = \frac{\delta\theta_F}{3\pi(n-k)} \tag{8-30}$$

$$V_3 = \frac{\delta R}{4} \tag{8-31}$$

This solution reduces to the Hohmann-type transfer for $\delta\theta_F = 0$ ($\Delta V_2 = 0$). The admissibility condition requires that

$$\delta\theta_F \geq 0 \ ; \ \delta R \geq 0 \tag{8-32}$$

$$0 \leq \frac{\delta\theta_F}{\delta R} \leq \frac{3\pi}{4}(n-k) \tag{8-33}$$

Since the maximum value of $n-k$ is $n-1$, the points which satisfy these conditions lie in the upper-half Hohmann-cost wedge of Fig. 8-1. The admissibility conditions which the reciprocal solution must satisfy are obtained by reversing the inequalities in Eqs. (8-32) and (8-33). These points then lie in the lower-half wedge.

The cost of this three-impulse transfer is the cost of a Hohmann transfer, $\delta R/2$. As seen by the expressions for the velocity changes, (Eqs. (8-29) - (8-31)), the transfer physically corresponds to applying a first impulse which is smaller than the first Hohmann impulse. An integral number of reference periods later (since $n-k$ is even) the original deficit is made up by the second impulse. The third impulse is then the same size as the second Hohmann impulse.

Case III:

For n even, k odd,

$$\begin{bmatrix} \delta R \\ \delta\tilde{\theta}_F \\ 0 \\ -\frac{3}{2}\,\delta R \end{bmatrix} = \begin{bmatrix} 0 & 4 & 0 \\ -3n\pi & -3k\pi & 0 \\ 0 & 0 & 0 \\ 1 & -7 & 1 \end{bmatrix} \begin{bmatrix} \Delta V_1 \\ \Delta V_2 \\ \Delta V_3 \end{bmatrix} \tag{8-34}$$

which has the solution

$$\Delta V_1 = \frac{\delta R}{4} - \frac{1}{4}\frac{k}{n}\,\delta R - \frac{\delta\theta_F}{3n\pi} \tag{8-35}$$

$$\Delta V_2 = \frac{\delta R}{4}. \tag{8-36}$$

$$\Delta V_3 = \frac{1}{4}\frac{k}{n}\,\delta R + \frac{\delta\theta_F}{3n\pi} \tag{8-37}$$

The admissibility condition requires

$$\delta R \geq 0 \tag{8-38}$$

$$-\frac{3k\pi}{4} \leq \frac{\delta\theta_F}{\delta R} \leq \frac{3\pi}{4}(n - k) \tag{8-39}$$

Since the maximum value of $n - k$ is $n - 1$ and the maximum value of k is $n - 1$, points satisfying condition (8-39) lie in the Hohmann-cost wedge. The cost of this three-impulse transfer is the Hohmann cost. The admissibility condition requires that the first impulse be no greater than the first Hohmann impulse. Thus at all times during the transfer the vehicle lies between the terminal orbits.

Case IV:

For n odd, k even

the first two columns of the matrix of Eq. (8-34) are interchanged. This results in the sizes of the first and second impulses being interchanged:

$$\Delta V_1 = \frac{\delta R}{4} \tag{8-40}$$

$$\Delta V_2 = \frac{\delta R}{4} - \frac{1}{4}\frac{k}{n}\,\delta R - \frac{\delta\theta_F}{3n\pi} \tag{8-41}$$

$$\Delta V_3 = \frac{1}{4}\frac{k}{n}\,\delta R + \frac{\delta\theta_F}{3n\pi} \tag{8-42}$$

In this case the first impulse is a full-strength Hohmann impulse.

In summary, a set of three-impulse solutions exists for the degenerate primer vector solution. The cost of these solutions is the Hohmann cost and the final states reached are among the same as those reached by a Hohmann transfer with initial and final coasting periods.

8.5 Four-Impulse Non-Unique Solutions

By analogy with the three-impulse solutions, consider a four-impulse solution for which the impulse times are half-reference periods apart. This can be extended by adding full reference periods to the time intervals between impulse without changing the cost. For impulses separated by half-reference periods ($\theta_1 = 3\pi$)

$$\begin{bmatrix} \delta R \\ \delta\tilde{\theta}_F \\ 0 \\ -\frac{3}{2}\,\delta R \end{bmatrix} = \begin{bmatrix} 4 & 0 & 4 & 0 \\ -9\pi & -6\pi & -3\pi & 0 \\ 0 & 0 & 0 & 0 \\ -7 & 1 & -7 & 1 \end{bmatrix} \begin{bmatrix} \Delta V_1 \\ \Delta V_2 \\ \Delta V_3 \\ \Delta V_4 \end{bmatrix} \tag{8-43}$$

Since the third row equation of (8-43) is satisfied identically, this set of equations represents 3 equations in the 4 unknown velocity changes. To obtain a solution, one of the velocity changes must be arbitrary. Let this be the first velocity change and denote its arbitrary magnitude by c. The solution to Eq. (8-43) is then:

$$\Delta V_1 = c \tag{8-44}$$

$$\Delta V_2 = \frac{\delta R}{4} - c - \frac{\delta\theta_F}{6\pi} \tag{8-45}$$

$$\Delta V_3 = \frac{\delta R}{4} - c \tag{8-46}$$

$$\Delta V_4 = c + \frac{\delta\theta_F}{6\pi} \tag{8-47}$$

Evidently, the cost of this transfer is also the Hohmann cost, $\delta R/2$. The admissibility condition, $\Delta V_i \geq 0$ requires

$$0 \leq c \leq \frac{\delta R}{4} \tag{8-48}$$

$$-\frac{6\pi c}{\delta R} \leq \frac{\delta\theta_F}{\delta R} \leq \frac{3\pi}{2} - \frac{6\pi c}{\delta R} \tag{8-49}$$

By taking the maximum and minimum allowable values of c, one sees that points that satisfy Eq. (8-49) also lie inside the Hohmann wedge of Fig. 8-1.

This transfer is then an example of a four-impulse non-unique solution which results from the degenerate prime vector solution.

Because the times of the impulse are not uniquely determined by the primer vector, n-impulse solutions which perform the rendezvous for the cost of a Hohmann transfer can also be constructed.

As in the three-impulse case, the rendezvous realized by the four-impulse transfer discussed here can also be accomplished by a two-impulse Hohmann transfer with initial and final coasting periods. The transfer time and the cost of the two transfers are the same.

Figure 8-2 gives an alternative representation of the region of reachable final state variations using these non-unique transfers.

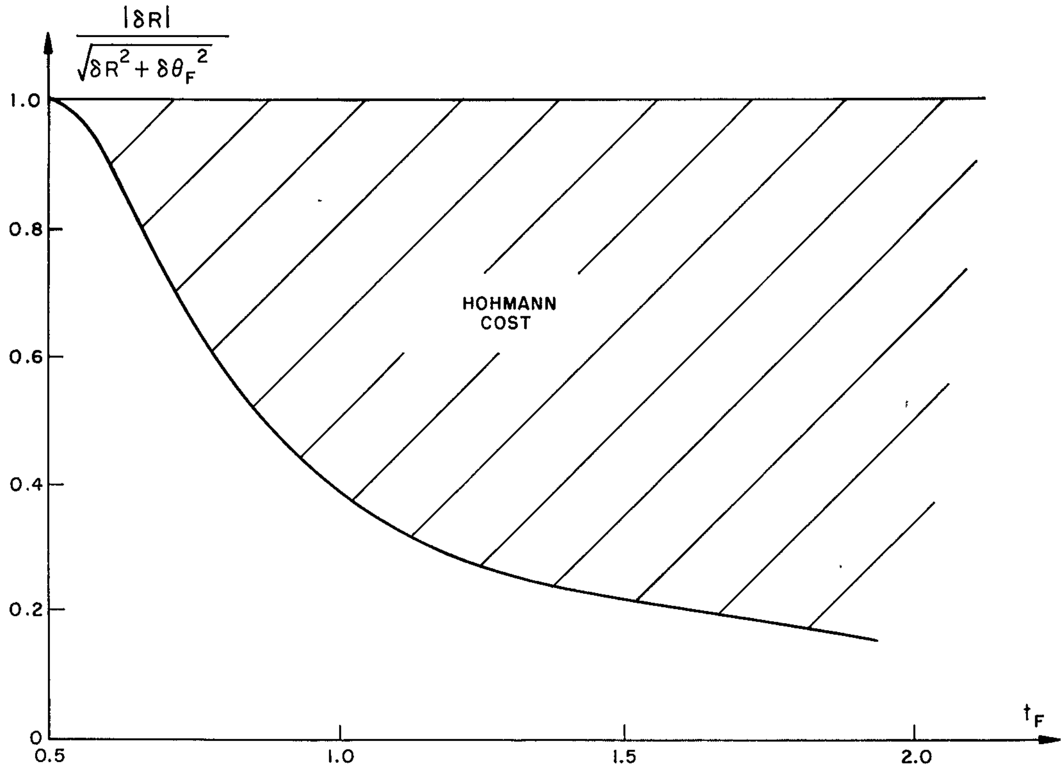

Fig. 8-2. Alternate display of region of Hohmann transfer.

CHAPTER 9

RESULTS AND CONCLUSIONS

9.1 Discussion of Results

The major results of this investigation are shown in the plot of final state variations for circle-to-circle coplanar rendezvous which are reached optimally using different numbers of impulses. Figure 9-1 summarizes the results obtained in the preceding chapters. Figure 9-2 is an alternate representation which allows the information to be displayed on a finite portion of the plane.

The types of thrust programs which theoretically could result in minimizing solutions to the rendezvous boundary value problem are two-, three-, and four-impulse transfers, as discussed in Section 4.2. As seen by Figs. 9-1 and 9-2, all of these possibilities are represented for the transfer times considered. In addition, some final state variations are attained optimally by means of a coasting period in the initial or final orbit.

9.2 Use of Optimal Multiple-Impulse Solutions for a Specific Rendezvous

To accomplish a specific rendezvous between coplanar, close circular orbits, the difference in the terminal radii, δR, and the initial target phase angle, β (Appendix B.6), would be the available information at $t = 0$. It would then be of interest to know the number of impulses and the cost of the rendezvous as a function of the transfer time.

Figure 9-3 displays, for an example ratio $\beta / \delta R$, the cost (in velocity requirement per radius difference) as a function of transfer time. The solid curve represents the cost of the optimal solution. The numbers beneath the curve denote the number of impulses.

As shown in Appendix B.6, the relationship between β and $\delta\theta_F$ is given (in dimensionless variables) by:

$$\delta\theta_F = \beta - \frac{3}{4}\,\delta R\; t_F$$

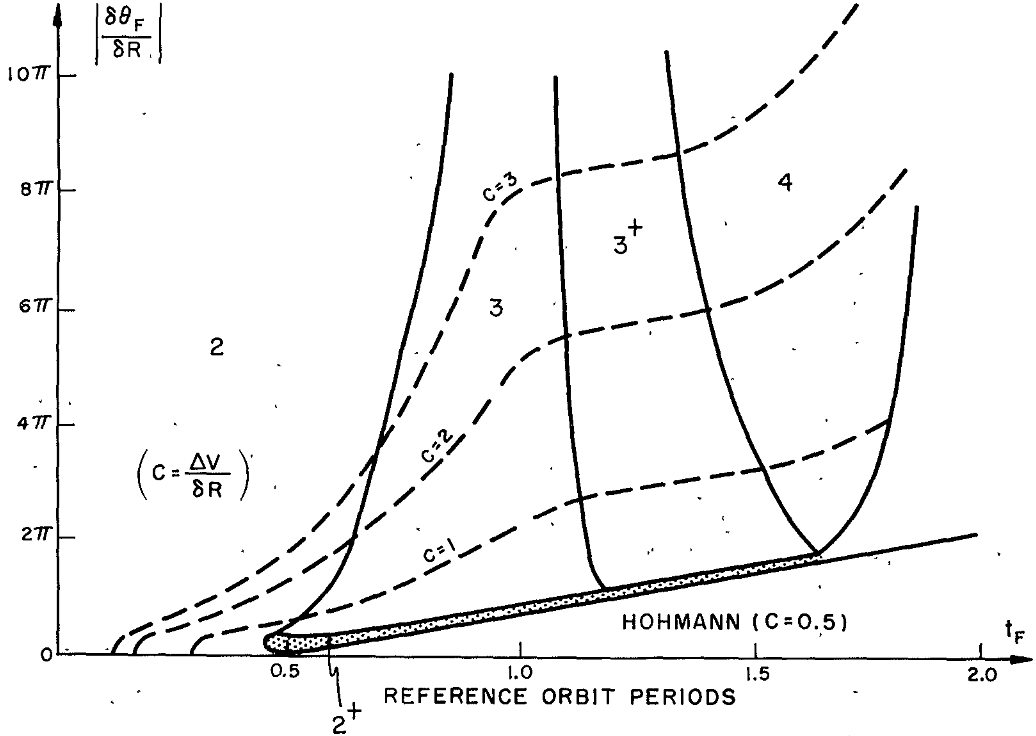

Fig. 9-1. Reachable final state variations. Optimal multiple-impulse solutions.

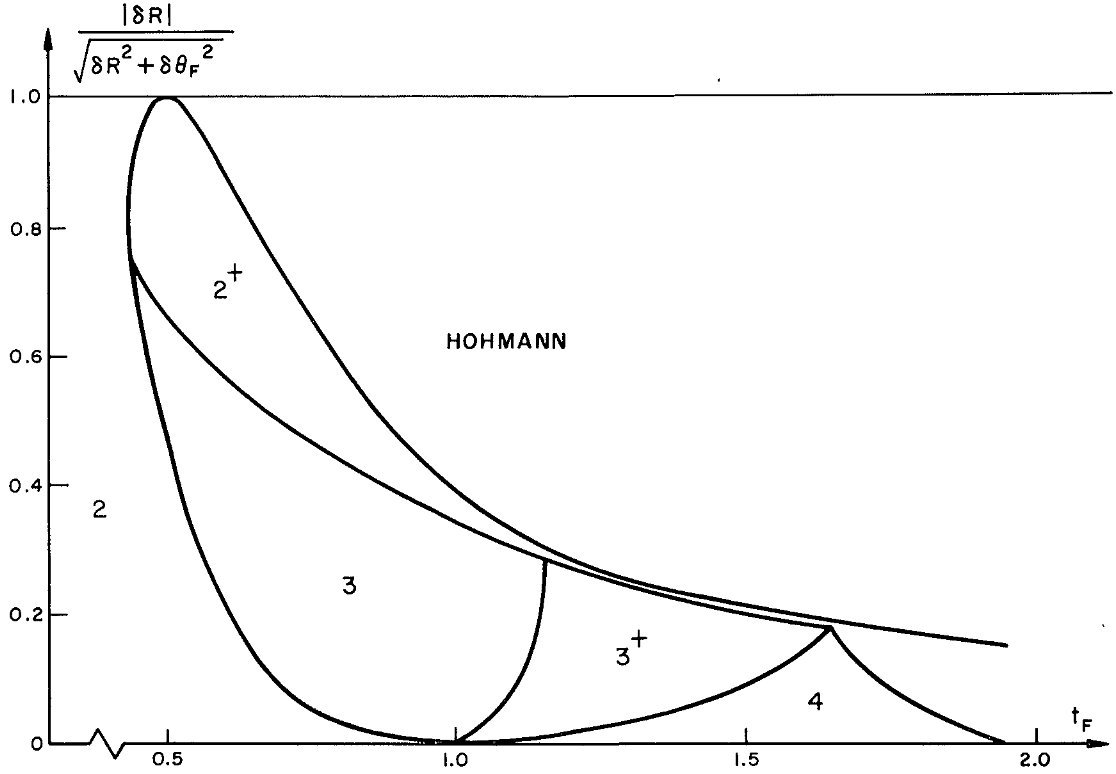

Fig. 9-2. Alternate display of reachable state variations.

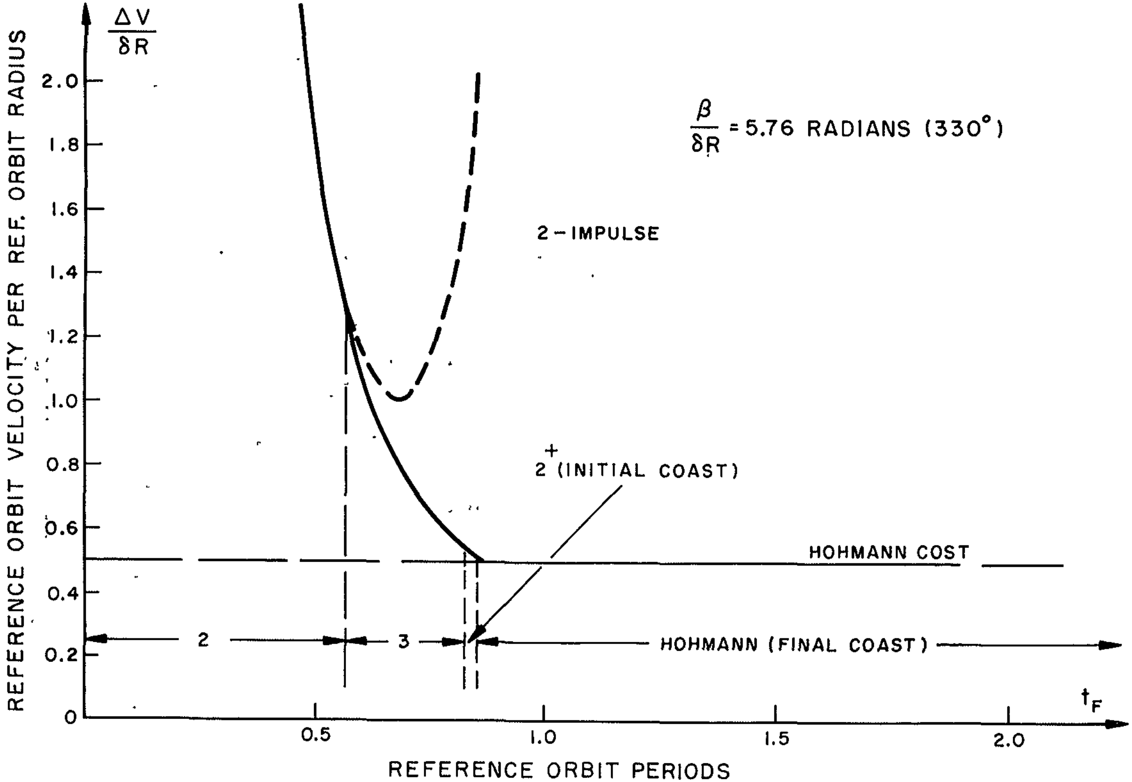

Fig. 9-3. Optimal cost as a function of transfer time for given initial conditions.

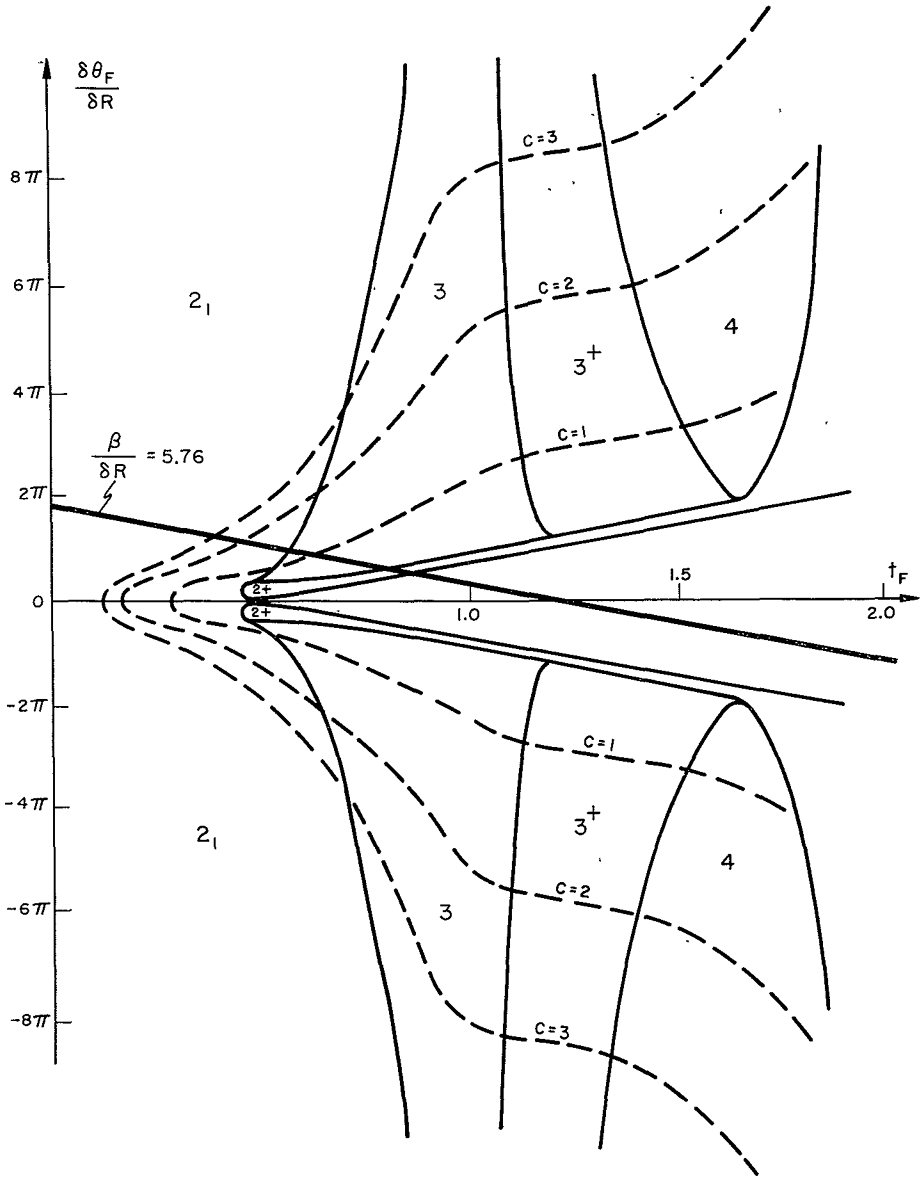

Fig. 9-3a. Reachable state variations for given value of $\beta/\delta R$ (see Fig. 9-3).

The curve of Fig. 9-3 corresponds to the slice through the plane of reachable final state variations shown in Fig. 9-3a.

For short transfer times the two-impulse transfer is optimal. For t_F larger than 0.55 reference orbit periods, three impulses become optimal. The dashed curve shows the two-impulse cost, which reaches a minimum and then rapidly increases due to the singularity at $t_F = 1$. At the minimum cost of the two-impulse transfer the three-impulse transfer offers approximately 20% savings in fuel over the two-impulse transfer. This saving increases with increasing transfer time as shown.

For a small range of transfer times for t_F slightly less than 0.86, two-impulses with initial coast is optimal. At $t_F = 0.86$ the absolute minimum of the Hohmann transfer is available. Since the time-in-flight for the Hohmann transfer is 0.5 reference periods, the transfer for $t_F = 0.86$ requires an initial coast of duration 0.36 reference periods. Geometrically this coast is the time necessary for the phase angle of the target to become the correct value for a Hohmann transfer.

For $t_F > 0.86$ the optimal transfer is the Hohmann transfer with a final coast of duration (t_F - 0.86) reference periods. Note that the optimal cost curve is either decreasing or constant as the transfer time increases.

Figure 9-4 shows an analogous curve for a much different value of $\beta/\delta R$. In this case at $t = 0$ the opportunity for a Hohmann transfer is past and will not recur for a time on the order of the synodic period of the terminal orbits. However, the optimal cost curve asymptotically approaches the Hohmann cost as the transfer time increases.

As in the previous case the two-impulse transfer is optimal for short transfer times. Between the two- and three-impulse optimal transfers is a region of two-impulse with final coast. In this region it is best to make the transfer corresponding to the minimum of the two-impulse cost curve and employ a final coast period. During this final coast the cost does not change, since the transfer is complete and one is merely coasting in the final orbit.

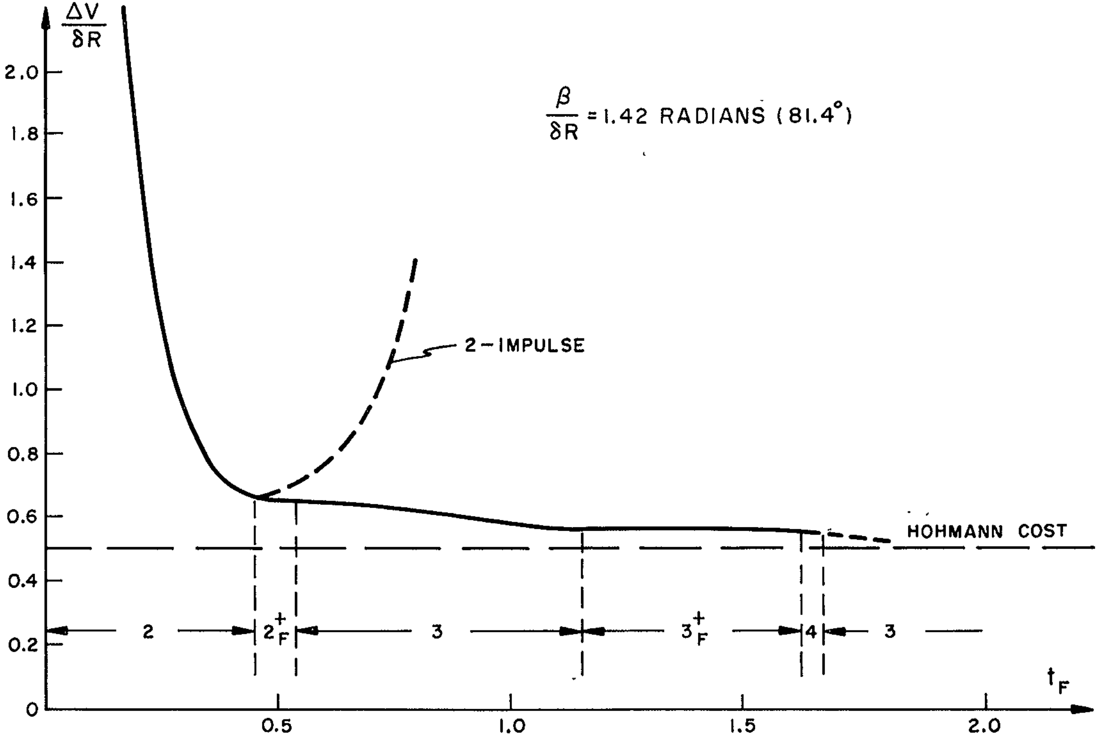

Fig. 9-4. Optimal cost as a function of transfer time for given initial conditions.

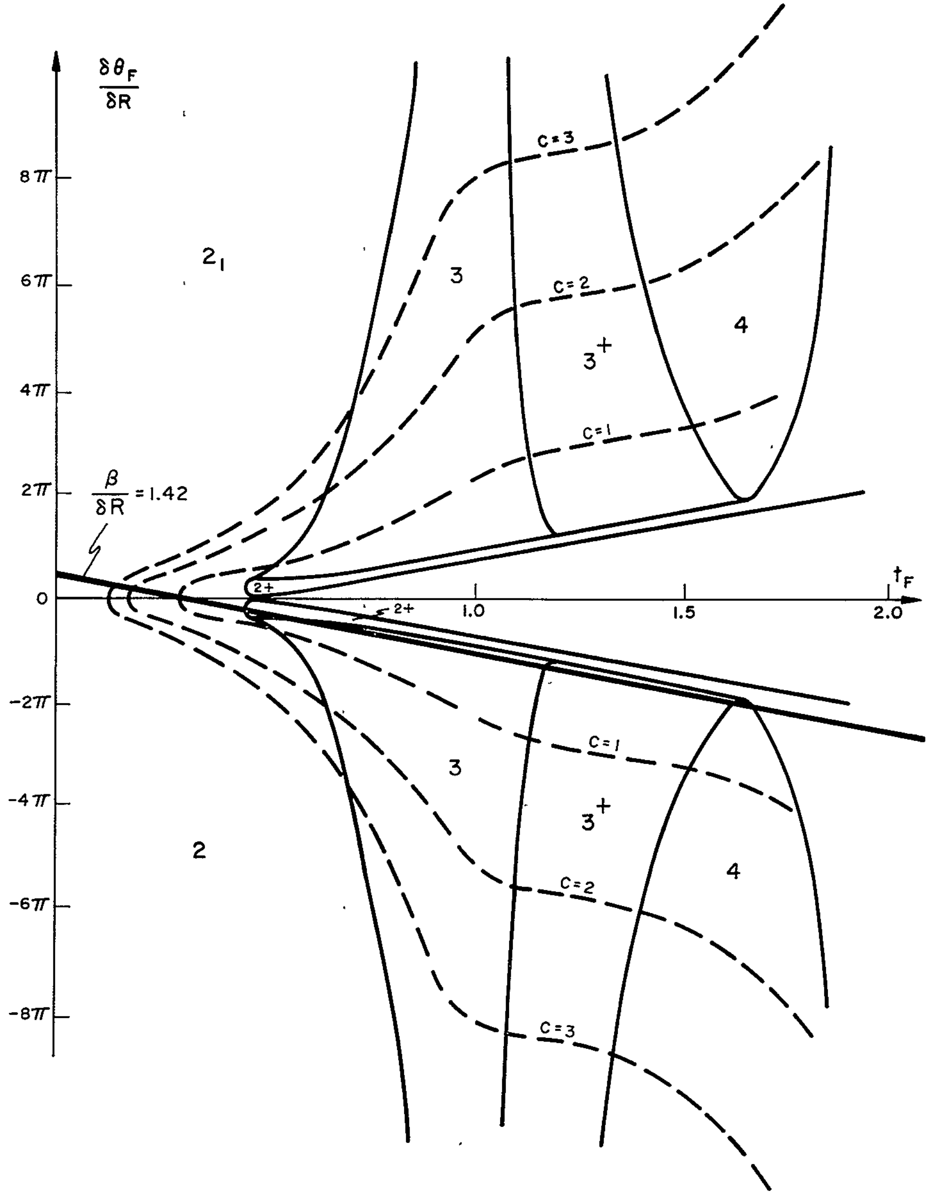

Fig. 9-4a. Reachable state variations for given value of $\beta/\delta R$ (see Fig. 9-4).

In a similar way, three-impulse with final coast solutions lie between three-impulse and four-impulse solutions, as shown in Fig. 9-4. The optimal cost curve is either decreasing or constant as the transfer time increases and will attain the minimum value of the Hohmann cost for a large enough transfer time.

9.3 Example Rendezvous Transfers

In an attempt to gain some geometrical insight into optimal multiple-impulse transfers, some example transfers are discussed in this section.

Figure 9-5 shows an optimal three-impulse rendezvous transfer and the two-impulse transfer for the same boundary conditions and transfer time. The launch velocity increment for both transfers is essentially tangential. The two-impulse transfer intercepts the target with an appreciable radial component of velocity. This requires a larger velocity increment to perform the rendezvous compared with the optimal three-impulse transfer, which arrives more tangentially.

The mid-course velocity change for the three-impulse transfer occurs at the point shown in Fig. 9-5. The dashed trajectory is the transfer which would result if no mid-course velocity change were made. As shown in the figure, this would cause the vehicle to pass inside the target. The effect of the mid-course velocity change is then to impart a tangential "nudge" to the vehicle which causes it to continue out to the target and arrive essentially tangentially. This three-impulse transfer corresponds to Fig. 9-4 for a transfer time of 0.75 reference periods.

Figure 9-6 shows a rendezvous for slightly different initial conditions and transfer time. In this case the two-impulse transfer with final coast is optimal. The second velocity increment performs the rendezvous; the remaining time is spent coasting in the final orbit. Both at launch and arrival, the corresponding two-impulse transfer has an appreciable radial velocity component.

9.4 Recommendations for Further Research

There seem to be two basic directions in which there is a need for further study. One direction is in the continued study of linearized

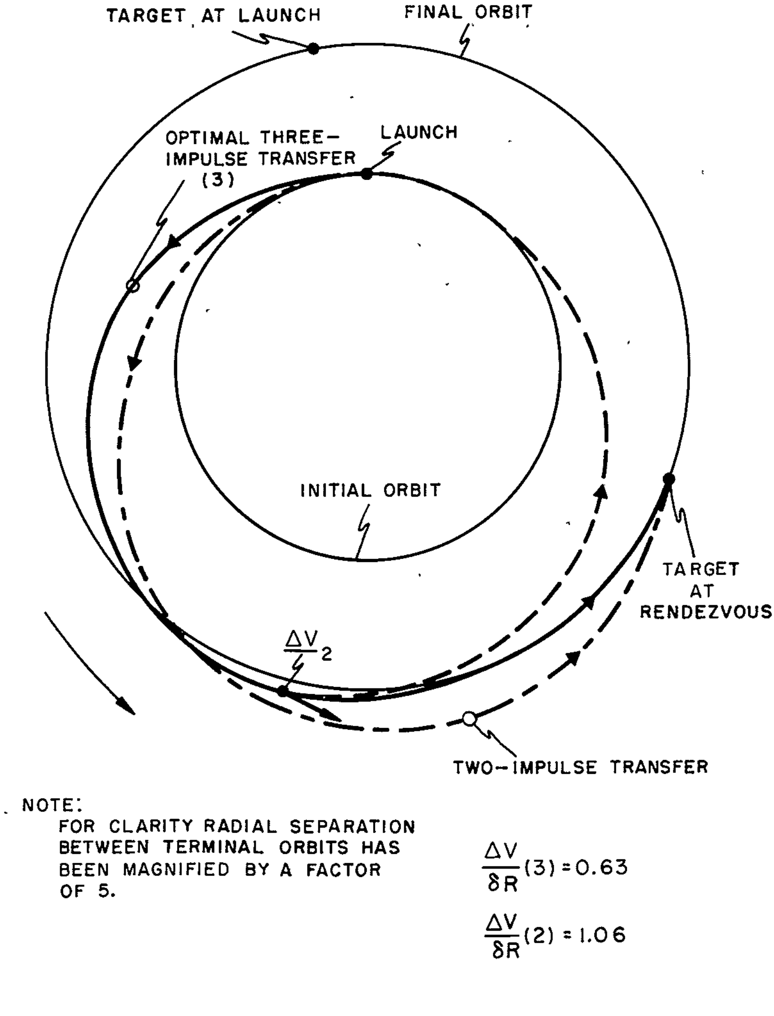

Fig. 9-5. Optimal three-impulse transfer.

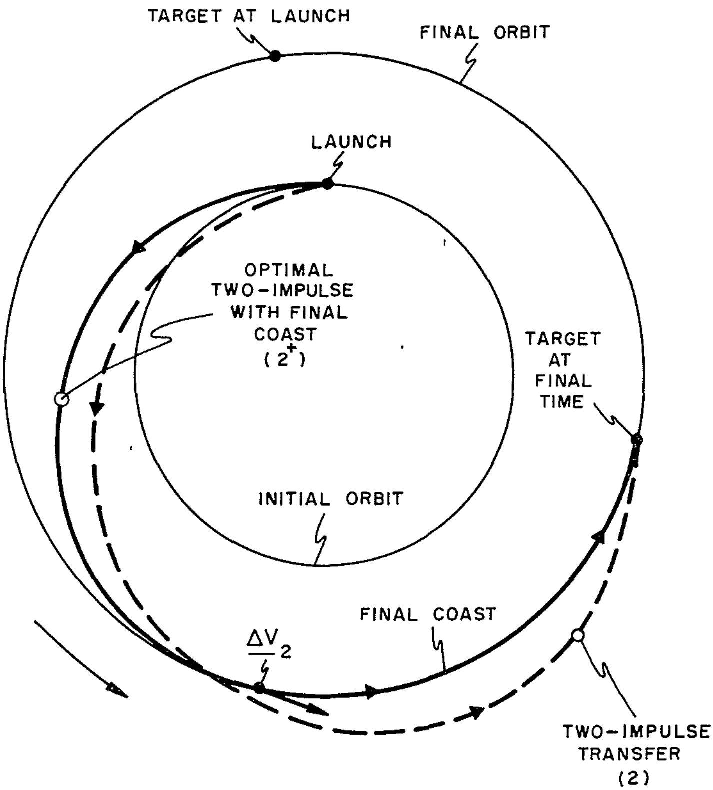

NOTE:
FOR CLARITY RADIAL SEPARATION BETWEEN TERMINAL ORBITS HAS BEEN MAGNIFIED BY A FACTOR OF 5.

$$\frac{\Delta V}{\delta R}(2^{+}) = 0.54$$

$$\frac{\Delta V}{\delta R}(2) = 1.15$$

Fig. 9-6. Optimal two-impulse transfer with final coast.

problems. This investigation of coplanar circular orbits has considered only the simplest case. Many primer vector solutions exist which satisfy the necessary conditions for an optimal transfer but do not yield admissible solutions to the restrictive boundary conditions of a circle-to-circle transfer. One intriguing example of this is the set of "one-loop" four-impulse solutions discussed in Chapter 5.

Another useful contribution in the direction of linearized problems would be to investigate optimal multiple-impulse solutions for non-circular reference trajectories. This type of investigation would be applicable to optimal linear guidance schemes using several velocity corrections.

Yet another useful contribution would be to determine a suitable way of categorizing the numerous optimal three-impulse solutions to the circle-to-circle case, in order to display the impulse times, magnitudes and directions for all the relevant initial conditions and transfer times.

The other basic direction in which further research is needed is in the study of optimal multiple-impulse solutions to the nonlinear problem of an inverse-square gravitational field. The solutions obtained for the linearized, coplanar, circle-to-circle problem should provide reasonably good initial conditions for a numerical solution to the nonlinear problem with inclined elliptical orbits. It is in the realm of the nonlinear problem that optimal multiple-impulse solutions are ultimately desired.

APPENDIX A

CONSTRUCTION OF PRIMER VECTOR SOLUTIONS FROM LOCUS DIAGRAM

A.1 Introduction

In this appendix the details of constructing primer vector solutions geometrically are discussed. The relevant equations for determining the arbitrary constants in the solution to the primer vector equations are given.

A.2 General Considerations

The radial and circumferential components of the primer vector are given by Eq. (2-20):

$$\begin{aligned} \lambda &= A(\cos\tau + 2B) \\ \mu &= A(-2\sin\tau - 3B\tau + c) \end{aligned} \qquad \text{(A-1)}$$

where

$$\tau = \omega(t - t_p) \qquad \text{(A-2)}$$

As mentioned in Section 2.6, these equations are a parametric description of a locus in the λ-μ plane. The constant A normalizes length in the plane, B determines the shape of the locus, C positions the locus along the μ-axis, and t_p corresponds to the initial value of $\tau(\tau = -\omega t_p$ at $t = 0)$.

The technique used to construct primer vector solutions which satisfy the necessary conditions involves choosing a locus shape by picking a value of the constant B. As solutions are constructed, this constant is varied incrementally in order to investigate all locus shapes of interest. Only $B \geq 0$ need be considered for the construction, since the solutions for $B < 0$ (the "reciprocal" solutions of Section 4.5) are obtained from the $B > 0$ solutions by inspection. In addition, for $B > \frac{2}{3}$, the locus has no loops; therefore only two-impulse optimal solutions can be constructed since the necessary tangency of the locus with the unit circle for a midcourse impulse is not possible.

For a given choice of B, the method of evaluating the other constants for the locus varies with the number of impulses being considered. These different methods are described in the sections which follow. It should be noted that, although fixed-time solutions are obtained, it is the constant B that is initially specified and not the transfer time. The value of the transfer time is a result obtained from the construction.

A. 3 Construction of Four-Impulse Primer Vector Solutions

As shown in Chapter 4, the fact that the locus must be tangent to the unit circle for two values of τ for a four-impulse solution requires that the center of the circle lie at a point on the μ-axis which is either in the center of a loop of the locus (Fig. 4-1) or midway between two loops (Fig. 4-2). For $B > 0$ this is accomplished by choosing the constant C to be either $3B\pi$ or zero, respectively. (See Fig. 2-3.) As a result, the impulse times are symmetric about the time mid-way through the transfer, represented by $\tau = \pi$ for $C = 3B\pi$ and by $\tau = 0$ for $C = 0$.

The normal to the locus intersects the μ-axis at a value $\hat{\mu}$ given by

$$\hat{\mu} = A\left[C - 3B\tau - \sin\tau\left(\frac{4B + 3\cos\tau}{3B + 2\cos\tau}\right)\right] \qquad \text{(A-3)}$$

At the time of the second impulse, τ_2, the locus must be tangent to the unit circle centered at (0, 0). (See Fig. A-1.) This requires that τ_2 be a solution to

$$0 = C - 3B\tau_2 - \sin\tau_2\left(\frac{4B + 3\cos\tau_2}{3B + 2\cos\tau_2}\right) \qquad \text{(A-4)}$$

The time of the third impulse, τ_3, also satisfies this equation and can be simply obtained from τ_2 by using the symmetry property of the impulse times. (In Fig. A-1 $\tau_3 = -\tau_2$.)

Since Eq. (A-4) has several solutions, care must be taken to ensure obtaining the desired solution. Once τ_2 is obtained, the constant A is evaluated to make the magnitude of the primer vector unity at time τ_2

$$A = \frac{1}{[(\cos\tau_2 + 2B)^2 + (C - 3B\tau_2 - \sin\tau_2)^2]^{1/2}} \qquad \text{(A-5)}$$

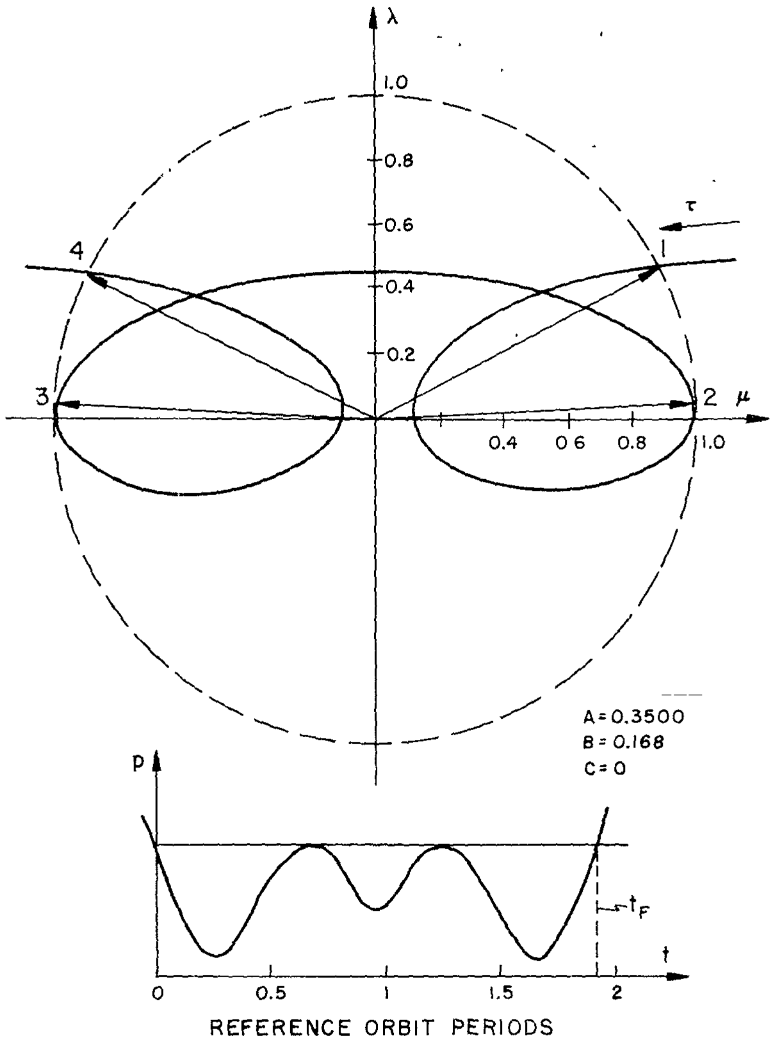

λ
1.0
0.8
0.6
0.4
0.2
τ
4
1
3
2
μ
0.4
0 6
0.8
1.0
A = 0.3500
B = 0.168
C = 0
p
t_F
t
0
0.5
1
1.5
2
REFERENCE ORBIT PERIODS

Fig. A-2.

The phasing constant, t_p, can be obtained from τ_1 (since the initial time is also the time of the first impulse $\tau_o = \tau_1$). However, the value of τ_o is not of primary importance, since only differences in τ are needed. The transfer time is $\tau_4 - \tau_1$, the second impulse occurs $\tau_2 - \tau_1$ after the first impulse, and so forth.

The unit vectors in the direction of the midcourse thrusts are given by (Fig. A-2):

$$\underline{u}_2 = \begin{bmatrix} \lambda(\tau_2) \\ \mu(\tau_2) \end{bmatrix} \; ; \; \underline{u}_3 = \begin{bmatrix} \lambda(\tau_2) \\ -\mu(\tau_2) \end{bmatrix} \tag{A-6}$$

To determine the time of the first impulse (and hence the fourth, by symmetry), one requires that τ_1 satisfy

$$\lambda^2(\tau_1) + \mu^2(\tau_1) = 1 \tag{A-7}$$

$\underline{u}_1$ and $\underline{u}_4$ are then evaluated in a manner analogous to Eq. (A-6).

Since the equations to determine the impulse times (Eqs. (A-4) and (A-7)) are transcendental, a numerical iteration is necessary to obtain the solution. Because of the multiplicity of solutions, the Secant Method[29] proved to be a more practical iteration scheme than the Newton-Rhapson Method[29] since the desired solution could be bounded before the iteration began.

A.4 Construction of Three-Impulse Primer Vector Solutions

As shown in Fig. 2-5, since only one tangency of the primer locus with the unit circle is required for a three-impulse solution, symmetry of the impulse times does not occur. In this case one chooses, for a given value of B, a convenient value of τ_2, the time of the second impulse. C is then evaluated to make μ of Eq. (A-3) zero:

$$C = 3B\tau_2 + \sin\tau_2 \left(\frac{4B + 3\cos\tau_2}{3B + 2\cos\tau_2} \right) \tag{A-8}$$

The constant A is evaluated by Eq. (A-5) to make the magnitude of the primer vector unity at time τ_2.

Using these values of A, B, and C, one incrementally increases τ from τ_2, travelling along the locus until

$$\lambda^2(\tau) + \mu^2(\tau) = 1 \tag{A-9}$$

The value of τ which satisfies Eq. (A-9) is the time of the third impulse, τ_3. The time of the first impulse is obtained by incrementally decreasing τ from τ_2 until Eq. (A-9) is satisfied. In each case, satisfaction of Eq. (A-9) to a desired accuracy requires a short iteration. With the impulse times evaluated, the components of the primer vector for these times are evaluated and a three-impulse primer vector solution is complete.

For the same locus shape, the initial choice of τ_2 is now incremented and the above procedure repeated to obtain a different three-impulse solution. Thus many different solutions are obtained from a given locus shape. When a given locus shape is exhausted of solutions, the value of the constant B is changed, as in the four-impulse case, and the entire procedure repeated.

APPENDIX B

THE LINEARIZED EQUATIONS OF MOTION

B.1 Equations of Motion and the Coriolis Operator

Newton's second law for a freely-falling body in a gravitational field is

$$p_I^2 \underline{R} = \underline{g}(\underline{R}) \tag{B-1}$$

where p is the derivative operator d/dt and $p_I^2 \underline{R}$ is the second derivative of the position vector relative to an observer in an inertial reference frame (considered to be non-rotating with respect to the distant galaxies).

For two-body motion,

$$\underline{g}(\underline{R}) = - \frac{\mu}{R^3} \underline{R} \tag{B-2}$$

The derivative of $\underline{R}$ relative to a rotating frame is related to the derivative in an inertial frame by the law of Coriolis. Let $\underline{\omega}$ be the angular velocity of the rotating frame with respect to the inertial frame. Then

$$p_I \underline{R} = p_R \underline{R} + \underline{\omega} \times \underline{R} = (p_R + \Omega) \underline{R} \tag{B-3}$$

where, for

$$\underline{R} = \begin{bmatrix} x \\ y \\ z \end{bmatrix}, \quad \Omega = \begin{bmatrix} 0 & -\omega_z & \omega_y \\ \omega_z & 0 & -\omega_x \\ -\omega_y & \omega_x & 0 \end{bmatrix} \tag{B-4}$$

The expression for the second derivative is obtained by applying the operator p_I to Eq. (B-3). Noting that

$$p_R(\Omega \underline{R}) = (p_R \Omega) \underline{R} + \Omega (p_R \underline{R}) \tag{B-5}$$

and that

$$p_I \Omega = p_R \Omega \triangleq \dot{\Omega} \tag{B-6}$$

one obtains

$$p_I^2 \underline{R} = [p_R^2 + \Omega(2p_R + \Omega) + \dot{\Omega}]\underline{R} \tag{B-7}$$

To summarize, the first and second derivative operators in the two reference frames are related by the well-known formulas:

$$\begin{aligned} p_I &= p_R + \Omega \\ p_I^2 &= p_R^2 + \Omega(2p_R + \Omega) + \dot{\Omega} \end{aligned} \tag{B-8}$$

B. 2 Linearization of the Equations of Motion

Motion of a vehicle which experiences only small deviations from a known reference solution to Eq. (B-1) can be approximated by the equations of motion linearized about the reference solution. Applying the first variation operator to Eq. (B-1),

$$\delta(p_I^2 \underline{R}) = G(\underline{R})\ \delta\underline{R} \tag{B-9}$$

where $G(\underline{R}) = \partial g/\partial \underline{r}$ is the gravity gradient matrix evaluated along the reference trajectory. If time is the independent variable for the linearization ($\delta t \equiv 0$), differentiation and variation are interchangeable. In terms of the state variation

$$\delta\underline{x}^I \triangleq \begin{bmatrix} \delta\underline{R} \\ p_I \delta\underline{R} \end{bmatrix} \tag{B-10}$$

the linearized equation of motion is

$$p_I \delta\underline{x}^I \quad \begin{bmatrix} 0 & I \\ G & 0 \end{bmatrix} \delta\underline{x}^I \tag{B-11}$$

Equation (B-11) is Eq. (3-7) written in more explicit notation. The solution to Eq. (B-11) is

$$\delta\underline{x}_j^I = \Phi_{ji}^I\ \delta\underline{x}_i^I \tag{B-12}$$

where Φ_{ji}^I is the state transition matrix of the system.

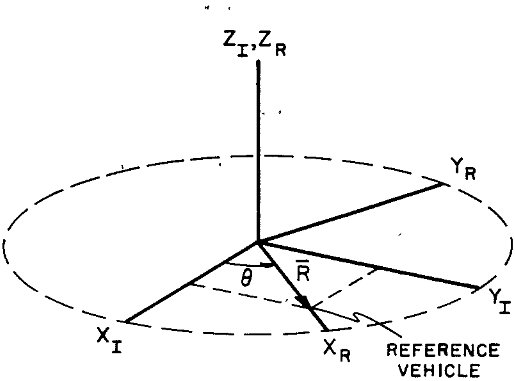

Fig. B-1.

Consider a coordinate frame which rotates with the radius vector to the vehicle in the reference orbit as shown in Fig. B-1. In these rotating coordinates,

$$\underline{R} = \begin{bmatrix} r \\ 0 \\ 0 \end{bmatrix} \quad ; \quad \delta\underline{R} = \begin{bmatrix} \delta r \\ r\,\delta\theta \\ \delta z \end{bmatrix} \tag{B-13}$$

For two-body motion

$$G = \frac{\mu}{R^5}\left[3\underline{R}\,\underline{R}^T - R^2 I\right] = \frac{\mu}{r^3}\begin{bmatrix} 2 & 0 & 0 \\ 0 & -1 & 0 \\ 0 & 0 & -1 \end{bmatrix} \tag{B-14}$$

This is the formulation used by Stern[18] in which $\delta \underline{x}^I$ is the state variation seen by an inertially non-rotating observer, coordinatized in a frame rotating with a vehicle in the reference orbit.

B. 3 State Variation Seen by a Rotating Observer

Another formulation, used by Hollister[30] is in terms of the state variation seen by a rotating observer. Let

$$\delta \underline{x}^R \quad \begin{bmatrix} \delta \underline{R} \\ p_R \, \delta \underline{R} \end{bmatrix} \tag{B-15}$$

$\delta \underline{x}^R$ is related to $\delta \underline{x}^I$ by a linear transformation. At time t_j:

$$\delta \underline{x}_j^I = T_j \, \delta \underline{x}_j^R \tag{B-16}$$

where

$$T_j = \begin{bmatrix} I & 0 \\ \Omega_j & I \end{bmatrix} \tag{B-17}$$

and

$$|T_j| = 1 \tag{B-18}$$

The differential equation analogous to Eq. (B-11) is then

$$p_R \, \delta \underline{x}^R = \begin{bmatrix} 0 & I \\ G - \Omega_j^2 - \dot{\Omega}_j & -2\Omega_j \end{bmatrix} \delta \underline{x}^R \tag{B-19}$$

The solution to this equation is

$$\delta \underline{x}_j^R = \Phi_{ji}^R \, \delta \underline{x}_i^R \tag{B-20}$$

where

$$\Phi_{ji}^R = T_j^{-1} \Phi_{ji}^I T_i \tag{B-21}$$

$\delta \underline{x}^R$ is the representation of the state variation used in this investigation.

B. 4. Equations Linearized about Circular Orbit

For a circular orbit of radius a, $\dot{\theta} = \omega =$ constant. If $\delta \underline{x}^R$ is coordinatized in the rotating frame, the components of the velocity variation are the derivatives of the position variation components. In these coordinates

$$G = \omega^2 \begin{bmatrix} 2 & 0 & 0 \\ 0 & -1 & 0 \\ 0 & 0 & -1 \end{bmatrix} \tag{B-22}$$

and Eq. (B-19) becomes

$$\begin{bmatrix} \delta \dot{r} \\ a\,\delta\dot{\theta} \\ \delta \dot{z} \\ \delta \ddot{r} \\ a\,\delta\ddot{\theta} \\ \delta \ddot{z} \end{bmatrix} = \left[\begin{array}{ccc|ccc} & 0 & & & I & \\ \hline 3\omega^2 & 0 & 0 & 0 & 2\omega & 0 \\ 0 & 0 & 0 & -2\omega & 0 & 0 \\ 0 & 0 & -\omega^2 & 0 & 0 & 0 \end{array}\right] \begin{bmatrix} \delta r \\ a\,\delta\theta \\ \delta z \\ \delta \dot{r} \\ a\,\delta\dot{\theta} \\ \delta \dot{z} \end{bmatrix} \tag{B-23}$$

The transition is then

$$\Phi_{ji} = \begin{bmatrix} 4 - 3\cos\alpha & 0 & 0 & \frac{\sin\alpha}{\omega} & \frac{2}{\omega}(1 - \cos\alpha) & 0 \\ 6(\sin\alpha - \alpha) & 1 & 0 & \frac{2}{\omega}(\cos\alpha - 1) & \frac{4\sin\alpha - 3\alpha}{\omega} & 0 \\ 0 & 0 & \cos\alpha & 0 & 0 & \frac{\sin\alpha}{\omega} \\ 3\omega\sin\alpha & 0 & 0 & \cos\alpha & 2\sin\alpha & 0 \\ 6\omega(\cos\alpha - 1) & 0 & 0 & -2\sin\alpha & 4\cos\alpha - 3 & 0 \\ 0 & 0 & -\omega\sin\alpha & 0 & 0 & \cos\alpha \end{bmatrix}$$

(B-24)

where $\alpha \triangleq \tau_j - \tau_i = \omega(t_j - t_i)$.

B. 5 Nondimensional State Variation

It is convenient to nondimensionalize the problem in terms of a characteristic length and time for the reference orbit. This can be done by measuring distances in multiples of circular reference orbit radius, a, and by defining a dimensionless time $\tau = \omega(t - t_p)$. The constant t_p allows a different origin for τ and t. The equation

$$a\,\delta\dot{\theta} = -\frac{3}{2}\omega\,\delta r \tag{B-25}$$

would then be written as

$$\frac{\delta\dot{\theta}}{\omega} = \frac{d}{d\tau}\,\delta\theta = -\frac{3}{2}\left(\frac{\delta r}{a}\right) \tag{B-26}$$

By choosing a set of units such that a = 1 and $\omega = 1$, the nondimensionalized variables $\delta\dot{\theta}/\omega$ and $\delta r/a$ are numerically equal to the original variables $\delta\dot{\theta}$ and δr. Therefore, in these units the original variables can be interpreted as dimensionless variables and Eq. (B-25) can be written as

$$\delta\dot{\theta} = -\frac{3}{2}\,\delta r \tag{B-27}$$

Distances are then measured in multiples of reference orbit radius and time is measured in multiples of the time to travel one radian on the reference orbit.

In these units:

Reference Orbit Radius	$a = 1$	
Reference Orbit Angular Velocity (mean motion)	$\omega = 1$	
Reference Orbital Velocity	$v = 1$	(B-28)
Reference Period	$P = 2\pi$	
Gravitational Constant	$\mu = 1$	

B. 6 Boundary Conditions for Circle-to-Circle Coplanar Rendezvous

As discussed in Section 4. 2, the specific problem to be investigated is rendezvous between two circular, coplanar orbits. The reference orbit is also a circular orbit of unit radius lying in the same plane. A trajectory lying in this plane can be described by a four-component state variation, since $\delta z \equiv 0$.

The state variation for the specific case of a body in a circular orbit close to the reference orbit is obtained by finding a solution to Eq. (B-23) for which δR and $\delta\dot{\theta}$ are constants.

The dimensionless state variation of a body in circular orbit of radius $1 + \delta a$ is:

$$\delta \underline{x}(\tau) = \begin{bmatrix} \delta r(\tau) \\ \delta\theta(\tau) \\ \delta\dot{r}(\tau) \\ \delta\dot{\theta}(\tau) \end{bmatrix} = \begin{bmatrix} \delta a \\ \delta\theta(\tau) \\ 0 \\ -\frac{3}{2}\delta a \end{bmatrix} \tag{B-29}$$

and, at any other time τ':

$$\delta \underline{x}(\tau') = \begin{bmatrix} \delta a \\ \delta\theta(\tau) - \frac{3}{2}\delta a(\tau' - \tau) \\ 0 \\ -\frac{3}{2}\delta a \end{bmatrix} \tag{B-30}$$

For the coplanar, circle-to-circle rendezvous, the reference orbit is chosen to lie half-way between the terminal orbits. Define δR to be the difference between the dimensionless final orbit radius and the dimensionless initial orbit radius. (Thus $\delta R < 0$ if the initial orbit is the outer terminal orbit.) At the initial time, τ_o (corresponding to $t = 0$), the vehicle is in the initial orbit as shown in Fig. B-2. Since the state variation is measured with respect to the reference point travelling in the reference orbit, it is convenient to choose the reference point at τ_o such that $\delta\theta_o = 0$. Then the dimensionless state variation at τ_o is

$$\delta \underline{x}_o = \begin{bmatrix} -\delta R/2 \\ 0 \\ 0 \\ \frac{3}{4}\delta R \end{bmatrix} \tag{B-31}$$

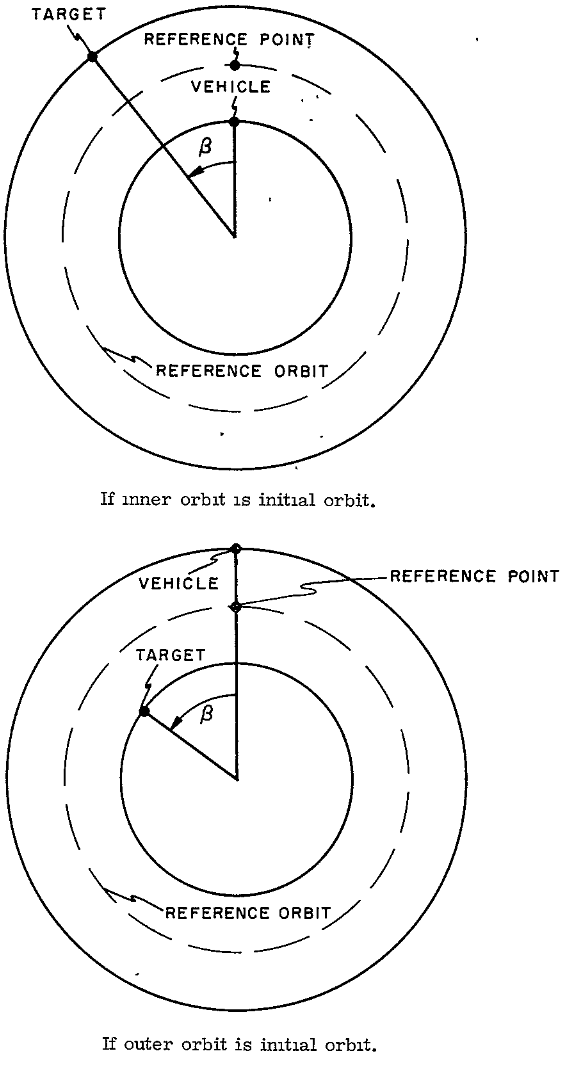

If inner orbit is initial orbit.

If outer orbit is initial orbit.

Fig. B-2. Geometry at t_o.

The state variation of the target is

$$\delta \underline{x}^T(\tau) = \begin{bmatrix} \delta R/2 \\ \delta\theta^T(\tau) \\ 0 \\ -\frac{3}{4}\delta R \end{bmatrix} \tag{B-32}$$

where, in terms of the initial phase angle, β (Fig. B-1),

$$\frac{\delta\theta^T}{\delta R} = \frac{\beta}{\delta R} - \frac{3}{4}(\tau - \tau_o) \tag{B-33}$$

The condition for rendezvous at τ_F is

$$\delta \underline{x}(\tau_F) = \delta \underline{x}^T(\tau_F) \tag{B-34}$$

so that

$$\frac{\delta\theta(\tau_F)}{\delta R} = \frac{\beta}{\delta R} - \frac{3}{4}(\tau_F - \tau_o) \tag{B-35}$$

B. 7 <u>State Variation Using True Longitude as Independent Variable</u>

As discussed in Section 3. 3, using true longitude as the independent variable[20] in the linearized equations may yield a more accurate approximation to the nonlinear rendezvous solution. $\delta \underline{y}$, representing the state variation using θ as the independent variable ($\delta\theta \equiv 0$) is obtained from $\delta \underline{x}$, the state variation using time as independent variable, by a linear transformation:

$$\delta \underline{y} = M\ \delta \underline{x} \tag{B-36}$$

Taking as components of $\delta \underline{y}$ the variation in radial position, time, out-of-plane position and their derivatives with respect to θ, Eq. (B-36) for a circular reference orbit is:

$$\begin{bmatrix} \delta r \\ \delta t \\ \delta z \\ \delta r' \\ \delta t' \\ \delta z' \end{bmatrix}_{\theta} = \left[\begin{array}{ccc|ccc} 1 & 0 & 0 & & & \\ 0 & -\frac{1}{a\omega} & 0 & & 0 & \\ 0 & 0 & 1 & & & \\ \hline & & & \frac{1}{\omega} & 0 & 0 \\ & 0 & & 0 & -\frac{1}{a\omega^2} & 0 \\ & & & 0 & 0 & \frac{1}{\omega} \end{array}\right] \begin{bmatrix} \delta r \\ a\,\delta\theta \\ \delta z \\ \delta\dot{r} \\ a\,\delta\dot{\theta} \\ \delta\dot{z} \end{bmatrix}_{t} \tag{B-37}$$

where the prime denotes differentiation with respect to θ. The matrix M is diagonal and constant. In the units of Section B.5 the diagonal elements have unit magnitude.

The differential equation for $\delta \underline{y}$ is related to the $\delta \underline{x}$ equation in the following way:

$$\delta\dot{\underline{x}} = F\,\delta\underline{x} \tag{B-38}$$

$$\delta\underline{y}' = \frac{1}{\omega}\,(MF + \dot{M})\,M^{-1}\,\delta\underline{y} \tag{B-39}$$

For a circular orbit, Eq. (B-39) is of the same form as Eq. (B-23):

$$\begin{bmatrix} \delta r' \\ \delta t' \\ \delta z' \\ \delta r'' \\ \delta t'' \\ \delta z'' \end{bmatrix} = \left[\begin{array}{ccc|ccc} & 0 & & & I & \\ \hline 3 & 0 & 0 & 0 & -2a\omega & 0 \\ 0 & 0 & 0 & \frac{2}{a\omega} & 0 & 0 \\ 0 & 0 & -1 & 0 & 0 & 0 \end{array}\right] \begin{bmatrix} \delta r \\ \delta t \\ \delta z \\ \delta r' \\ \delta t' \\ \delta z' \end{bmatrix} \tag{B-40}$$

The solution to Eq. (B-39) is

$$\delta\underline{y}_j = \boldsymbol{\Psi}_{ji}\,\delta\underline{y}_i \tag{B-41}$$

where

$$\boldsymbol{\Psi}_{ji} = M_j\,\boldsymbol{\Phi}_{ji}\,M_i^{-1} \tag{B-42}$$

The subscripts on M apply if M is time-varying, as in the elliptical case.

The boundary value problems (Section 3.5) for the two state variables are related by:

$$\delta \underline{x}_F = \Phi_{Fo}\, \delta \underline{x}_o + W\, \underline{\Delta V} \tag{B-43}$$

$$\delta \underline{y}_F = \Psi_{Fo}\, \delta \underline{y}_o + M_F\, W\, \underline{\Delta V} \tag{B-44}$$

APPENDIX C

SYLVESTER'S LAW[31]

Given two conformable matrices

$$k\,(m \times n)$$

$$L(n \times q)$$

the rank of kL, denoted by $\rho(kL)$, is related to $\rho(k)$ and $\rho(L)$ in the following way:

$$\rho(k) + \rho(L) - n \leq \rho(kL) \leq \min \left\{ \rho(k), \rho(L) \right\} \tag{C-1}$$

In the application to Section 6.6

$$H = \Phi_{HF} W \tag{C-2}$$

$\rho(\Phi_{HF}) = 4$ since Φ_{HF} is (4×4) and nonsingular

$\rho(W) \leq 3$ since W is (4×3)

Substituting into Eq. (C-1):

$$\rho(W) \leq \rho(\Phi_{HF} W) \leq \rho(W) \tag{C-3}$$

Therefore

$$\rho(\Phi_{HF} W) = \rho(W) \tag{C-4}$$

$$\rho(H) = \rho(W) \tag{C-5}$$

The rank of H is equal to the rank of W.

LIST OF REFERENCES

1. Hohmann, W., "Die Erreichbarkeit der Himmelskoerper," Oldenbourg, Munich (1925), The Attainability of Heavenly Bodies, NASA Technical Translation F-44 (1960).

2. Lawden, D. F., "Interplanetary Rocket Trajectories," Chapter 1, Advances in Space Science, 1, edited by F. I. Ordway III, Academic Press, N.Y., 1-53 (1959).

3. Lawden, D. F., "Impulsive Transfer Between Elliptical Orbits," Chapter 11 of Optimization Techniques, G. Leitmann, editor, Academic Press, N.Y., 323-351 (1962).

4. Lawden, D. F., Optimal Trajectories for Space Navigation, Butterworths, London (1963).

5. Breakwell, J. V., "The Optimization of Trajectories," SIAM Journal Vol. 7 No. 2, June 1959.

6. Edelbaum, T. N., "How Many Impulses," AIAA Third Aerospace Sciences Meeting, N.Y., Preprint No. 66-7 (1966).

7. Shternfeld, A., Soviet Space Science, Basic Books, Inc., New York, 109-11 (1959).

8. Edelbaum, T. N., "Some Extensions of the Hohmann Transfer Maneuver," ARS Journal 29, 864-865 (1959).

9. Hoelker, R. F. and Silber, R., "The Bi-elliptical Transfer Between Coplanar Circular Orbits," Proc. 4th Symposium Ballistic Missile and Space Technology, Los Angeles (1959).

10. Marchal, C., "Transferts Optimaux entre Orbites Elliptiques (Durée Indifférente)," presented at XVI IAF Congress, Athens (1965).

11. Edelbaum, T. N., "Minimum Impulse Transfers in the Near Vicinity of a Circular Orbit," Journal of the Astronautical Sciences, Vol. XIV, No. 2, 66-73 (1967).

12. Gobetz, F. W., "Optimum Transfers Between Hyperbolic Asymptotes," AIAA Journal 1, 2034-2041 (1963).

13. Marchal, C., "Transferts Optimaux entre Orbites Hyperboliques," presented at XVII IAF Congress, Madrid (1966).

14. Lion, P. M. and Handelsmann, M., "The Primer Vector on Fixed-Time Impulsive Trajectories," AIAA Fifth Aerospace Sciences Meeting, N. Y., January 1967.

15. Marec, J., "Rendez-vous Impulsionnels Optimaux de Longue Duree entre Orbites Quasi-Circulaires Proches, Coplanaires ou non," presented at colloquium "Advanced Problems and Methods for Space Flight Optimization," Liege (1967).

16. Doll, J. R. and Gobetz, F. W., "Three-Impulse Interplanetary Rendezvous Trajectories," presented at AAS Symposium, Huntsville (1966).

17. Leitmann, G., An Introduction to Optimal Control, McGraw-Hill, N. Y. (1966).

18. Stern, R. G., "Interplanetary Midcourse Guidance Analysis," Sc. D. Thesis, Dept. of Aeronautics and Astronautics, MIT (1963).

19. Gobetz, F. W., "Optimal Variable-Thrust Transfer of a Power-Limited Rocket between Neighboring Circular Orbits," AIAA Journal Vol. 2, No. 2 (1964).

20. Stern, R. G. and Potter, J. E., "Linearized Orbit Theory with True Longitude as the Independent Variable," to be presented at 2nd IFAC Symposium, Vienna, Sept. 1967.

21. Neustadt, L. W., "Optimization, A Moment Problem and Nonlinear Programming," SIAM Journal on Control 2, 33-53 (1964).

22. Stern, R. G. and Potter, J. E., "Optimization of Midcourse Velocity Corrections," IFAC Symposium on Automatic Control in the Peaceful Use of Space, Stavanger, Norway (1965).

23. Potter, J. E., "Four Impulse Orbit Transfers," to appear.

24. Winston, B. P., "Optimal Four-Impulse Transfers between Two Nearby Orbits," S. M. Thesis, Dept. of Aeronautics and Astronautics, MIT (1966).

25. Hildebrand, F. B., Methods of Applied Mathematics, Prentice-Hall Inc., N. J. (1952).

26. Kelley, H. J., Kopp, R. E., and Moyer, H. G., "Singular Extremals," Chapter 3 of Topics in Optimization, G. Leitmann, editor, Academic Press, N. Y. (1967).

27. McIntyre, J. E. and Crocco, L., "Optimal Transfer Between Close Circular Orbits Using the Pontryagin Maximum Principle," AIAA Aerospace Sciences Meeting, N. Y., Preprint No. 64-29 (1964).

28. Barrar, R. B., "An Analytic Proof that the Hohmann-Type Transfer is the True Minimum Two-Impulse Transfer," Astronautica Acta 9, 1-11 (1963).

29. Hildebrand, F. B., Introduction to Numerical Analysis, McGraw-Hill, N. Y. (1956).

30. Hollister, W. M., "The Mission for a Manned Expedition to Mars," Sc. D. Thesis, Dept. of Aeronautics and Astronautics, MIT (1963).

31. Marcus, M., "Basic Theorems in Matrix Theory," National Bureau of Standards Applied Mathematics Series, 57, U. S. Government Printing Office (1960).

BIOGRAPHICAL SKETCH

John Edward Prussing was born on August 19, 1940 in Oak Park, Illinois. He attended public schools in Oak Park and Libertyville, Illinois and graduated from Libertyville-Fremont Township High School in 1958.

Mr. Prussing entered M. I. T. as an undergraduate in 1958. In 1963 he received the degrees of Bachelor of Science and Master of Science in the Honors Program of the M. I. T. Department of Aeronautics and Astronautics. His Master's thesis was in the field of Adaptive Control Systems.

During his graduate study Mr. Prussing has been a Research Assistant and Staff Member at the M. I. T. Instrumentation Laboratory, Dynamics Research Corporation Fellow, Teaching Assistant in the Department of Aeronautics and Astronautics, and Research Assistant at the M. I. T. Experimental Astronomy Laboratory.

While at the Experimental Astronomy Laboratory he co-authored an article with Prof. Walter M. Hollister on Venus flyby trajectories. His teaching experience is in inertial guidance techniques and in interplanetary trajectory analysis. He is a member of Sigma Xi and Sigma Gamma Tau honorary fraternities.

Mr. Prussing is married to the former Laurel Victoria Lunt. They have one daughter, Heidi Elizabeth.